2018

A Study of African Savanna Vegetation Structure, Patterning, and Change

Christoffer R. Axelsson
South Dakota State University

A STUDY OF AFRICAN SAVANNA VEGETATION STRUCTURE, PATTERNING, AND CHANGE

BY

CHRISTOFFER R. AXELSSON

A dissertation submitted in partial fulfillment of the requirements for the

Doctor of Philosophy

Major in Geospatial Science and Engineering

Specialization in Remote Sensing Geography

South Dakota State University

2018

A STUDY OF AFRICAN SAVANNA VEGETATION STRUCTURE, PATTERNING, AND CHANGE

This dissertation is approved as a creditable and independent investigation by a candidate for the Doctor of Philosophy in Geospatial Science and Engineering and is acceptable for meeting the dissertation requirements for this degree. Acceptance of this does not imply that the conclusions reached by the candidates are necessarily the conclusions of the major department.

Niall P. Hanan, Ph.D.
Dissertation Advisor Date

Geoffrey M. Henebry, Ph.D.
Director, GSCE Date

Dean, Graduate School Date

ACKNOWLEDGEMENTS

This research was supported by the NASA Terrestrial Ecology Program, the National Science Foundation (Coupled Natural-Human Systems Program), and the Geospatial Sciences Center of Excellence (GSCE) at South Dakota State University. First and foremost, I sincerely thank my academic advisor Dr. Niall Hanan, and the committee members Dr. Geoff Henebry, Dr. Michael Wimberly, Dr. Alisa Gallant, and Dr. David Clay. I have had great support from Dr. Hanan's research group, both at SDSU and at NMSU, as well as staff and students at GSCE. Special thanks to my officemates, Francis and Fangjun. I thank Jamie Nickeson for providing me with the satellite data necessary for the analyses. The high resolution satellite data were provided by NASA's Commercial Archive Data (cad4nasa.gsfc.nasa.gov) under the National Geospatial-Intelligence Agency's NextView license agreement. Thanks to Sujan Parajuli and Dinesh Shrestha for their work with classifying the imagery. Finally, I thank Njoki and staff at national parks and nature reserves in Kenya for a very memorable field work experience.

CONTENTS

ABBREVIATIONS

AfSIS	Africa Soil Information Service
BRT	Boosted Regression Tree
CO_2	Carbon Dioxide
CRU	Climatic Research Unit
cv	Coefficient of Variation
DEM	Digital Elevation Model
ENVI™	Environment for Visualizing Images
FAO	Food and Agriculture Organization
FAOSTAT	Food and Agriculture Organization Corporate Statistical Database
GPS	Global Positioning System
ha	hectare
IDL™	Interactive Data Language
ISODATA	Iterative Self-Organizing Data Analysis Technique
ISRIC	International Soil Reference Information Centre
LAI	Leaf Area Index
m	meter
MAP	Mean Annual Precipitation
MODIS	Moderate Resolution Imaging Spectrometer
MPa	Megapascal
NASA	National Aeronautics and Space Administration
NDVI	Normalized Difference Vegetation Index
NP	National Park
OLS	Ordinary Least Squares

PVP	Periodic Vegetation Pattern
RPC	Rapid Positioning Coordinate
SAR	Simultaneous Autoregression
SLA	Specific Leaf Area
SRTM	Shuttle Radar Topography Mission
TRMM	Tropical Rainfall Measuring Mission
UN	United Nations
VHR	Very High Resolution

ABSTRACT

A STUDY OF AFRICAN SAVANNA VEGETATION STRUCTURE, PATTERNING, AND CHANGE

CHRISTOFFER AXELSSON

2018

African savannas cover roughly half of the continent, are home to a great diversity of wildlife, and provide ecosystem services to large populations. Savannas showcase a great diversity in vegetation structure, resulting from variation in climatic, edaphic, topographic, and biological factors. Fires play a large role as savannas are the most frequently burned ecosystems on Earth. To study how savanna vegetation structure shifts with environmental factors, it is necessary to gather site data covering the full gradient of climatic and edaphic conditions. Several earlier studies have used coarse resolution satellite remote sensing data to study variation in woody cover. These woody cover estimates have limited accuracy in drylands where the woody component is relatively small, and the data cannot reveal more detailed information on the vegetation structure. We therefore know little about how other structural components, tree densities, crown sizes, and the spatial pattern of woody plants, vary across environmental gradients.

This thesis aimed to examine how woody vegetation structure and change in woody cover vary with environmental conditions. The analyses depended on access to very high spatial resolution (<1 m) satellite imagery from sites spread across African savannas. The high resolution data combined with a crown delineation method enabled me to estimate variation in tree densities, mean crown size and the level of aggregation among woody

plants. With overlapping older and newer imagery at most of the sites, I was also able to estimate change in woody cover over a 10-year period. I found that higher woody plant aggregation is associated with drier climates, high rainfall variability, and fine-textured soils. These same factors were also indicative of the areas where highly organized periodic vegetation patterns were found. The study also found that observed increases in woody cover across the rainfall gradient is more a result of increasing crown sizes than variation in tree density. The analysis of woody cover change found a mean increase of 0.25 % per year, indicating an ongoing trend of woody encroachment. I could not attribute this trend to any of the investigated environmental factors and it may result from higher atmospheric CO_2 concentrations, which has been proposed in other studies. The most influential predictor of woody cover change in the analysis was the difference between potential woody cover and initial woody cover, which highlights the role of competition for water and density dependent regulation when studying encroachment rates. The second most important predictor was fire frequency.

To better understand and explain the dominant ecosystem processes controlling savanna vegetation structure, I constructed a spatially explicit model that simulates the growth of herbaceous and woody vegetation in a landscape. The model reproduced several of the trends in woody vegetation structure earlier found in the remote sensing analysis. These include how tree densities and crowns sizes respond differently to increases in precipitation along the full rainfall range, and the factors controlling the spatial pattern of trees in a landscape.

1 INTRODUCTION

1.1 Factors that shape savanna systems

Savannas are composed of an open woody canopy with a continuous layer of herbaceous vegetation. They cover roughly an eighth of the global land surface and over half of the African continent (Scholes & Archer, 1997). The extent of the savanna biome is controlled by environmental factors, primarily rainfall, rainfall seasonality, fire, and herbivory (Lehmann et al., 2011). Systems with rainfall below ~750 $mm\ yr^{-1}$ generally lack the climatic prerequisites for forming closed canopies. These are called water-limited savannas as they are prevented by water shortage from forming closed woody canopies. Rainfall supports the growth of woody plants and broadly defines the potential upper limit of woody cover in a landscape (Figure 1.1b; Sankaran et al., 2005). Savannas are also common in areas with rainfall above 750 $mm\ yr^{-1}$, where disturbances (fire and browsing) can suppress woody vegetation and keep it from converting into forest (Sankaran et al., 2008). Rainfall and disturbances thus strongly influence the extent of the savanna biome by supporting and suppressing woody cover. Furthermore, observations of the variation in woody cover indicate that the distribution is bimodal with a drop in the presence of savannas with 50-70 % tree cover, indicative of the presence of alternative stable states (Figure 1.1b; Hirota et al., 2011; Staver et al., 2011a).

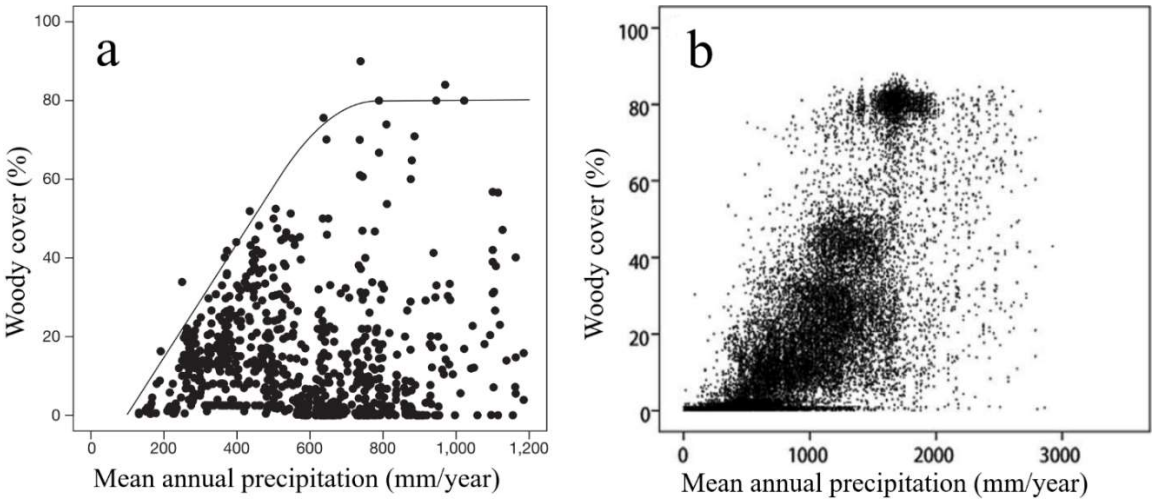

Figure 1.1 (a) Derived relationship between potential woody cover and mean annual precipitation (MAP) at African savanna sites (Sankaran et al., 2005). (b) Woody cover estimates for Africa showing a bifurcated distribution with fewer sites in the 50-70 % range (Hirota et al., 2011).

Especially in higher rainfall savannas (1000-2000 $mm\,yr^{-1}$), the wet environment provides excellent conditions for herbaceous biomass growth which can be transformed into high fire intensities that kill and top-kill woody plants. This creates a positive feedback loop between herbaceous growth, intense fires, and suppression of woody vegetation, that can maintain an open savanna landscape as a stable state under high rainfall conditions (Staver et al., 2011b). Frequent fires are thus a key component of mesic savannas and savanna systems are by far the most frequently burned ecosystems on Earth (Andela et al., 2017; Archibald et al., 2013). At woody cover higher than ~40 %, herbaceous productivity and the connectivity of grassy fuels is reduced due to light limitations leading to fewer and less intense fires (Archibald et al., 2009). If woody cover in mesic savannas surpasses this threshold, the woody cover may continue to expand until the system reaches a closed canopy state. This can explain the lack of sites in the 50-70 %

range (Figure 1.1b). Rainfall seasonality also plays an important role for the fire regime and the distribution of savannas. Lehmann et al. (2011) found that rainfall seasonality is the most influential factor for predicting the worldwide distribution of savannas in the mesic climate zone. A long dry season cures fuels and creates optimal conditions for fire occurrence. Systems with a dry season longer than 6 months are therefore more likely to burn (Archibald et al., 2009). High rainfall seasonality can also directly affect woody communities by constraining sapling survival during the long dry season. While internal feedback loops can act to keep an ecosystem in a stable state, woody communities are seldom stable in the longer term (Gillson, 2004). They naturally undergo periods of growth and decline, and interannual variation in rainfall and fauna populations is the norm. Mesic savannas, where the vegetation is not in equilibrium with the climate, may transition between open savanna and closed forest states over larger time frames of centuries to millennia (Hoffmann et al., 2012).

Woody cover is also influenced by soil type, which controls the partitioning of rainfall into evapotranspiration, drainage, and runoff (Fernandez-Illescas et al., 2001). Noy-Meir (1973) proposed that an inverse texture effect controls how woody plants are affected differently by soil texture in drier (~<500 mm/year) and wetter systems. The higher hydraulic conductivity of coarse-textured soils leads to deeper soil water infiltration, which limits evaporation from the top soil layer. In addition, coarse-textured soils have lower water losses from runoff generation. Woody plants thereby benefit from coarse-textured soils in drier systems. The lower water-holding capacity of coarse-textured soils also leads to higher water losses through drainage to groundwater, which is thought to be a more dominant flux in wetter systems. The inverse texture hypothesis thus posits that

woody plants in wetter systems are favored by fine-textured soils. While there have been several observations of lower woody productivity on clayey soils in drylands (Lane et al., 1998; Williams et al., 1996), the exact mechanism for this is still being debated. Fensham, Butler, & Foley (2015) suggested that growth is hampered by the higher wilting point on clayey soils which impedes water extraction.

1.2 Competition and facilitation between plants

In addition to external factors, such as rainfall, savanna systems are shaped by complex tree-grass and tree-tree interactions. These interactions often involve competition for resources, but are sometimes facilitative in that plants may improve local growth conditions (Brooker et al., 2008). Water is a scarce resource for much of the year in the seasonal tropics and plants need coping mechanisms to survive the dry season (Schwinning et al., 2004). Herbaceous vegetation can both compete with and facilitate the growth of woody vegetation. They have relatively shallow roots and rely more on soil moisture in the upper soil layers compared to the more deep-rooted woody vegetation. Differences in rooting depth is most pronounced in arid systems ($< 500\ mm\ yr^{-1}$), where investing in deeper roots is more important, while woody and herbaceous vegetation can have similar mean rooting depths in humid systems (Schenk & Jackson, 2002). As herbaceous vegetation consumes water in the upper soil layer, it reduces flow to deeper soil layers where woody vegetation has sole access to the resource (Holdo & Brocato, 2015). Overlapping root networks is thus not a prerequisite for competition, and grasses have been shown to suppress the growth of woody plants regardless of their sizes (Riginos, 2009). Competition with grasses might be most critical, though, in the early stages of plant development before deeper roots have been established (February et al., 2013). Adult

woody plants will extract water from shallow soil depths as long as it is available, but also have the option to switch to deeper layers when necessary (Kulmatiski & Beard, 2013). There is thus competition for water both between trees and between trees and herbaceous vegetation. With increasing plant size, both trees, shrubs, and herbaceous vegetation increase the vertical and lateral extension of their root systems (Schenk & Jackson, 2002). But, while most herbaceous plants only has minor lateral extension and mainly competes for water underneath its canopy, woody plants can have laterally extensive root systems that extend far beyond the crown radius (Schenk & Jackson, 2002; Scholes, 2003). Individual woody plants thus compete for resources over far larger areas than individual herbs and grasses. There are also differences in the timing of resource consumption in seasonal systems. Compared to grasses, trees more quickly expand their leaf area at the start of the growing season and retain them longer after the rains end (Scholes, 2003). There are thus periods in both the beginning and after the rainy season when trees do not compete with herbaceous vegetation.

In addition to competing for resources, plants may also modify the environment in ways that facilitate growing conditions locally. Both woody and herbaceous vegetation provide shading of the ground, and their root networks increase macroporosity of the soils which enhances infiltration of rainwater (Thompson et al., 2010). Shading reduces water losses through evaporation and provides a locally cooler microclimate (Breshears et al., 1998). Whether the net effect of plant interactions is competitive or facilitative depends on several factors including overall resource availability, time of the year, degree of shading, growth stage of the plant, and species type. A prerequisite for facilitative interactions is some kind of resource limitation or need that

can be alleviated by neighboring plants. With more severe resource limitations, facilitative effects are more important and therefore more likely to be stronger than negative effects from competition. This observation has given rise to the stress-gradient hypothesis which states that facilitative interactions increase with increasing environmental stress (He et al., 2013). Woody plants generally have a positive effect on herbaceous growth in drier savannas ($\sim < 700\ mm\ yr^{-1}$) where conservation of water resources is more critical, while it is negative in more humid systems (Dohn et al., 2013; Moustakas et al., 2013). Both living and dead herbaceous vegetation provide beneficial effects, and the net effect on woody sapling growth can therefore shift from strongly negative (through active competition) to strongly positive (through passive facilitation) as grasses wilt (Resco de Dios et al., 2014). Adult woody plants can act as nurse plants with facilitative effects on both herbaceous vegetation and saplings growing underneath or nearby their canopy (Hoffmann, 1996). Furthermore, shading can be beneficial up to a certain level where the negative effect of light shortage overtakes the positive effect of cooling. The net effect along a gradient of shading is therefore unimodal and can be either facilitative or suppressive of the undergrowth, depending on degree of shading and shade-tolerance of the shaded species (Holmgren et al., 2012). Woody plants with a low canopy are more effective at filtering out most of the local light and are therefore generally more suppressive, while taller trees filter out less light and can provide intermediate shading over a relatively large area (Blaser et al., 2013).

There are additional means of competition and facilitation associated with specific woody species that can have a considerable effect on surrounding vegetation. Some species use hydraulic lift to transport water from deeper soil layers to the surface via

a tap root, to the benefit of both itself and surrounding vegetation (Goldstein et al., 2008). Nitrogen fixing plants enhance local growing conditions in the understory by increasing the nutritional value of the soil (Blaser et al., 2013). An example of competitive interactions is the use of allelochemicals to suppress the growth of neighboring plants (Rolo et al., 2012).

1.3 From patchiness to periodic vegetation patterns

In areas where facilitative mechanisms dominate at shorter ranges, the spatial pattern of the vegetation tends to be more aggregated. The soil quality in vegetated patches is further improved by litter fall and a higher concentration of animal droppings near trees (Belsky, 1994; Ludwig et al., 2004). In drier areas, this can lead to vegetated patches in an otherwise bare landscape. Partly due to increased macroporosity near roots, vegetated patches also exhibit higher infiltration capacity than bare soils (De Boever et al., 2016; Niemeyer et al., 2014). The differences in infiltration capacity are more pronounced in water-limited systems (Thompson et al., 2010), and on fine-textured soils which feature lower hydraulic conductivity (D. J. Eldridge & Freudenberger, 2005). Bare inter-patch areas can then act as runoff zones that distribute rainwater to nearby vegetated patches. The amount of water redistribution can be further enhanced in the presence of soil crusts that obstruct soil pores (Pueyo et al., 2013), and hardpans that limit infiltration to deeper soil layers (Penny et al., 2013). Vegetation at such sites can form periodic vegetation patterns with sharp contrasts between the bare runoff zones and vegetated patches. Depending on water availability and topography, periodic vegetation may feature spotted, labyrinthine, gapped, or banded patterns (Figure 1.2; Deblauwe et al., 2011). In Africa, such vegetation patterns are most common in the Sahelian zone and in the Horn of Africa.

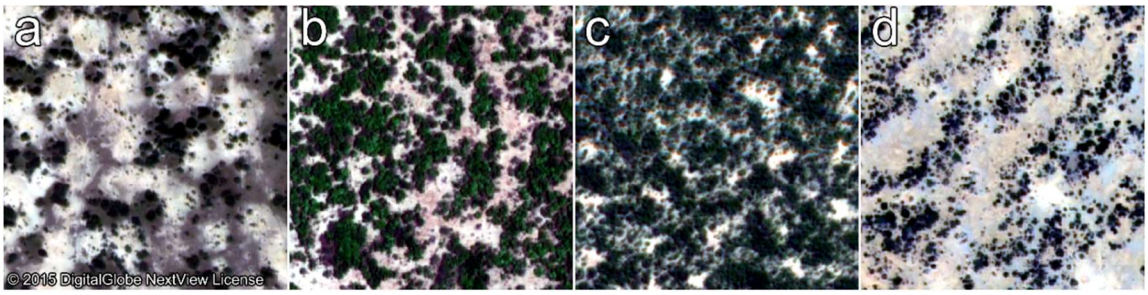

Figure 1.2 Examples of periodic vegetation patterns: (a) spotted pattern, (b) labyrinthine pattern, (c) gapped pattern, and (d) banded pattern. Imagery provided by NASA's Commercial Archive Data.

1.4 Woody encroachment

Encroachment of trees and shrubs has been observed worldwide and its drivers and consequences have been heavily debated over the past decades. Reports of invasions or thickening of shrubs in arid and semiarid grasslands (Van Auken, 2009), gap-filling in woodlands (Lunt et al., 2010), and expansion of forest into savannas (R. Fensham et al., 2005) have all been linked to a global trend of more woody plants. There is no clear consensus on the exact mechanisms that drive this development, but increased atmospheric CO_2 levels (Higgins & Scheiter, 2012) and a global trend of fire frequency reduction (Andela et al., 2017; Marlon et al., 2008) stand out as the main candidates. Both of these factors likely play important roles, but at the global scale it is not straightforward to assign clear causal relationships with either. The number of interacting factors and internal feedbacks complicate any analysis of savanna ecosystems. The role of fire is well established, but its relationship with woody vegetation is circular. While frequent fires are efficient at suppressing woody vegetation, less woody vegetation generally leads to more fires. In systems where humans do not impose a fire regime, it can thus be difficult to

disentangle the effect of fire on the vegetation from how the vegetation influences the fire regime.

Livestock grazing has been linked to encroachment through several different causal pathways, for example, seed dispersal (Brown & Carter, 1998; González-Roglich et al., 2015), soil compaction (Castellano & Valone, 2007), and altering soil moisture conditions by removing competing grasses (Ward & Esler, 2011). These are viable mechanisms that likely contribute to and speed up encroachment in specific cases. A more indirect effect commonly associated with livestock introductions is the removal of wild browsers (Archer et al., 2017). The main causal pathway from grazing to woody encroachment is, however, via suppression of fire. Grazing removes fine grassy fuels which decreases fire frequency and intensity (Archer et al., 2017).

The effect of CO_2 concentrations on vegetation is most evident in chamber tests where plants are subjected to elevated CO_2 concentrations. Such experiments show variable responses that depend on plant functional type, photosynthetic pathway, as well as interactions with nutrient and climatic factors (Körner, 2006; Robinson et al., 2012; Wang et al., 2012). There is evidence that elevated CO_2 leads to increased competitiveness of woody species with strong responses on photosynthesis, stem growth, root development, and aerial expansion, that are most pronounced among younger trees (Kgope et al., 2010; Morgan et al., 2007). The difference in photosynthetic pathway between C_3 trees and C_4 grasses is often invoked as a reason for greater competitiveness of woody species. Some growth experiments indicate that the C_3 photosynthetic pathway becomes increasingly competitive at higher CO_2 levels (Poorter & Navas, 2003; Wang et al., 2012). However, other experiments indicate similar responses in C_3 and C_4 grasses where both have the

potential to benefit from elevated CO_2, mainly by increased water-use efficiency (Morgan et al., 2007; Owensby et al., 1997). Plant type (woody vs herbaceous) appears to be a stronger predictor of growth response to CO_2 than the photosynthetic pathway. Young trees have the added benefit of accumulating biomass responses over many years whereas annual grasses reset their growth cycle every year (Körner, 2006). There is, thus, ample evidence to suggest that elevated CO_2 concentrations can support woody encroachment.

In natural environments, it is difficult to disentangle the effect of elevated CO_2 from other possible drivers such as changes to grazing or fire regimes. There are, however, observations of encroachment also on sites that have been subjected to constant disturbance regimes for longer time periods (Buitenwerf et al., 2012; Stevens et al., 2016). It is also clear that vegetation growth interacts with atmospheric CO_2 levels, and any consistent trend in terrestrial carbon accumulation will affect atmospheric CO_2 concentrations. In fact, estimates and modelling of trends in atmospheric carbon and biologic sequestration point to semi-arid systems as an important terrestrial carbon sink, which is consistent with the trend of woody encroachment (Ahlström et al., 2015).

It is clear that greater woody proliferation has important consequences on ecosystem processes, biochemical cycles (especially the carbon cycle), biodiversity, and the provision of ecosystem services (Archer et al., 2017). Consequences can be seen as either positive or detrimental depending on the view-point. Biomass accumulation in savannas acts as a terrestrial sink of anthropogenic CO_2 emissions, which can offset some of the carbon lost through deforestation. On the other hand, many encroached lands are used as pastures and, here, the woody plants are viewed as a threat to livestock productivity (Anadón et al., 2014). There is, however, also the view that many of the negative effects

associated with encroachment in pastures are caused by unsustainable grazing regimes. Eldridge and Soliveres (2014) argued that overgrazing has confounded the scientific community, leading it to believe that encroachment causes land degradation when in fact both are driven by unsustainable grazing regimes (Figure 1.3).

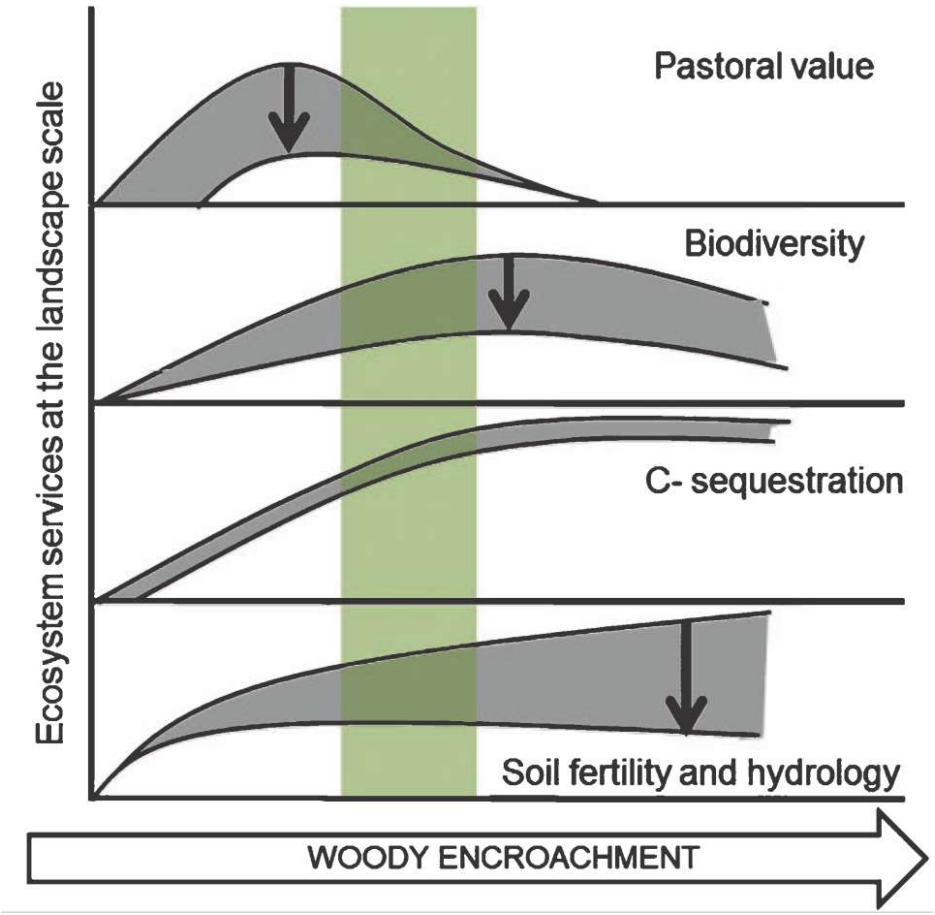

Figure 1.1 Different levels of woody cover optimizes different ecosystem services (from Eldridge & Soliveres (2014)). The pastoral value is maximized at a woody cover around 6-10%, and biodiversity is maximized at around 30-40%. The green stripe indicates a range suitable for all services. The downward arrows indicate the effect of grazing.

1.5 Remote sensing of woody vegetation properties and change in woody cover

The use of satellite data has become the key technology for large-scale assessment and monitoring of vegetation. Medium to coarse resolution multispectral products based on reflectance in the visible and near infrared bands, such as Landsat and MODIS, have proved valuable for estimating woody cover and change in woody cover at continental and global scales (Hansen et al., 2013). In systems with woody cover <~ 25%, it is however still difficult to accurately estimate woody cover from coarse resolution imagery due to the variable reflectance from soils and herbaceous vegetation (Gaughan et al., 2013; Gessner et al., 2013; Hansen et al., 2005). In addition, the commonly used Landsat and MODIS Vegetation Continuous Fields products are calibrated for trees above 5 m height and are therefore ill-suited for shrub-dominated landscapes (Hansen et al., 2005). One alternative that has been used is passive microwave data, which is sensitive to the water content in vegetation and therefore total biomass (Liu et al., 2013). By matching the intra-annual variation in water content to known phenological patterns in woody and herbaceous vegetation, it is possible to derive a proxy for woody cover. Brandt et al. (2017) used this methodology to estimate change in woody cover across the African continent and found an increasing trend in woody cover in drylands. This type of wall-to-wall analyses are important since most of the evidence for woody encroachment are based on field studies and aerial photography covering smaller areas. Small encroachment rates over large areas can have significant impacts on biomass accumulation numbers, but these can to a large degree be offset by more dramatic negative effects from localized disturbances (Campbell et al., 2012). Any large-scale inventory of the net change in woody cover must therefore sample a sufficiently large area to accurately capture both positive and negative fluxes.

There is also a risk for biased site selection. Heavily disturbed sites might be avoided, and some researchers might be drawn to areas where encroachment is known to occur.

Very high spatial resolution imagery (VHR; < 1m resolution), either aerial photography or satellite-based, have been used extensively for mapping change in woody cover. The high resolution results in a smaller proportion of mixed pixels, and individual trees are often clearly distinguishable. They are thus suitable for mapping woody vegetation also in areas with very sparse woody canopy and is sometimes used as validation data for estimates from coarser products (Bastin et al., 2017; Karlson et al., 2015). Additionally, the use of VHR imagery enables extracting more detailed information based on individual plants. The extraction of data on individual plants requires some kind of tree crown delineation algorithm. Several such algorithms have been proposed, many of which are based on the eCognition software (Bunting & Lucas, 2006; Rasmussen et al., 2011). If crown delineation is carried out successfully, it can enable estimation of the sizes of crowns, the density of trees, and the spatial pattern of trees in the landscape. These properties reveal information about the function of the ecosystem, the demography of the woody community, and the processes that shape it. If the pattern of woody plants is aggregated, we would expect that facilitative tree-tree interactions are at play. A regular tree pattern would indicate that competitive interactions dominate. Furthermore, analysis of how variation in woody properties relate to environmental variables, such as climate, soil type, and fire frequency, can expand our understanding of the processes that shape savannas.

1.6 Research Objectives

1.6.1 Analyzing vegetation structure and its spatial organization across environmental gradients

Several previous studies have analyzed variation in woody cover across African savannas and tried to link it to environmental factors (e.g. Bucini & Hanan, 2007; Good & Caylor, 2011). However, these studies used woody cover estimates from coarse-scale satellite products (MODIS) with limited reliability in mixed systems with low woody cover. My research uses sites extracted from VHR data sampled across African savannas for more accurate estimates of woody cover. The use of VHR, in combination with a crown delineation algorithm, further enables the derivation of crown density, crown sizes, and the level of spatial aggregation among woody plants. As far as I know, there has not been any previous analysis on how these woody vegetation properties vary across African savannas. By linking variation in woody cover, crown density, mean crown size, and level of aggregation to environmental factors (precipitation, soil texture, topography, and fire frequency), we expand our knowledge of the processes that shape woody communities in savanna systems.

Research question #1

Do vegetation structure and spatial patterns among woody plants vary predictably with climatic, edaphic, and topographic conditions in African savannas?

1.6.2 Assessing woody encroachment in African rangelands

On the African continent, local and regional studies in Southern Africa (Roques et al., 2001; Wigley et al., 2010), East Africa (Dalle et al., 2006), and West Africa

indicate a trend of increasing woody cover in African savannas. This trend is also supported by a meta-analysis by Stevens et al. (2017). These studies use a multitude of methods with varying temporal scales. There is, however, a need for continental studies that employ the same methodology on data from the same time period. This study estimates change in woody cover from samples in overlapping older (2002-2006) and newer (2011-2016) high resolution imagery. Estimates of change in woody cover is linked to environmental factors to clarify how dynamics in woody communities relate to water availability, fire frequency, livestock densities, soil texture and population density.

Research question #2

Is there a trend of ongoing woody encroachment in African savannas, and how are the dynamics of woody communities influenced by environmental conditions?

1.6.3 Simulating the processes that shape vegetation structure in African savannas

The first two research questions deal with observing variation in vegetation structure in relation to environmental factors. It is, however, not always straightforward to make the correct interpretations regarding the underlying ecosystem processes. Patterns we see in savanna landscapes emerge from both competitive and facilitative tree-tree and tree-grass interactions. Different mechanisms work over different spatial length-scales which also depend on the sizes of the trees. A spatially explicit vegetation model can be useful for explaining and visualizing how these mechanisms interact in shaping the observed landscapes. I therefore set out to construct a savanna landscape simulation model where the vegetation is influenced by the same factors that were examined in research question #1. The model mechanisms are based on a literature review with later adjustments and

calibrations based on observations from the remote sensing analysis. If it is possible to reproduce the observed trends, the model can serve to explain the underlying processes and highlight in which way they do or do not conform to our general understanding of savanna systems.

Research question #3

Is it possible to reproduce the observed trends in vegetation structure using a simulation model, and what are the main driving processes underlying the observed vegetation patterns according to model simulations?

1.7 Thesis structure

The thesis is organized into five chapters with chapters 2-4 covering the three research questions. Chapter 2 describes an analysis of woody vegetation structure using remote sensing (research question #1), chapter 3 studies woody cover change (research question #2), and chapter 4 presents an analysis using a savanna vegetation model (research question #3). The final chapter of the thesis synthesizes and discusses findings from the research.

1.8 References

Ahlström, A., Raupach, M. R., Schurgers, G., Smith, B., Arneth, A., Jung, M., . . . Jain, A. K. (2015). The dominant role of semi-arid ecosystems in the trend and variability of the land CO2 sink. *Science, 348*(6237), 895-899.

Anadón, J. D., Sala, O. E., Turner, B., & Bennett, E. M. (2014). Effect of woody-plant encroachment on livestock production in North and South America. *Proceedings of the National Academy of Sciences, 111*(35), 12948-12953.

Andela, N., Morton, D., Giglio, L., Chen, Y., van der Werf, G., Kasibhatla, P., . . . Kloster, S. (2017). A human-driven decline in global burned area. *Science, 356*(6345), 1356-1362.

Archer, S. R., Andersen, E. M., Predick, K. I., Schwinning, S., Steidl, R. J., & Woods, S. R. (2017). Woody plant encroachment: causes and consequences. In D. D. Briske (Ed.), *Rangeland Systems* (pp. 25-84): Springer.

Archibald, S., Lehmann, C. E., Gómez-Dans, J. L., & Bradstock, R. A. (2013). Defining pyromes and global syndromes of fire regimes. *Proceedings of the National Academy of Sciences, 110*(16), 6442-6447.

Archibald, S., Roy, D. P., van Wilgen, B. W., & Scholes, R. J. (2009). What limits fire? An examination of drivers of burnt area in southern Africa. *Global Change Biology, 15*(3), 613-630.

Bastin, J.-F., Berrahmouni, N., Grainger, A., Maniatis, D., Mollicone, D., Moore, R., . . . Abraham, E. M. (2017). The extent of forest in dryland biomes. *Science, 356*(6338), 635-638.

Belsky, A. J. (1994). Influences of trees on savanna productivity: tests of shade, nutrients, and tree-grass competition. *Ecology, 75*(4), 922-932.

Blaser, W. J., Sitters, J., Hart, S. P., Edwards, P. J., & Venterink, H. O. (2013). Facilitative or competitive effects of woody plants on understorey vegetation depend on N-fixation, canopy shape and rainfall. *Journal of Ecology*.

Brandt, M., Rasmussen, K., Peñuelas, J., Tian, F., Schurgers, G., Verger, A., . . . Fensholt, R. (2017). Human population growth offsets climate-driven increase in woody vegetation in sub-Saharan Africa. *Nature Ecology & Evolution, 1*, 0081.

Breshears, D. D., Nyhan, J. W., Heil, C. E., & Wilcox, B. P. (1998). Effects of woody plants on microclimate in a semiarid woodland: soil temperature and evaporation in canopy and intercanopy patches. *International Journal of Plant Sciences, 159*(6), 1010-1017.

Brooker, R. W., Maestre, F. T., Callaway, R. M., Lortie, C. L., Cavieres, L. A., Kunstler, G., . . . Anthelme, F. (2008). Facilitation in plant communities: the past, the present, and the future. *Journal of Ecology, 96*(1), 18-34.

Brown, J. R., & Carter, J. (1998). Spatial and temporal patterns of exotic shrub invasion in an Australian tropical grassland. *Landscape ecology, 13*(2), 93-102.

Bucini, G., & Hanan, N. P. (2007). A continental-scale analysis of tree cover in African savannas. *Global Ecology and Biogeography, 16*(5), 593-605.

Buitenwerf, R., Bond, W., Stevens, N., & Trollope, W. (2012). Increased tree densities in South African savannas:> 50 years of data suggests CO2 as a driver. *Global Change Biology*.

Bunting, P., & Lucas, R. (2006). The delineation of tree crowns in Australian mixed species forests using hyperspectral Compact Airborne Spectrographic Imager (CASI) data. *Remote Sensing of Environment, 101*(2), 230-248.

Campbell, J. L., Kennedy, R. E., Cohen, W. B., & Miller, R. F. (2012). Assessing the carbon consequences of western juniper (Juniperus occidentalis) encroachment across Oregon, USA. *Rangeland Ecology & Management, 65*(3), 223-231.

Castellano, M., & Valone, T. (2007). Livestock, soil compaction and water infiltration rate: evaluating a potential desertification recovery mechanism. *Journal of Arid Environments, 71*(1), 97-108.

Dalle, G., Maass, B. L., & Isselstein, J. (2006). Encroachment of woody plants and its impact on pastoral livestock production in the Borana lowlands, southern Oromia, Ethiopia. *African Journal of Ecology, 44*(2), 237-246.

De Boever, M., Gabriels, D., Ouessar, M., & Cornelis, W. (2016). Influence of Acacia Trees on Near-Surface Soil Hydraulic Properties in Arid Tunisia. *Land Degradation & Development, 27*(8), 1805-1812.

Deblauwe, V., Couteron, P., Lejeune, O., Bogaert, J., & Barbier, N. (2011). Environmental modulation of self-organized periodic vegetation patterns in Sudan. *Ecography, 34*(6), 990-1001.

Dohn, J., Dembélé, F., Karembé, M., Moustakas, A., Amévor, K. A., & Hanan, N. P. (2013). Tree effects on grass growth in savannas: competition, facilitation and the stress-gradient hypothesis. *Journal of Ecology, 101*(1), 202-209.

Eldridge, D., & Soliveres, S. (2014). Are shrubs really a sign of declining ecosystem function? Disentangling the myths and truths of woody encroachment in Australia. *Australian Journal of Botany*.

Eldridge, D. J., & Freudenberger, D. (2005). Ecosystem wicks: woodland trees enhance water infiltration in a fragmented agricultural landscape in eastern Australia. *Austral Ecology, 30*(3), 336-347.

February, E. C., Higgins, S. I., Bond, W. J., & Swemmer, L. (2013). Influence of competition and rainfall manipulation on the growth responses of savanna trees and grasses. *Ecology, 94*(5), 1155-1164.

Fensham, R., Fairfax, R., & Archer, S. (2005). Rainfall, land use and woody vegetation cover change in semi-arid Australian savanna. *Journal of Ecology, 93*(3), 596-606.

Fensham, R. J., Butler, D. W., & Foley, J. (2015). How does clay constrain woody biomass in drylands? *Global Ecology and Biogeography, 24*(8), 950-958.

Fernandez-Illescas, C. P., Porporato, A., Laio, F., & Rodriguez-Iturbe, I. (2001). The ecohydrological role of soil texture in a water-limited ecosystem. *Water Resources Research, 37*(12), 2863-2872. doi:10.1029/2000wr000121

Gaughan, A. E., Holdo, R. M., & Anderson, T. M. (2013). Using short-term MODIS time-series to quantify tree cover in a highly heterogeneous African savanna. *International Journal of Remote Sensing, 34*(19), 6865-6882.

Gessner, U., Machwitz, M., Conrad, C., & Dech, S. (2013). Estimating the fractional cover of growth forms and bare surface in savannas. A multi-resolution approach based on regression tree ensembles. *Remote Sensing of Environment, 129*, 90-102.

Gillson, L. (2004). Evidence of hierarchical patch dynamics in an East African savanna? *Landscape ecology, 19*(8), 883-894.

Goldstein, G., Meinzer, F. C., Bucci, S. J., Scholz, F. G., Franco, A. C., & Hoffmann, W. A. (2008). Water economy of Neotropical savanna trees: six paradigms revisited. *Tree Physiology, 28*(3), 395-404.

González-Roglich, M., Swenson, J. J., Villarreal, D., Jobbágy, E. G., & Jackson, R. B. (2015). Woody Plant-Cover Dynamics in Argentine Savannas from the 1880s to 2000s: The Interplay of Encroachment and Agriculture Conversion at Varying Scales. *Ecosystems*, 1-12.

Good, S. P., & Caylor, K. K. (2011). Climatological determinants of woody cover in Africa. *Proceedings of the National Academy of Sciences, 108*(12), 4902-4907.

Hansen, M. C., Potapov, P. V., Moore, R., Hancher, M., Turubanova, S., Tyukavina, A., . . . Loveland, T. (2013). High-resolution global maps of 21st-century forest cover change. *Science, 342*(6160), 850-853.

Hansen, M. C., Townshend, J. R., DeFries, R. S., & Carroll, M. (2005). Estimation of tree cover using MODIS data at global, continental and regional/local scales. *International Journal of Remote Sensing, 26*(19), 4359-4380.

He, Q., Bertness, M. D., & Altieri, A. H. (2013). Global shifts towards positive species interactions with increasing environmental stress. *Ecology letters*.

Higgins, S. I., & Scheiter, S. (2012). Atmospheric CO2 forces abrupt vegetation shifts locally, but not globally. *Nature, 488*(7410), 209-212.

Hirota, M., Holmgren, M., Van Nes, E. H., & Scheffer, M. (2011). Global resilience of tropical forest and savanna to critical transitions. *Science, 334*(6053), 232-235.

Hoffmann, W. A. (1996). The effects of fire and cover on seedling establishment in a neotropical savanna. *Journal of Ecology*, 383-393.

Hoffmann, W. A., Geiger, E. L., Gotsch, S. G., Rossatto, D. R., Silva, L. C., Lau, O. L., . . . Franco, A. C. (2012). Ecological thresholds at the savanna-forest boundary: how plant traits, resources and fire govern the distribution of tropical biomes. *Ecology letters*.

Holdo, R. M., & Brocato, E. R. (2015). Tree–grass competition varies across select savanna tree species: a potential role for rooting depth. *Plant Ecology, 216*(4), 577-588.

Holmgren, M., Gómez-Aparicio, L., Quero, J. L., & Valladares, F. (2012). Non-linear effects of drought under shade: reconciling physiological and ecological models in plant communities. *Oecologia, 169*(2), 293-305.

Karlson, M., Ostwald, M., Reese, H., Sanou, J., Tankoano, B., & Mattsson, E. (2015). Mapping tree canopy cover and aboveground biomass in Sudano-Sahelian woodlands using Landsat 8 and random forest. *Remote Sensing, 7*(8), 10017-10041.

Körner, C. (2006). Plant CO2 responses: an issue of definition, time and resource supply. *New Phytologist, 172*(3), 393-411.

Kulmatiski, A., & Beard, K. H. (2013). Root niche partitioning among grasses, saplings, and trees measured using a tracer technique. *Oecologia, 171*(1), 25-37.

Lane, D. R., Coffin, D. P., & Lauenroth, W. K. (1998). Effects of soil texture and precipitation on above-ground net primary productivity and vegetation structure across the Central Grassland region of the United States. *Journal of Vegetation Science, 9*(2), 239-250.

Lehmann, C. E., Archibald, S. A., Hoffmann, W. A., & Bond, W. J. (2011). Deciphering the distribution of the savanna biome. *New Phytologist, 191*(1), 197-209.

Liu, Y. Y., Dijk, A. I., McCabe, M. F., Evans, J. P., & Jeu, R. A. (2013). Global vegetation biomass change (1988–2008) and attribution to environmental and human drivers. *Global Ecology and Biogeography, 22*(6), 692-705.

Ludwig, F., de Kroon, H., Berendse, F., & Prins, H. H. (2004). The influence of savanna trees on nutrient, water and light availability and the understorey vegetation. *Plant Ecology, 170*(1), 93-105.

Lunt, I. D., Winsemius, L. M., McDonald, S. P., Morgan, J. W., & Dehaan, R. L. (2010). How widespread is woody plant encroachment in temperate Australia? Changes in woody vegetation cover in lowland woodland and coastal ecosystems in Victoria from 1989 to 2005. *Journal of Biogeography, 37*(4), 722-732.

Marlon, J. R., Bartlein, P. J., Carcaillet, C., Gavin, D. G., Harrison, S. P., Higuera, P. E., . . . Prentice, I. (2008). Climate and human influences on global biomass burning over the past two millennia. *Nature Geoscience, 1*(10), 697-702.

Morgan, J. A., Milchunas, D. G., LeCain, D. R., West, M., & Mosier, A. R. (2007). Carbon dioxide enrichment alters plant community structure and accelerates shrub growth

in the shortgrass steppe. *Proceedings of the National Academy of Sciences, 104*(37), 14724-14729.

Moustakas, A., Kunin, W. E., Cameron, T. C., & Sankaran, M. (2013). Facilitation or competition? Tree effects on grass biomass across a precipitation gradient. *PloS one, 8*(2), e57025.

Niemeyer, R., Fremier, A., Heinse, R., Chávez, W., & DeClerck, F. (2014). Woody vegetation increases saturated hydraulic conductivity in dry tropical Nicaragua. *Vadose Zone Journal, 13*(1).

Noy-Meir, I. (1973). Desert ecosystems: environment and producers. *Annual review of Ecology and Systematics, 4*, 25-51.

Owensby, C., Ham, J., Knapp, A., Bremer, D., & Auen, L. (1997). Water vapour fluxes and their impact under elevated CO2 in a C4-tallgrass prairie. *Global Change Biology, 3*(3), 189-195.

Penny, G. G., Daniels, K. E., & Thompson, S. E. (2013). Local properties of patterned vegetation: quantifying endogenous and exogenous effects. *Philosophical Transactions of the Royal Society of London A: Mathematical, Physical and Engineering Sciences, 371*(2004), 20120359.

Poorter, H., & Navas, M. L. (2003). Plant growth and competition at elevated CO2: on winners, losers and functional groups. *New Phytologist, 157*(2), 175-198.

Pueyo, Y., Moret-Fernández, D., Saiz, H., Bueno, C., & Alados, C. (2013). Relationships Between Plant Spatial Patterns, Water Infiltration Capacity, and Plant Community Composition in Semi-arid Mediterranean Ecosystems Along Stress Gradients. *Ecosystems*, 1-15.

Rasmussen, M. O., Göttsche, F.-M., Diop, D., Mbow, C., Olesen, F.-S., Fensholt, R., & Sandholt, I. (2011). Tree survey and allometric models for tiger bush in northern Senegal and comparison with tree parameters derived from high resolution satellite data. *International Journal of Applied Earth Observation and Geoinformation, 13*(4), 517-527.

Resco de Dios, V. R., Weltzin, J. F., Sun, W., Huxman, T. E., & Williams, D. G. (2014). Transitions from grassland to savanna under drought through passive facilitation by grasses. *Journal of Vegetation Science*.

Riginos, C. (2009). Grass competition suppresses savanna tree growth across multiple demographic stages. *Ecology, 90*(2), 335-340.

Robinson, E. A., Ryan, G. D., & Newman, J. A. (2012). A meta-analytical review of the effects of elevated CO2 on plant–arthropod interactions highlights the importance of interacting environmental and biological variables. *New Phytologist, 194*(2), 321-336.

Rolo, V., López-Díaz, M., & Moreno, G. (2012). Shrubs affect soil nutrients availability with contrasting consequences for pasture understory and tree overstory production and nutrient status in Mediterranean grazed open woodlands. *Nutrient Cycling in Agroecosystems, 93*(1), 89-102.

Roques, K., O'connor, T., & Watkinson, A. (2001). Dynamics of shrub encroachment in an African savanna: relative influences of fire, herbivory, rainfall and density dependence. *Journal of Applied Ecology, 38*(2), 268-280.

Sankaran, M., Hanan, N. P., Scholes, R. J., Ratnam, J., Augustine, D. J., Cade, B. S., . . . Ludwig, F. (2005). Determinants of woody cover in African savannas. *Nature, 438*(7069), 846-849.

Sankaran, M., Ratnam, J., & Hanan, N. (2008). Woody cover in African savannas: the role of resources, fire and herbivory. *Global Ecology and Biogeography, 17*(2), 236-245.

Schenk, H. J., & Jackson, R. B. (2002). Rooting depths, lateral root spreads and below-ground/above-ground allometries of plants in water-limited ecosystems. *Journal of Ecology, 90*(3), 480-494.

Scholes, R. (2003). Convex relationships in ecosystems containing mixtures of trees and grass. *Environmental and resource economics, 26*(4), 559-574.

Scholes, R., & Archer, S. (1997). Tree-grass interactions in savannas. *Annual review of Ecology and Systematics, 28*, 517-544.

Schwinning, S., Sala, O. E., Loik, M. E., & Ehleringer, J. R. (2004). Thresholds, memory, and seasonality: understanding pulse dynamics in arid/semi-arid ecosystems. *Oecologia, 141*(2), 191-193.

Staver, A. C., Archibald, S., & Levin, S. A. (2011a). The global extent and determinants of savanna and forest as alternative biome states. *Science, 334*(6053), 230-232.

Staver, A. C., Archibald, S., & Levin, S. A. (2011b). Tree cover in sub-Saharan Africa: Rainfall and fire constrain forest and savanna as alternative stable states. *Ecology, 92*(5), 1063-1072.

Stevens, N., Erasmus, B., Archibald, S., & Bond, W. (2016). Woody encroachment over 70 years in South African savannahs: overgrazing, global change or extinction aftershock? *Phil. Trans. R. Soc. B, 371*(1703), 20150437.

Stevens, N., Lehmann, C. E., Murphy, B. P., & Durigan, G. (2017). Savanna woody encroachment is widespread across three continents. *Global Change Biology, 23*(1), 235-244.

Thompson, S., Harman, C., Heine, P., & Katul, G. (2010). Vegetation-infiltration relationships across climatic and soil type gradients. *Journal of Geophysical Research: Biogeosciences (2005–2012), 115*(G2).

Van Auken, O. (2009). Causes and consequences of woody plant encroachment into western North American grasslands. *Journal of Environmental Management, 90*(10), 2931-2942.

Wang, D., Heckathorn, S. A., Wang, X., & Philpott, S. M. (2012). A meta-analysis of plant physiological and growth responses to temperature and elevated CO2. *Oecologia, 169*(1), 1-13.

Ward, D., & Esler, K. J. (2011). What are the effects of substrate and grass removal on recruitment of Acacia mellifera seedlings in a semi-arid environment? *Plant Ecology, 212*(2), 245-250.

Wigley, B. J., Bond, W. J., & Hoffman, M. (2010). Thicket expansion in a South African savanna under divergent land use: local vs. global drivers? *Global Change Biology, 16*(3), 964-976.

Williams, R., Duff, G., Bowman, D., & Cook, G. (1996). Variation in the composition and structure of tropical savannas as a function of rainfall and soil texture along a large-scale climatic gradient in the Northern Territory, Australia. *Journal of Biogeography, 23*(6), 747-756.

2 PATTERNS IN WOODY VEGETATION STRUCTURE ACROSS AFRICAN SAVANNAS

Axelsson, C. R., & Hanan, N. P. (2017). Patterns in woody vegetation structure across African savannas. *Biogeosciences, 14*(13), 3239.

Abstract

Vegetation structure in water-limited systems is to a large degree controlled by ecohydrological processes, including mean annual precipitation (MAP) modulated by the characteristics of precipitation and geomorphology that collectively determine how rainfall is distributed vertically into soils or horizontally in the landscape. We anticipate that woody canopy cover, crown density, crown size, and the level of spatial aggregation among woody plants in the landscape, will vary across environmental gradients. A high level of woody plant aggregation is most distinct in periodic vegetation patterns (PVPs), which emerge as a result of ecohydrological processes such as runoff generation and increased infiltration close to plants. Similar, albeit weaker, forces may influence the spatial distribution of woody plants elsewhere in savannas. Exploring these trends can extend our knowledge of how semi-arid vegetation structure is constrained by rainfall regime, soil type, topography, and disturbance processes such as fire. Using high spatial resolution imagery, a flexible classification framework, and a crown delineation method, we extracted woody vegetation properties from 876 sites spread over African savannas. At each site, we estimated woody cover, mean crown size, crown density, and the degree of aggregation among woody plants. This enabled us to elucidate the effects of rainfall regimes (MAP and seasonality), soil

texture, slope, and fire frequency on woody vegetation properties. We found that previously documented increases in woody cover with rainfall is more consistently a result of increasing crown size than increasing density of woody plants. Along a gradient of mean annual precipitation from the driest (<200 mm/yr) to the wettest (1200-1400 mm/yr) end, mean estimates of crown size, crown density, and woody cover increased by 233 %, 73 %, and 491 % respectively. We also found a unimodal relationship between mean crown size and sand content suggesting that maximal savanna tree-sizes do not occur in either coarse sands or heavy clays. When examining the occurrence of PVPs, we found that the same factors that contribute to the formation of PVPs also correlate with higher levels of woody plant aggregation elsewhere in savannas and that rainfall seasonality plays a key role for the underlying processes.

2.1 Introduction

African savannas are complex tree-grass systems controlled by combinations of climate, soil, and disturbance processes such as fire and herbivory (Sankaran et al., 2008). In dry savannas, water availability determines the establishment, growth and survival of plants and competitive plant traits are often of a water saving nature (Chesson et al., 2004; Pillay & Ward, 2014). Abiotic environmental factors, such as the rainfall regime, soil type, and topography, impact ecohydrological processes by controlling infiltration rates, runoff generation, and available water capacity, which in turn impact the growth and survival of woody plants in the landscape (Ludwig et al., 2005). Climate, both rainfall patterns and temperatures, could change in many parts of Africa (Gan et al., 2016), and the effect on vegetation will depend on how those pressures interact with other abiotic and biotic factors. In addition to ecohydrological factors, savannas are heavily influenced

by the frequency and intensity of fires (Bond, 2008), as well as herbivore regimes (Sankaran et al., 2008), which often combine to suppress woody cover to levels well below its climatic potential (Sankaran et al., 2005). A thorough understanding of the underlying processes that influence savanna vegetation structure is key to assessing the future resilience and productivity of these ecosystems.

Across environmental gradients we expect to see variation in woody vegetation properties, including individual-level characteristics (mean crown size) and population-level characteristics (crown density, woody cover, and the spatial distribution of plants in the landscape). Woody cover is fundamentally a function of crown sizes and crown density and by studying these components individually, it is possible to attain important insight into the function of ecosystems and what ecosystem services they provide. Two landscapes with similar woody cover but different sizes of individual trees will sequester different amounts of carbon (Shackleton & Scholes, 2011), harbor different fauna (Riginos & Grace, 2008), and differ in biogeochemical dynamics (Veldhuis, Hulshof, et al., 2016). The level of spatial aggregation among woody plants can help us understand facilitative and competetive processes determining survival of seedlings and saplings. Woody plants increase water infiltration and local accumulation of soil and nutrient resources, as well as altering sub-canopy microclimates (Barbier et al., 2014; Dohn et al., 2016; Gómez-Aparicio et al., 2008). These short-range facilitative effects usually operate at spatial scales of a few meters, but may increase the degree of aggregation among woody plants at larger scales (Scanlon et al., 2007; Xu et al., 2015). Overland flows of water can be especially effective at redistributing resources over longer distances, in some conditions leading to the emergence of periodic vegetation patterns (PVPs; Rietkerk & van de Koppel, 2008;

Valentin et al., 1999). Contrasting infiltration rates between bare and vegetated patches lead to redistribution of water and soil resources which reinforces an organized pattern. While soil texture type has been weakly associated with the occurrence of PVPs (Deblauwe et al., 2008), the impervious conditions of the bare patches are generally caused by shallow soil depths, hardpans, or soil crusts (McDonald et al., 2009). On flat ground, PVPs take the form of spotted, labyrinthine, or gapped patterns depending on soil water availability. On a gentle slope, they develop into vegetated bands that run parallel to contour lines (Valentin et al., 1999). While PVPs have been studied extensively, their formative processes are seldom linked to ecohydrological processes in other types of savanna landscapes.

To analyze how woody cover, crown size, crown density and the spatial pattern of trees vary with environmental gradients, we need to map the landscape at the level of individual trees. Satellite-based high spatial resolution (HSR; <4 m) sensors have the necessary degree of detail for this task. Papers delineating individual trees from HSR in African savannas have shown promising results (Karlson et al., 2014; Rasmussen et al., 2011), but these studies are generally restricted to small geographical areas. In this paper we present an analysis of woody properties sampled across the diverse water-limited savannas of Africa using a combination of WorldView, Quickbird and GeoEye satellite data ($\leq$ 0.61 m resolution) from 876 sites. The woody components of the sites were classified and delineated into individual tree crowns, from which we derived estimates of mean crown size, crown density, woody cover, and the degree of aggregation among woody plants. We then analyzed how these woody vegetation properties vary with rainfall regime (MAP and seasonality), soil texture, slope, and fire frequency using a boosted regression tree (BRTs) approach. The dataset contains sites from several areas with PVPs

and we also investigated the environmental factors associated with the occurrence of highly organized periodic patterns.

2.2 Data and Methodology

Our methodological approach included a flexible classification approach based on unsupervised classification, tree crown delineation, and boosted regression tree analysis (Figure 2.1).

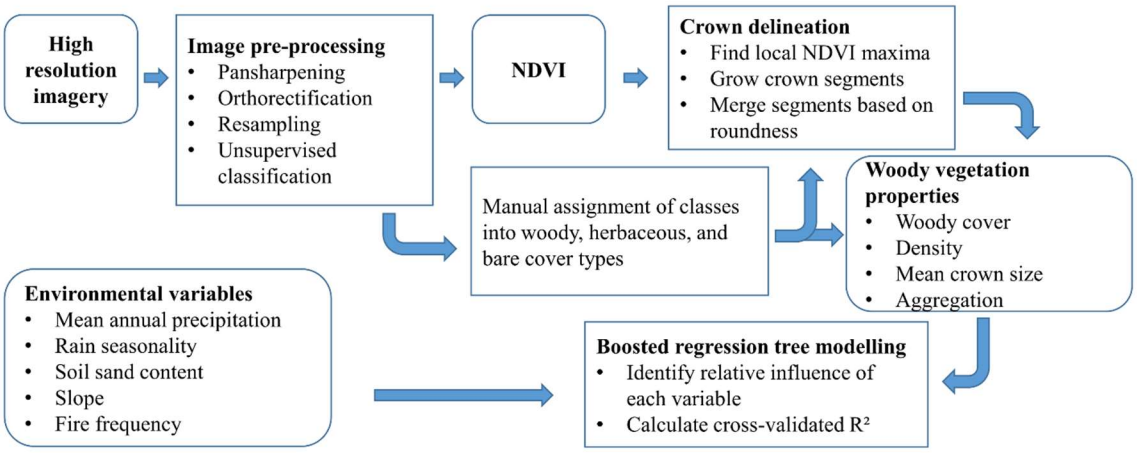

Figure 2.1 Methodological workflow showing datasets (rounded boxes) and methods (square boxes) used to estimate woody vegetation structure and analyze relationships with environmental variables.

2.2.1 Satellite data and sampling strategy

We used data from WorldView-2, WorldView-3, GeoEye-1, and Quickbird-2 satellites, with varying ground resolutions (≤0.61 m for panchromatic data and ≤2.44 m for the multispectral bands). The sampling frame for the analysis was sub-Saharan African savannas with a minimum of anthropogenic disturbances. When acquiring data, we adopted

a sampling strategy with imagery distributed across Africa in rangelands as defined by the Anthropogenic biomes product (Ellis & Ramankutty, 2008) (Figure 2.2), which helped us identify and avoid areas with high anthropogenic impact.Focus was on selecting recent images (2011-2016) when trees were in full leaf (generally in mid to late growing season) and avoid areas of high human population density. The selection process was also influenced by a second study on change detection where we needed overlapping imagery from two points in time. We excluded images with view angles >25° or cloud cover >20%. Following these criteria, we acquired imagery in 48 regions, within which we sampled 240 x 240 m sites for use in the analysis. Within-image site-selection followed a systematic sampling approach and was guided by a 0.04° longitude/latitude grid which served as a base for site locations. In some cases, however, the location of sites was adjusted to avoid areas where vegetation structure was clearly influenced by topography (rocky outcrops, streams, and gullies), or anthropogenic activity (settlements, roads, active or fallow agriculture). Sample locations influenced by topographic or anthropogenic effects were either moved to a nearby location or eliminated from the analysis. During the later classification process, we found that some sites could not be classified reliably due to either low image quality, or a lack of contrast between trees and the herbaceous background. These sites were also eliminated. In the end, we ended up with a total of 876 sites (Figure 2.2).

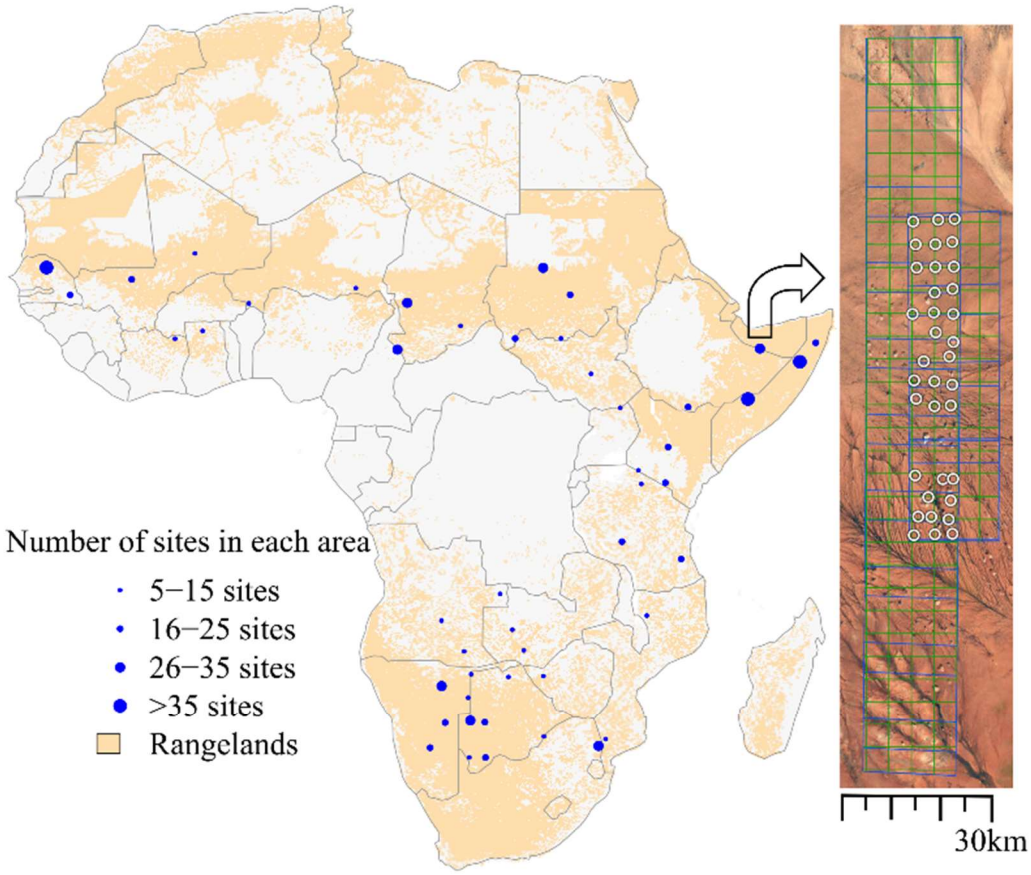

Figure 2.2 Location of the 48 study areas, containing 876 study sites, spread out over African rangelands. The rangeland areas are from the Anthropogenic biomes product (Ellis & Ramankutty, 2008), and symbol size for study areas is proportional to the number of study sites in each. The map to the right shows a study area on the border between Somalia and Ethiopia and exemplifies the sampling strategy for study sites (white rings). The placement of sites was guided by a 0.04° longitude/latitude grid (green lines) in areas with overlapping older and newer satellite imagery (blue lines).

2.2.2 Preprocessing and classification of satellite data

Once the locations of sites were established, each site was preprocessed using IDL scripts in ENVI 5.2. This included Gram-Schmidt pan-sharpening of the blue, green, red, and infrared bands, and orthorectification using embedded RPC-information and an SRTM v2 DEM (Farr et al., 2007). The orthorectified images were resampled using a nearest neighbor method to a standard 0.6 m ground resolution creating a 400 x 400 pixel (240 x 240 m) image centered over each site. We then ran unsupervised ISODATA classification on the pan-sharpened images to create 18 spectrally different classes, which were smoothed using a kernel size of 3 pixels. Following preprocessing, the 18 spectrally distinct classes were manually assigned to woody, herbaceous and bare cover classes using a custom-built software in R. The software includes several tools to facilitate accurate and efficient classifications, including a tool to split a class into two spectrally different classes if it appears to contain more than one land cover type, and a tool to remove minor inconsistencies such as a single herbaceous pixel in the middle of a tree crown.

2.2.3 Crown delineation

After the 240 x 240 m image constituting each study site was classified into woody, herbaceous, and bare soil components, a crown delineation process was run to aggregate woody pixels into individual tree crown polygons. The method uses the classified woody layer (as the “forest mask”) together with NDVI from the pansharpened imagery and is based on the assumption that woody plants have higher NDVI at the center of the crown, where branches and leaves are dense, and declining NDVI towards the outer edges of the crown where branch and leaf density tend to be lower. The first step in the delineation process is to identify local maxima in NDVI. If the center pixel in the 3 x 3

pixel neighborhood is a maximum, it is given a unique segment ID and serves as a seed for a crown segment. The second step involves iterative growth of segments in all directions, but only to woody pixels with lower NDVI than the neighboring segment pixel. In the third step, neighboring segments are merged if the resulting crown is rounder than both of the two neighboring segments. Since the merging criteria can be fulfilled for several segment neighbors, a segment is only merged once in each iteration and the merging order is based on the roundness of the resulting segments. Here, roundness is calculated as the area of the segment divided by the area of a minimum bounding circle. Round segments thereby get values close to one, while more complex segment forms have lower roundness. This step is re-iterated until rounder segments cannot be formed (Figure 2.3). We also added a maximum crown size limit so that segments are not merged if the resulting crown is larger than the area of a circle with diameter 40 m, as trees larger than this size are very rare throughout the sampling frame. The method was implemented in C code and has several traits in common with previous delineation methods (e.g. Bunting & Lucas, 2006; Culvenor, 2002; Karlson et al., 2014; Pouliot & King, 2005) which generally were developed and tuned for a specific landscape type. The method by Bunting & Lucas (2006) is perhaps the most similar since it also identifies segment seeds using local maxima of a vegetation index, iteratively expands to neighboring pixels, and has iterations of segment merging. That method was developed using the eCognition software and has some additional steps not included in our method, such as post-splitting of segments and the initial generation of a forest mask. In our methodology, the forest mask (woody areas) was already established using the semi-automatic approach described above.

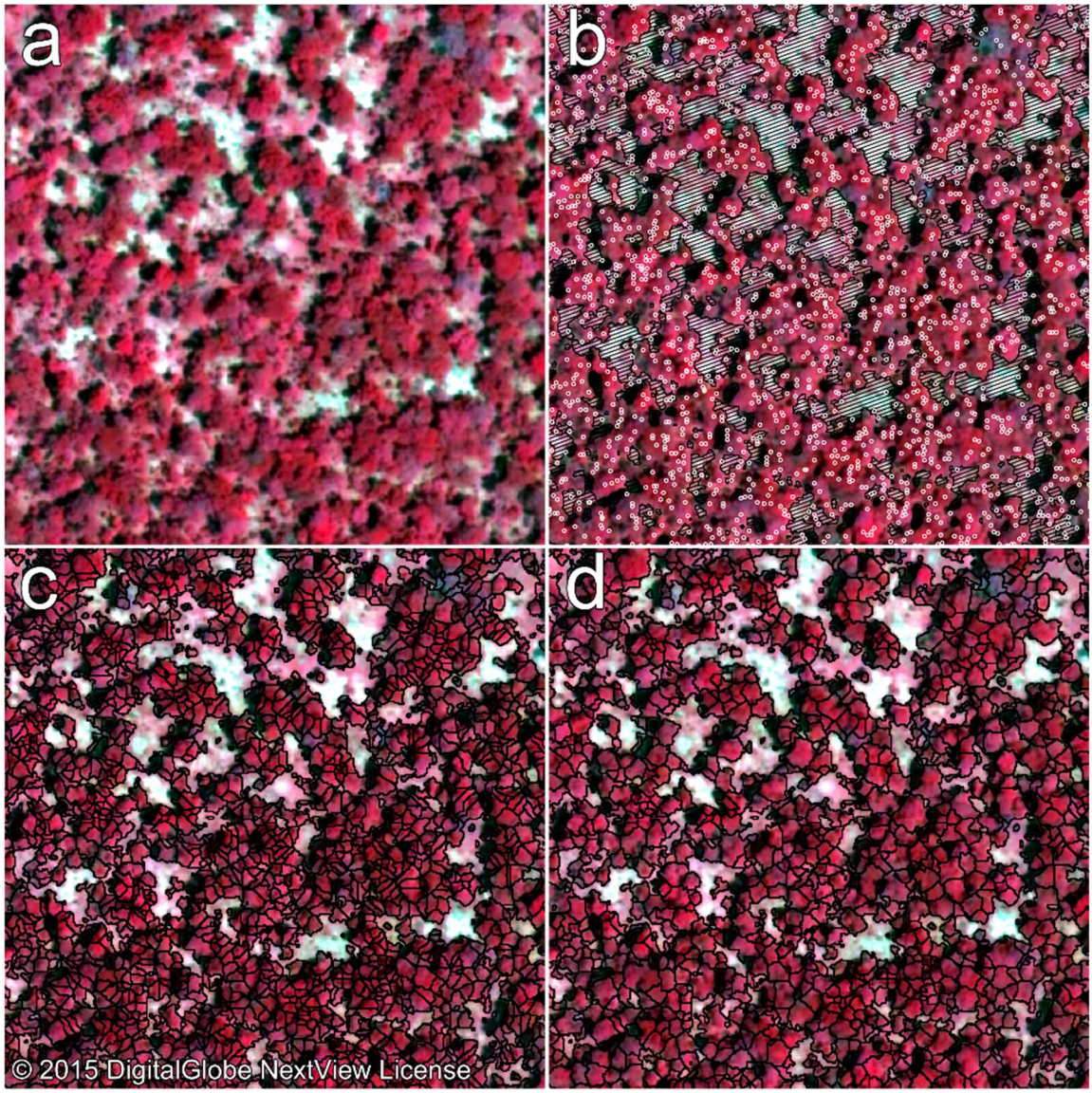

Figure 2.3 Crown delineation steps for a woodland site in Zambia. (a) Pan-sharpened false-color image, (b) Local NDVI maxima as white points and the non-woody areas shown as striped polygons, (c) Crown segments before merging, and (d) and the final crown polygons following crown merging.

The delineated crowns played an important role in this analysis because they were used for calculating crown density, crown sizes, and woody plant aggregation. Our analysis of the derived woody properties did not focus on absolute numbers but on how

they vary across environmental gradients under the assumption that errors were propagated consistently over space. A visual inspection of all sites indicated that the crown delineation consistently produced crown layers that looked realistic when overlaying the imagery. We recognize, however, that it is extremely difficult to accurately delineate tree canopies in areas where crowns overlap. In some cases, a large tree crown may be falsely divided into small canopies or a cluster of shrubs may be grouped together into one crown (Rasmussen et al., 2011). It is important that the rate of falsely divided and falsely grouped crowns is balanced since excessive division of large trees into smaller leads to higher estimates of both crown density and aggregation. We evaluated the performance of the classification and delineation methodology using field data from sites in Kenya (Appendix A). This showed that crowns smaller than ~2 m diameter were not reliably detected in the imagery. The validation analysis resulted in relatively strong agreement between estimated and field measured woody properties with R-squares of 0.69 (mean crown size), 0.82 (crown density), and 0.77 (woody cover) when crowns smaller than 2 m diameter were removed from the field data set. We did, however, find that particularly large and spread-out crowns were subdivided, leading to underestimation of crown sizes and overestimation of crown density.

2.2.4 Environmental variables

The rainfall data were extracted from the Tropical Rainfall Measuring Mission (TRMM) 3B42 v7 product (0.25° x 0.25°) for the years 1998-2015 (Huffman et al., 2007). In addition to mean annual precipitation (MAP), we used rainfall seasonality represented by the coefficient of variation of mean monthly rainfalls. For soil data we used the sand

content in the top soil layer (0-5cm) from the ISRIC/AfSIS 250 meter soil property maps of Africa (Hengl et al., 2015). To represent topography we used slope (%) derived from SRTM v2 (3 arc-seconds) elevation data (Farr et al., 2007). Fire frequency (fire events/year) was calculated using the MODIS MCD64A1 collection 5.1 burned area product (500m resolution) for the years 2001-2015 (Giglio et al., 2009). To avoid registering fires identified in adjacent months as separate fires, we counted fire events in consecutive months as a single fire. The extraction of raster values was based on nearest neighbor to the center point of each site in all cases except the TRMM data, for which we used bilinear interpolation due to its coarse resolution.

2.2.5 Statistical analysis of woody vegetation properties and the local environment

We derived four statistical properties of woody vegetation from each image: mean crown size (m^2), density (crowns/ha), woody cover (%), and spatial aggregation of woody plants. Aggregation was calculated from the center points of the crown polygons. We used Ripley's K transformed to Besag's L-function to estimate aggregation at distances from 1 to 60 m (Besag, 1977; Ripley, 1977). Calculations were made using the spatstat R package with isotropic edge correction. The L-function was normalized by subtracting the distance so that 0 represents a random pattern and positive values indicate aggregation. For the analysis, we used the L-function at 20 m to represent aggregation as this distance is longer than the typical diameter of savanna trees and within length-scales of facilitative tree-tree effects. When analyzing crown sizes and aggregation, we excluded all sites with a crown density of 10 crowns/ha or less due to their low sample size for these metrics. We used boosted regression trees (BRT, in the dismo R package) to relate woody properties to

the environmental variables. Its advantages include the ability to model non-linear relationships and to identify interactions between variables (Elith et al., 2008). When generating the BRTs, we used family = gaussian, tree complexity = 3, learning rate = 0.01, and bag fraction = 0.5 as model parameters. R^2, calculated through 10-fold cross-validation, was used for evaluating the strength of the relationships.

The dataset includes several sites with PVPs, which often are treated as a special case because of their striking appearance (Figure 2.4). It is of interest to examine the environmental conditions associated with the occurrence of PVPs as well as those associated with aggregated woody populations in savannas without PVPs. We therefore separated sites with periodic vegetation from the rest and generated an additional set of models. The category with periodic vegetation contained 149 sites situated in Somalia, Senegal, Chad, Mali, Niger, Namibia, and Sudan. The identification was based on visual inspection, and all sites with traits of periodic patterning (spotted, labyrinthine, gapped or banded) were put in the PVP category. We created one model for predicting aggregation among all sites, one for predicting aggregation among sites with no PVPs, and a third for predicting the occurrence PVPs. In the latter model, all PVP sites were given the value 1 and the rest 0, and the BRT family parameter was set to “bernoulli”, appropriate for binomially distributed data.

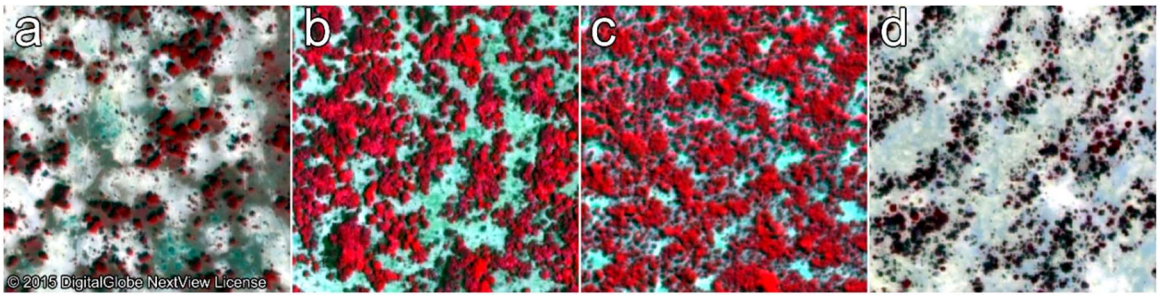

Figure 2.4 False-color imagery of periodic vegetation patterns identified among the sites: (a) spotted pattern in Senegal, (b) labyrinthine pattern in Mali, (c) gapped pattern in Niger, (d) banded pattern in Somalia. Sites with PVPs were identified visually by the authors.

2.3 Results

We started by calculating frequency distributions of the four woody properties divided into three rainfall categories (Figure 2.5). The more arid savannas (<400 mm/year) typically featured smaller crown sizes, lower crown density and woody cover, and higher levels of aggregation than sites in the wetter categories.

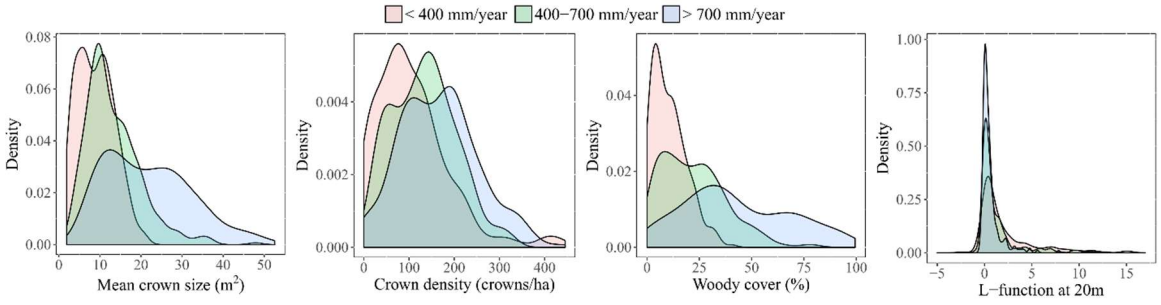

Figure 2.5 Frequency distributions of mean crown size, crown density, woody cover and aggregation calculated for different MAP ranges.

2.3.1 Mean crown size, density, and woody cover

Boxplots with woody properties divided into MAP bins (Figure 2.6) show that woody cover and crown sizes increased more sharply with increasing rainfall than crown densities. Along the rainfall gradient from the driest (<200 mm/yr) to the wettest (1200-1400 mm/yr) end, mean estimates of crown size, crown density, and woody cover increased

by 233 %, 73 %, and 491 % respectively. The BRT models for woody cover and mean crown size had high cross-validated R^2 (0.73 and 0.68) and the same environmental factors that control woody cover also had a large influence over crown sizes (Table 2.1). In both cases, MAP had the largest relative influence followed by rain seasonality. While MAP had a clear positive influence on both woody cover and crown sizes, it was more difficult to interpret the influence of rain seasonality (Figure 2.7). Woody cover had a weak unimodal response to sand content, that was driven by the relationship between crown size and sand content (Figure 2.7). Fire frequency resulted in weak negative responses on all woody properties.

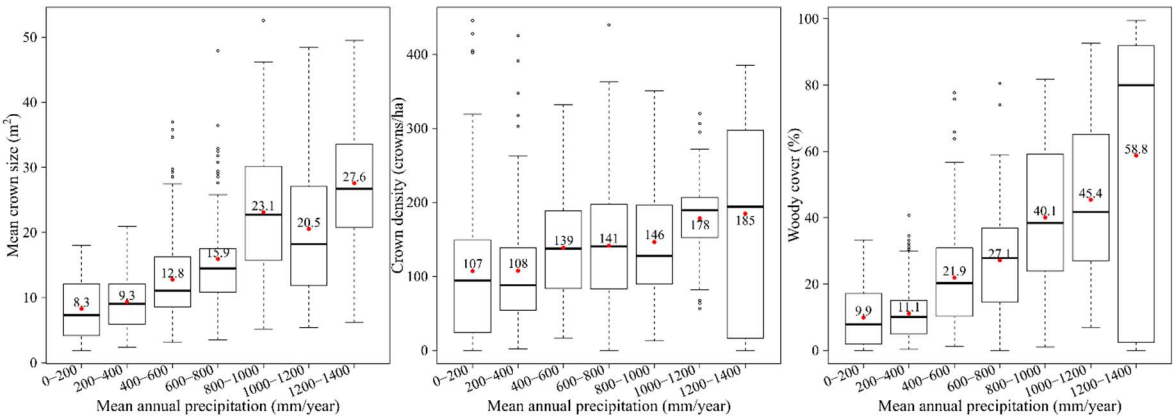

Figure 2.6 Boxplots of estimates of crown size, crown density, and woody cover along a rainfall gradient. Red points denote the means. Between the driest (<200 mm/yr) and wettest (1200-1400 mm/yr) categories, mean estimates of crown size, crown density, and woody cover increased by 233 %, 73 %, and 491 % respectively.

Table 2.1 Relative influence of each environmental variable and the cross-validated R^2 from the BRT models when modeling woody cover, crown density, and mean crown size.

Variables	Mean Crown Size	Crown density	Woody cover

MAP	45%	33%	47%
Rain seasonality	21%	37%	23%
Sand content	17%	13%	10%
Slope	11%	13%	10%
Fire frequency	6%	4%	11%
Cross-validated R^2	0.68	0.49	0.73

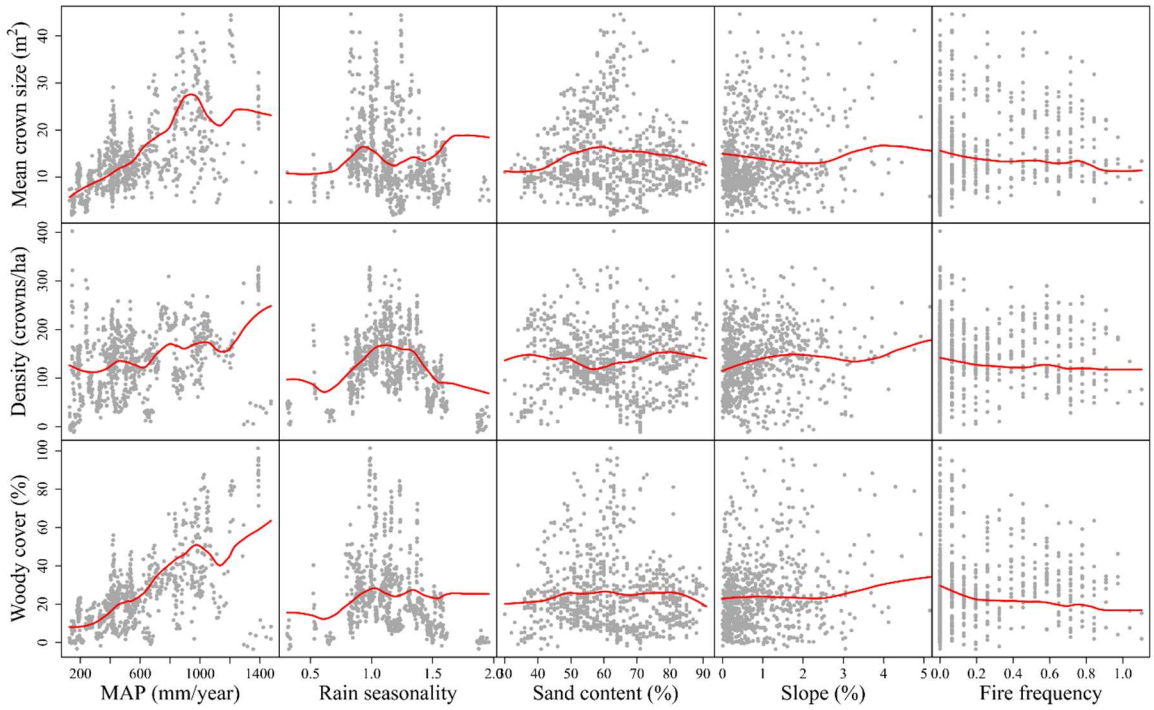

Figure 2.7 Modeled BRT responses ("partial dependencies") of woody canopy properties to each environmental variable when accounting for the average effect of the other four variables. The red lines are smoothed representations of the responses, with fitted values (model predictions based on the original data) for each of the 876 sites shown as grey dots. The x-axis for the slope predictor was truncated at 5% to highlight the response in the bulk of the data.

2.3.2 Woody plant aggregation

Our estimates of aggregation were based on the L-statistic (at 20 m) minus the distance, meaning positive values signal aggregated woody populations and negative values indicate dispersed populations (Figure 2.8). The large majority (82 %) of sites had positive values, indicating a rarity of dispersed woody populations in African savannas. There was little difference in the results for aggregation when sites with periodic patterns were included or not (Table 2.2). Higher levels of aggregation were generally associated with high seasonality, low MAP, fine-textured soils, and relatively flat terrain. These factors were also influential in determining the areas where periodic vegetation patterns occur. In fact, periodic patterns were absent in areas with MAP above 750mm, rain seasonality below 1.1, a sand content above 75%, and slopes steeper than 3.8%.

Table 2.2 Relative influence of each environmental variable and the cross-validated R^2 from the BRT models when modeling woody aggregation (L-function at 20 m) and occurrence of PVPs. In the latter model, all sites with PVPs were given the value 1 and the rest the value 0.

Variables	Aggregation (all sites)	Aggregation (non-periodic sites)	Occurrence PVPs
MAP	28%	16%	20%
Rain seasonality	44%	51%	46%
Topsoil Sand	14%	16%	21%
Slope	14%	17%	1%
Fire frequency	1%	0%	10%
Cross-validated R^2	0.31	0.29	0.83

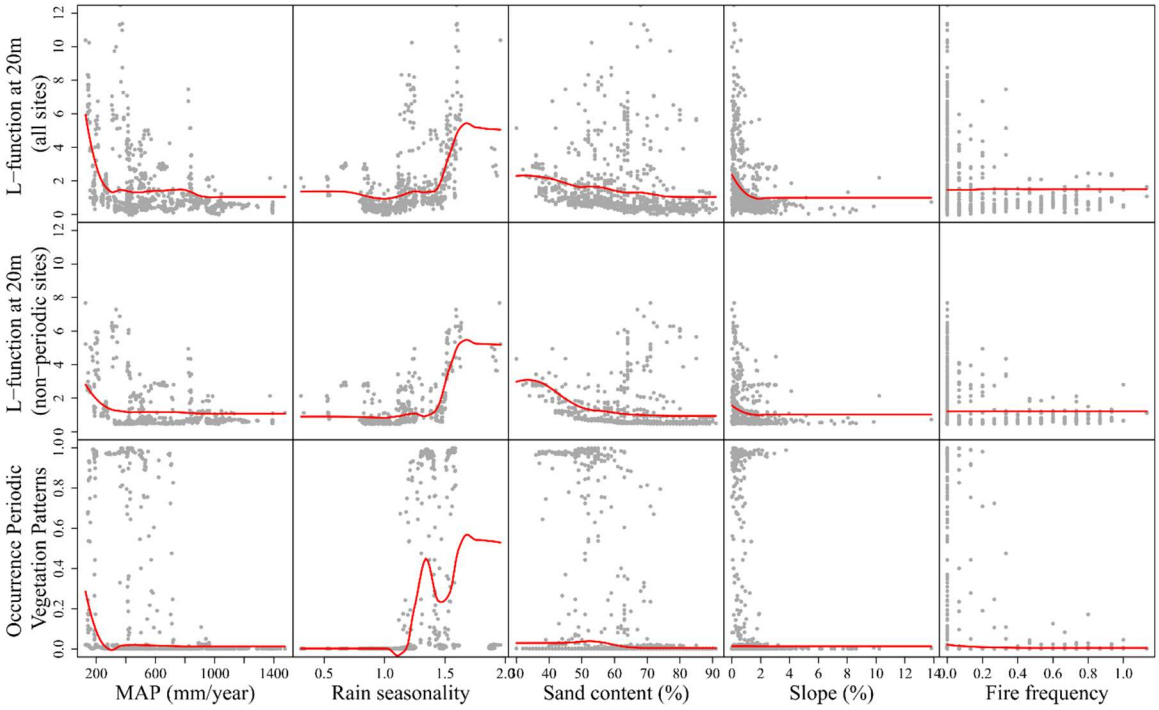

Figure 2.8 Modeled BRT responses ("partial dependencies") for predictions of under what conditions PVPs occur (top), and woody aggregation (L-statistic at 20 m) for all sites not categorized as having periodic patterns (bottom). The response for each environmental variable accounts for the average effect of the other four variables. The red lines are smoothed representations of the responses overlaying the fitted values (model predictions based on the original data; grey dots).

Additional insight was drawn from analyzing aggregation along distances and with the data categorized into PVPs and subdivisions based on MAP and soil texture (Figure 2.9). All categories were dispersed at short distances because each crown takes up space and there is bound to be a short distance between the center points of adjacent plants. Sites with PVPs had the highest levels of aggregation reaching a maximum at around 25 m

(Figure 2.9). The combination with wetter climes (≥600 mm MAP) on coarse-textured soils (≥60% sand) featured lower levels of aggregation than the other categories.

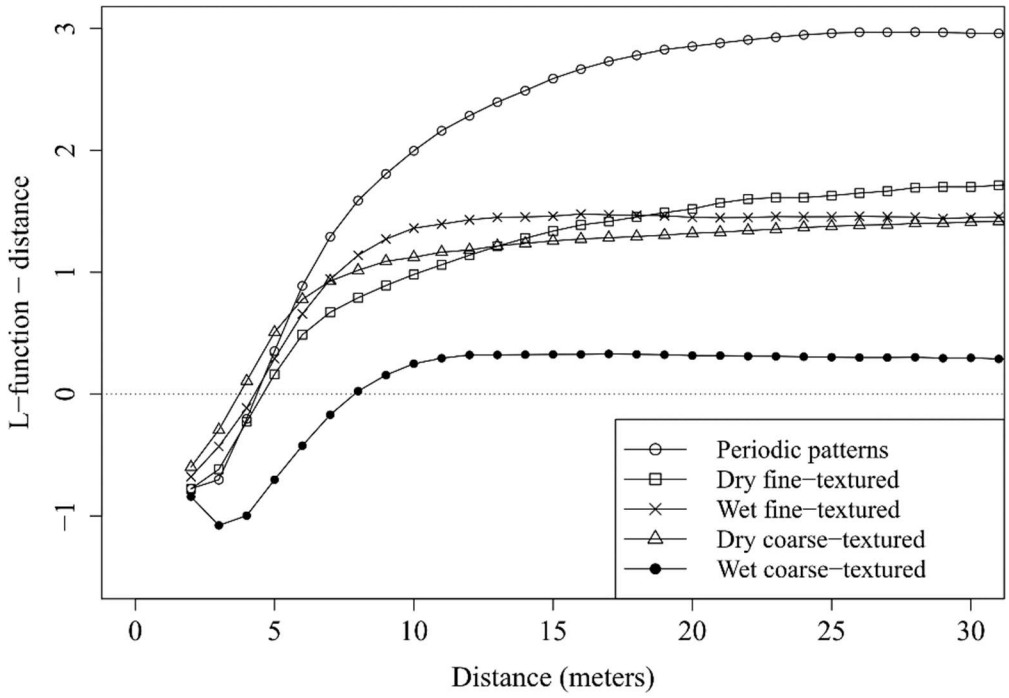

Figure 2.9 Level of aggregation among tree crowns calculated using Ripley's K transformed to Besag's L-function. The figure shows the mean values of five categories: sites with periodic vegetation patterns, and four subdivisions based on mean annual precipitation and soil texture. Sites classified as having periodic patterns were not included in the latter subdivisions. Sites with MAP below 600 mm were categorized as dry whereas sites with a sand content below 60% were categorized as fine-textured.

2.4 Discussion

2.4.1 Dividing woody cover into density and crown size components

Numerous authors have investigated how woody canopy cover varies across African savannas in response to variation in environmental variables (Good & Caylor, 2011; Sankaran et al., 2005; Staver et al., 2011). Given that tropical savannas cover about an eighth of Earth's land surface (Scholes & Archer, 1997) and contributes heavily to the global carbon cycle (Poulter et al., 2014), it is important to understand the makeup of these variations in terms of crown sizes and tree densities. By separating woody cover into mean crown size and density we were able to analyze whether they respond differently to environmental factors and how they combine to drive landscape-scale woody cover across the continent. Our results suggest that crown sizes respond more strongly to rainfall than crown density (Figure 2.6). This indicates that the commonly observed relationship of increasing woody cover with MAP in African savannas (e.g. Sankaran et al., 2005) is more a result of increasing size of trees than increasing tree density, at least in savannas with MAP < 700 mm.

We also found a unimodal relationship between crown sizes and soil texture that was not present in the results for crown density (Figure 2.7). Soil properties have a considerable effect on the water cycle and a few studies have noticed that woody growth is suppressed on clayey soils in drylands (Lane et al., 1998; Sankaran et al., 2005; Williams et al., 1996). Recently, Fensham et al. (2015) showed that the effect is likely due to the higher wilting point on clays which limits the soil moisture available for plants to extract. A combination of low rainfall and fine-textured soils can lead to very low soil water potentials and impact the vegetation in a way reminiscent of even drier conditions. In our

results, the relationship appears unimodal with suppression on both the clayey and the sandiest end. Woody growth is then controlled by available soil moisture which can be limited by either a high wilting point on clayey soils or low field capacity on sandy soils. Our results suggest these constraints affect the size of woody plants and not their abundance. Crown densities were most strongly influenced by rainfall seasonality and appears to have a unimodal response function (Figure 2.7). The sites with very low rainfall seasonality (<0.8) were all situated in the western part of East Africa (Serengeti, Masai Mara, and northern Uganda) in a region with bi-modal rainfall distributions and far lower seasonality that further east. Many of these sites had low woody densities and cover but likely for other reasons than rainfall seasonality. Elephant densities are thought to be a key driver of woody cover in the Mara-Serengeti ecosystem (Morrison et al., 2016). Browsing, especially by elephants, has a great impact on woody structure (Sankaran et al., 2013) and is a key factor we did not capture in this analysis. If we focus on sites with rainfall seasonality above 0.8, there is a more linear relationship with lower crown density and cover in areas with high rainfall seasonality which could be associated with the long periods of high water stress in more seasonal systems. Lehmann et al. (2014) found that high rainfall seasonality can constrain canopy closure and is an important predictor for the presence of savanna.

Overall, the estimated woody properties were more strongly influenced by rainfall amounts and seasonality than by soil, slope, and fire. Fire frequency had a weak negative association with both woody cover, crown sizes, and densities. Fire has, however, an interactive relationship with vegetation structure (Archibald et al., 2009) and this

analysis cannot separate the effect of fire on vegetation from impacts of vegetation structure on the fire regime.

2.4.2 Woody plant aggregation and the occurrence of periodic vegetation patterns

In accordance with previous research (Deblauwe et al., 2008), we found that the formation of highly aggregated PVPs is associated with specific environmental conditions. Periodic patterns are most likely to occur in areas with high rainfall seasonality, low mean annual rainfall, on fine-textured soils, and on flat or gently sloping terrain (Figure 2.8). These are factors that influence ecohydrological processes such as the propensity to form overland flows during rainfall events (Valentin et al., 1999). The results are in agreement with a global study on the biogeography of PVPs by Deblauwe et al. (2008) who found similar effects in regions with strong seasonal variation in temperature and more constant rainfall (Australia and Mexico) and in regions with distinct rainfall seasonality but more constant temperatures (Africa). Our analysis further shows that the same factors that contribute to PVP emergence are associated with higher levels of aggregation among woody plants elsewhere in African savannas. PVPs thus appear under conditions that naturally favor local facilitation and patchiness. However, the vegetation at many sites with these conditions do not exhibit highly organized periodic patterns which could be related to soil properties other than texture. The dominant process in the formation of PVPs is a significant overland flow from bare to vegetated patches which requires near impervious soils. This property is typically associated with shallow soil depths, physical crusts, or hardpans (Leprun, 1999; McDonald et al., 2009), and is not strongly dependent on soil texture.

Previous literature have linked local aggregation and patchiness in savannas to fire frequency (Veldhuis, Rozen-Rechels, et al., 2016), seed dispersal (Pueyo et al., 2008), runoff-erosion processes (Ludwig et al., 2005), and short-range facilitation through modified microclimate close to nurse plants (Holmgren & Scheffer, 2010). With increasing abiotic stress, we expect stronger tree-tree facilitation in accordance with the stress gradient hypothesis (He et al., 2013). In our analysis, the most influential predictor for modeling aggregation was rainfall seasonality (Table 2.2), a factor that could influence plant dynamics in more than one way. The pronounced dry season associated with highly seasonal systems exerts a strong abiotic pressure, especially on juvenile trees with less developed root systems. Juvenile survival through the dry season is likely higher in the shelter of nearby trees. Over time, a bias in survival rates may lead to higher aggregation among adult trees. Once the wet season arrives, it often comes in heavy downpours which can quickly saturate the top soil leading to overland flows. This leads to both redistribution of water resources to woody patches with higher infiltration rates, and redistribution of litter and soil resources (Ludwig et al., 2005). The more concentrated rains may also alleviate competition for water during the growing season leading to facilitation being the dominant force in highly seasonal drylands. There was also a clear relationship between fine-textured soils and higher aggregation. Fine-textured soils increase runoff through lower infiltration rates and may also amplify stress during the dry season through their higher wilting point. Sites with the combination of coarse-textured soils (≥60% sand) and wetter climes (≥600 mm MAP) stood out in the analysis by being far less aggregated (Figure 2.9). This points to the interactive effects of these variables. We found no link between fire frequency and aggregation and a weak relationship with slope favoring

aggregation on flat or gently sloping terrain. This relationship can also be explained in terms of overland flows. Steeper slopes tend to create drainage rills leading the water downhill which break up the local patch-interpatch redistribution of resources (Saco & Moreno-de las Heras, 2013).

2.5 Conclusions

Using high spatial resolution imagery, a flexible classification framework, and a crown delineation methodology, we estimated several key woody vegetation properties in African savannas and analyzed how these vary with local environmental conditions. We find that woody cover, crown sizes, and woody plant densities are more strongly influenced by rainfall amounts and seasonality than by soil texture, slope, and fire frequency. Of specific interest is that mean crown size responded more strongly to mean annual rainfall than plant densities, indicating that the commonly observed relationships between woody cover and rainfall (e.g. Sankaran et al., 2005) is more a result of increasing crown sizes than changes in crown density. Larger crown sizes were associated with mid-textured soils and appeared suppressed on both clays and very sandy soils. The level of aggregation among woody plants was most strongly related to rainfall seasonality, as was the occurrence of PVPs. Similar processes that influence patchiness in savannas also contribute to the formation of PVPs, with impermeable soil conditions being the possible difference between a patchy savanna landscape and highly organized periodic vegetation.

2.6 Appendix A: Validation of Estimated Woody Vegetation Properties using Field Data from Kenya

This appendix describes a validation analysis of estimated mean crown size, crown density, and woody cover using field data collected in southern Kenya during September-October 2015. Plots were established in five protected areas: Tsavo West NP, Tsavo East NP, Amboseli NP, Ol Pejeta wildlife conservancy, and Il Ngwesi group ranch (Figure A1). In total, we established 28 plots with at least four plots in each protected area. The size of plots varied with the density of trees and shrubs, ranging from 350m² to 8000m² with a median at 1450m² (38x38m). The positions of plot corners were determined with a GPS and the positions of trees and shrubs within each plot were measured with a laser rangefinder from the plot corners. Using measuring tape, we determined the diameter of crowns along the longest axis and on the perpendicular. From these two measurements, we later calculated crown sizes assuming elliptic crown shapes. We acquired the best available high resolution imagery covering the sites from 2012 or later. In some cases, this resulted in imagery of lower quality (few green leaves on the trees) than the imagery used in the continental analysis.

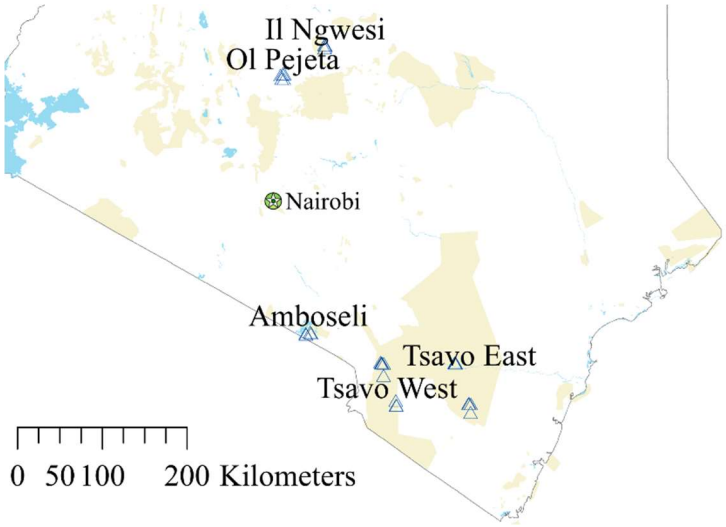

Figure A1 Map of the five protected areas in southern Kenya where field work was conducted. The positions of individual plots are marked with blue triangles.

Our analysis of detection ratios (Figure A2) indicated a detection threshold of ~ 2 m below which smaller trees and shrubs were not reliably detected, while most individuals with crown diameter > 3 m were detected. The detection ratios were likely negatively influenced by the sometimes low quality of the imagery and the time difference between image acquisition and field work (often 2-3 years).

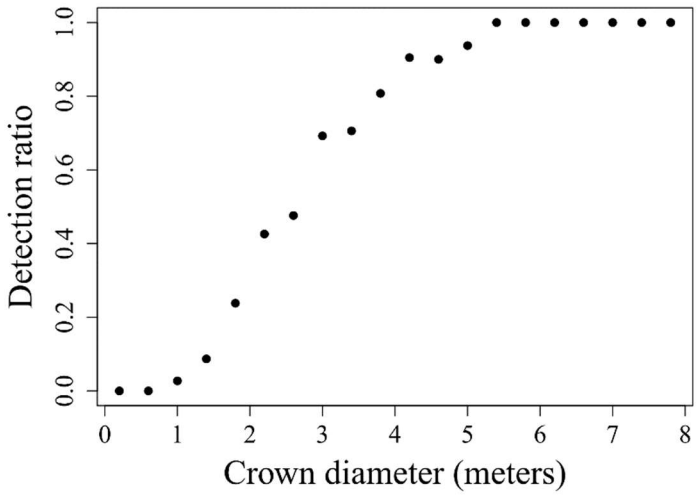

Figure A2 Detection ratios of woody plants in classified imagery at field work sites. The values were calculated as mean detection ratios for trees divided into bins of width 40 cm.

When calculating the relationship between estimated and field measured woody properties (Figure A3), we excluded all field measured trees and shrubs with a diameter less than the 2 m detection threshold. Estimates of the woody properties then fall relatively close to the one-to-one line. The four sites in Amboseli were dominated by large umbrella thorn acacias (*Vachellia tortilis*) with particularly large and spread out crowns (Figure A4). The spread-out architecture of these crowns makes them appear as several distinct crowns from above, and the delineation algorithm did not identify them as single trees. The large majority of our sites in the continental analysis do not contain this type of trees which are relatively rare across all of African savannas. Since they dominated all four sites in Amboseli, we determined they were overrepresented in the field data set and therefore chose to exclude the Amboseli sites when calculating R^2 for mean crown size and crown density. We also excluded one site in Ol Pejeta (OLP3) where the smaller trees lacked green leaves in the imagery and could not be detected.

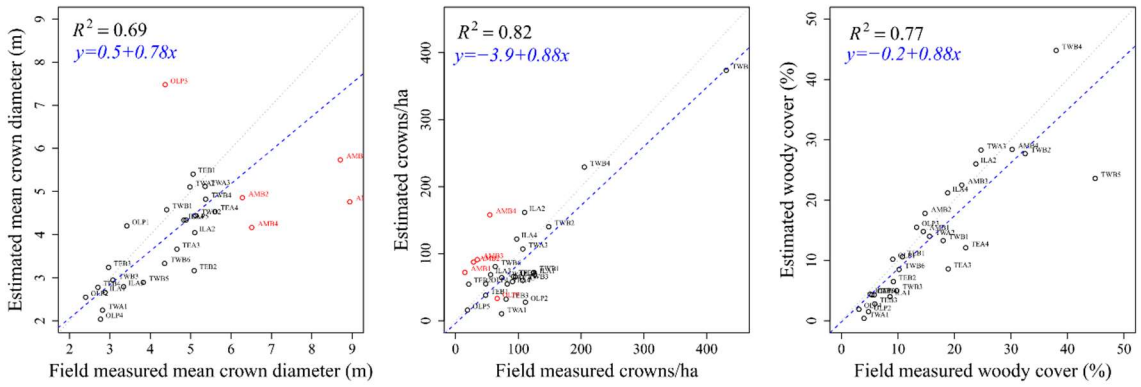

Figure A3 Validation of estimated mean crown size, crown density, and woody cover. The Amboseli sites and one site in Ol Pejeta were excluded when calculating R^2 for mean crown size and crown density. These sites are shown in red color.

Figure A4 Vachellia tortilis at a field work site in Amboseli NP, Kenya. The left image shows two trees with overlapping crowns, with the second being further back on the left. The right image shows the same trees in false color satellite imagery. The spread out architecture of the canopy make them appear as several distinct crowns. The camera symbol roughly indicates the position from which the ground photo was taken.

2.7 References

Archibald, S., Roy, D. P., van Wilgen, B. W., & Scholes, R. J. (2009). What limits fire? An examination of drivers of burnt area in southern Africa. *Global Change Biology, 15*(3), 613-630.

Barbier, N., Bellot, J., Couteron, P., Parsons, A. J., & Mueller, E. N. (2014). Short-Range Ecogeomorphic Processes in Dryland Systems. In *Patterns of Land Degradation in Drylands* (pp. 85-101): Springer.

Besag, J. (1977). Comments on Ripley's paper. *Journal of the Royal Statistical Society B, 39*(2), 193-195.

Bond, W. J. (2008). What limits trees in C4 grasslands and savannas? *Annual Review of Ecology, Evolution, and Systematics, 39*, 641-659.

Bunting, P., & Lucas, R. (2006). The delineation of tree crowns in Australian mixed species forests using hyperspectral Compact Airborne Spectrographic Imager (CASI) data. *Remote Sensing of Environment, 101*(2), 230-248.

Chesson, P., Gebauer, R. L., Schwinning, S., Huntly, N., Wiegand, K., Ernest, M. S., . . . Weltzin, J. F. (2004). Resource pulses, species interactions, and diversity maintenance in arid and semi-arid environments. *Oecologia, 141*(2), 236-253.

Culvenor, D. S. (2002). TIDA: an algorithm for the delineation of tree crowns in high spatial resolution remotely sensed imagery. *Computers & Geosciences, 28*(1), 33-44.

Deblauwe, V., Barbier, N., Couteron, P., Lejeune, O., & Bogaert, J. (2008). The global biogeography of semi-arid periodic vegetation patterns. *Global Ecology and Biogeography, 17*(6), 715-723.

Dohn, J., Augustine, D. J., Hanan, N. P., Ratnam, J., & Sankaran, M. (2016). Spatial vegetation patterns and neighborhood competition among woody plants in an East African savanna. *Ecology*.

Elith, J., Leathwick, J. R., & Hastie, T. (2008). A working guide to boosted regression trees. *Journal of Animal Ecology, 77*(4), 802-813.

Ellis, E. C., & Ramankutty, N. (2008). Putting people in the map: anthropogenic biomes of the world. *Frontiers in Ecology and the Environment, 6*(8), 439-447.

Farr, T. G., Rosen, P. A., Caro, E., Crippen, R., Duren, R., Hensley, S., . . . Roth, L. (2007). The shuttle radar topography mission. *Reviews of Geophysics, 45*(2), 1-33. doi:10.1029/2005RG000183

Fensham, R. J., Butler, D. W., & Foley, J. (2015). How does clay constrain woody biomass in drylands? *Global Ecology and Biogeography, 24*(8), 950-958.

Gan, T. Y., Ito, M., Hülsmann, S., Qin, X., Lu, X., Liong, S., . . . Koivusalo, H. (2016). Possible climate change/variability and human impacts, vulnerability of drought-prone regions, water resources and capacity building for Africa. *Hydrological Sciences Journal*, 1-18.

Giglio, L., Loboda, T., Roy, D. P., Quayle, B., & Justice, C. O. (2009). An active-fire based burned area mapping algorithm for the MODIS sensor. *Remote Sensing of Environment, 113*(2), 408-420.

Gómez-Aparicio, L., Zamora, R., Castro, J., & Hódar, J. A. (2008). Facilitation of tree saplings by nurse plants: Microhabitat amelioration or protection against herbivores? *Journal of Vegetation Science, 19*(2), 161-172.

Good, S. P., & Caylor, K. K. (2011). Climatological determinants of woody cover in Africa. *Proceedings of the National Academy of Sciences, 108*(12), 4902-4907.

He, Q., Bertness, M. D., & Altieri, A. H. (2013). Global shifts towards positive species interactions with increasing environmental stress. *Ecology letters*.

Hengl, T., Heuvelink, G. B., Kempen, B., Leenaars, J. G., Walsh, M. G., Shepherd, K. D., . . . Tamene, L. (2015). Mapping soil properties of Africa at 250 m resolution: Random forests significantly improve current predictions. *PloS one, 10*(6), e0125814.

Holmgren, M., & Scheffer, M. (2010). Strong facilitation in mild environments: the stress gradient hypothesis revisited. *Journal of Ecology, 98*(6), 1269-1275.

Huffman, G. J., Bolvin, D. T., Nelkin, E. J., Wolff, D. B., Adler, R. F., Gu, G., . . . Stocker, E. F. (2007). The TRMM multisatellite precipitation analysis (TMPA): Quasi-global, multiyear, combined-sensor precipitation estimates at fine scales. *Journal of Hydrometeorology, 8*(1), 38-55.

Karlson, M., Reese, H., & Ostwald, M. (2014). Tree crown mapping in managed woodlands (parklands) of semi-arid West Africa using Worldview-2 imagery and geographic object based image analysis. *Sensors, 14*(12), 22643-22669.

Lane, D. R., Coffin, D. P., & Lauenroth, W. K. (1998). Effects of soil texture and precipitation on above-ground net primary productivity and vegetation structure across the Central Grassland region of the United States. *Journal of Vegetation Science, 9*(2), 239-250.

Lehmann, C. E. R., Anderson, T. M., Sankaran, M., Higgins, S. I., Archibald, S., Hoffmann, W. A., . . . Bond, W. J. (2014). Savanna Vegetation-Fire-Climate Relationships Differ Among Continents. *Science, 343*(6170), 548-552. doi:10.1126/science.1247355

Leprun, J. C. (1999). The influences of ecological factors on tiger bush and dotted bush patterns along a gradient from Mali to northern Burkina Faso. *Catena, 37*(1), 25-44.

Ludwig, J. A., Wilcox, B. P., Breshears, D. D., Tongway, D. J., & Imeson, A. C. (2005). Vegetation patches and runoff-erosion as interacting ecohydrological processes in semiarid landscapes. *Ecology, 86*(2), 288-297.

McDonald, A. K., Kinucan, R. J., & Loomis, L. E. (2009). Ecohydrological interactions within banded vegetation in the northeastern Chihuahuan Desert, USA. *Ecohydrology, 2*(1), 66-71.

Morrison, T. A., Holdo, R. M., & Anderson, T. M. (2016). Elephant damage, not fire or rainfall, explains mortality of overstorey trees in Serengeti. *Journal of Ecology, 104*(2), 409-418.

Pillay, T., & Ward, D. (2014). Competitive effect and response of savanna tree seedlings: comparison of survival, growth and associated functional traits. *Journal of Vegetation Science, 25*(1), 226-234.

Pouliot, D., & King, D. (2005). Approaches for optimal automated individual tree crown detection in regenerating coniferous forests. *Canadian Journal of Remote Sensing, 31*(3), 255-267.

Poulter, B., Frank, D., Ciais, P., Myneni, R. B., Andela, N., Bi, J., . . . Liu, Y. Y. (2014). Contribution of semi-arid ecosystems to interannual variability of the global carbon cycle. *Nature, 509*(7502), 600-603.

Pueyo, Y., Kefi, S., Alados, C., & Rietkerk, M. (2008). Dispersal strategies and spatial organization of vegetation in arid ecosystems. *Oikos, 117*(10), 1522-1532.

Rasmussen, M. O., Göttsche, F.-M., Diop, D., Mbow, C., Olesen, F.-S., Fensholt, R., & Sandholt, I. (2011). Tree survey and allometric models for tiger bush in northern Senegal and comparison with tree parameters derived from high resolution satellite data. *International Journal of Applied Earth Observation and Geoinformation, 13*(4), 517-527.

Rietkerk, M., & van de Koppel, J. (2008). Regular pattern formation in real ecosystems. *Trends in ecology & evolution, 23*(3), 169-175.

Riginos, C., & Grace, J. B. (2008). Savanna tree density, herbivores, and the herbaceous community: bottom-up vs. top-down effects. *Ecology, 89*(8), 2228-2238.

Ripley, B. D. (1977). Modelling spatial patterns. *Journal of the Royal Statistical Society. Series B (Methodological), 39*(2), 172-212.

Saco, P. M., & Moreno-de las Heras, M. (2013). Ecogeomorphic coevolution of semiarid hillslopes: Emergence of banded and striped vegetation patterns through interaction of biotic and abiotic processes. *Water Resources Research, 49*(1), 115-126.

Sankaran, M., Augustine, D. J., & Ratnam, J. (2013). Native ungulates of diverse body sizes collectively regulate long-term woody plant demography and structure of a semi-arid savanna. *Journal of Ecology, 101*(6), 1389-1399.

Sankaran, M., Hanan, N. P., Scholes, R. J., Ratnam, J., Augustine, D. J., Cade, B. S., . . . Ludwig, F. (2005). Determinants of woody cover in African savannas. *Nature, 438*(7069), 846-849.

Sankaran, M., Ratnam, J., & Hanan, N. (2008). Woody cover in African savannas: the role of resources, fire and herbivory. *Global Ecology and Biogeography, 17*(2), 236-245.

Scanlon, T. M., Caylor, K. K., Levin, S. A., & Rodriguez-Iturbe, I. (2007). Positive feedbacks promote power-law clustering of Kalahari vegetation. *Nature, 449*(7159), 209-212.

Scholes, R., & Archer, S. (1997). Tree-grass interactions in savannas. *Annual review of Ecology and Systematics, 28*, 517-544.

Shackleton, C., & Scholes, R. (2011). Above ground woody community attributes, biomass and carbon stocks along a rainfall gradient in the savannas of the central lowveld, South Africa. *South African Journal of Botany, 77*(1), 184-192.

Staver, A. C., Archibald, S., & Levin, S. A. (2011). Tree cover in sub-Saharan Africa: Rainfall and fire constrain forest and savanna as alternative stable states. *Ecology, 92*(5), 1063-1072.

Valentin, C., d'Herbès, J.-M., & Poesen, J. (1999). Soil and water components of banded vegetation patterns. *Catena, 37*(1), 1-24.

Veldhuis, M. P., Hulshof, A., Fokkema, W., Berg, M. P., & Olff, H. (2016). Understanding nutrient dynamics in an African savanna: local biotic interactions outweigh a major regional rainfall gradient. *Journal of Ecology, 104*(4), 913-923. doi:10.1111/1365-2745.12569

Veldhuis, M. P., Rozen-Rechels, D., Roux, E., Cromsigt, J. P., Berg, M. P., & Olff, H. (2016). Determinants of patchiness of woody vegetation in an African savanna. *Journal of Vegetation Science, 28*(1), 93-104. doi:10.1111/jvs.12461

Williams, R., Duff, G., Bowman, D., & Cook, G. (1996). Variation in the composition and structure of tropical savannas as a function of rainfall and soil texture along a large-scale climatic gradient in the Northern Territory, Australia. *Journal of Biogeography, 23*(6), 747-756.

Xu, C., Holmgren, M., Van Nes, E. H., Maestre, F. T., Soliveres, S., Berdugo, M., . . . Scheffer, M. (2015). Can we infer plant facilitation from remote sensing? a test across global drylands. *Ecological Applications, 25*(6), 1456-1462.

3 RATES OF WOODY ENCROACHMENT IN AFRICAN SAVANNAS REFLECT WATER CONSTRAINTS AND FIRE DISTURBANCE

Axelsson CR, Hanan NP. Rates of woody encroachment in African savannas reflect water constraints and fire disturbance. JBiogeogr. 2018. https://doi.org/10.1111/jbi.13221

Abstract

Aim (1) To estimate current rates of woody encroachment across African savannas. (2) Identify relationships between change in woody cover and potential drivers, including water constraints, fire frequency, and livestock density. The found relationships led us to pursue a third goal: (3) use temporal dynamics in woody cover to estimate potential woody cover.

Location Sub-Saharan African savannas

Methods The study used very high spatial resolution (VHR) satellite imagery at sites with overlapping older (2002-2006) and newer (2011-2016) imagery to estimate change in woody cover. We sampled 596 sites in 38 separate areas across African savannas. Areas with high anthropogenic impact were avoided in order to more clearly identify the influence of environmental factors. Relationships between woody cover change and potential drivers were identified using linear regression and simultaneous auto-regression, where the latter accounts for spatial auto-correlation.

Results The mean annual change in woody cover across our study areas was 0.25 % per year. Although we cannot explain the general trend of encroachment based on our data, we found that change rates were positively correlated with the difference between potential

woody cover and actual woody cover (a proxy for water availability; $P<0.001$), and negatively correlated with fire frequency ($P<0.01$). Using the relationship between rates of encroachment and initial cover, we estimated potential woody cover at different rainfall levels.

Main conclusions The results indicate that woody encroachment is ongoing and widespread across African savannas. The fact that the difference between potential and actual cover was the most significant predictor highlights the central role of water availability and tree-tree competition in controlling change in woody populations, both in water-limited and mesic savannas. Our approach to derive potential woody cover from the woody cover change trajectories demonstrates that temporal dynamics in woody populations can be used to infer resource limitations.

3.1 Introduction

Change in woody cover in sub-Saharan Africa is characterized by decreases in populated areas and a slow but steady increase in remote areas, generally referred to as woody (or shrub) encroachment (Brandt, Rasmussen, et al., 2017). Woody encroachment in grasslands and savannas is a global phenomenon and its causes and consequences have been frequently debated over the last decades (D'Odorico et al., 2012). Consequences of encroachment have long been described as malign, being detrimental to livestock productivity by reducing grass cover and incurring expenses for shrub removal (Van Auken, 2009). On the other hand, increasing carbon stocks in drylands can offset carbon losses of deforestation, and enhance the provision of fuelwood and timber resources (Birhane et al., 2017). Higher woody canopy cover also affects biodiversity and local hydrological processes, including evapotranspiration, runoff generation, and rainfall

interception (Archer et al., 2017; Honda & Durigan, 2016). Since it impacts critical ecological processes and peoples' livelihoods, we need a thorough understanding of the extent and rate at which encroachment occurs, and improved understanding of why it occurs, to inform rational management and adaptation strategies.

Several potential causal factors have been linked to encroachment, including climate change (Brandt, Rasmussen, et al., 2017), changes in precipitation intensity (Kulmatiski & Beard, 2013), livestock grazing (Roques et al., 2001), fire suppression (Dalle et al., 2006), and increasing atmospheric CO_2 concentrations (Bond & Midgley, 2012; Buitenwerf et al., 2012). In Africa, the disappearance of free-roaming elephants may also have contributed to the overall trend (Daskin et al., 2016; Stevens et al., 2016). Given the ubiquity of encroachment observations in different parts of the world, the two potential main drivers are increasing CO_2 concentrations and the expansion of livestock grazing. Elevated CO_2 levels can increase the efficiency of photosynthesis and plant water-use, leading to enhanced growth among many woody species (Ainsworth & Long, 2005; Kgope et al., 2010; Morgan et al., 2007). The expansion of livestock grazing has been associated with reductions to fire frequency and intensity, and often the removal of wild browsers (Archer et al., 2017). Browsing and fire both suppress woody seedlings and saplings, and are necessary components of higher-rainfall savannas where they can maintain a mixed tree-grass state under rainfall amounts well above levels sufficient to support a closed canopy (Bond, 2008; Sankaran et al., 2013).

Irrespective of the dominant driver, it is clear that encroachment interacts with rainfall which defines the resource-based potential woody cover of tropical savannas. Sankaran et al. (2005) found a linear relationship between potential woody cover and mean

annual precipitation up to ~650 mm/year in African savannas, beyond which canopy closure was possible (albeit not always realized due to natural and anthropogenic disturbances). An extension of this relationship can be found in tropical and temperate forests where the upper bound of above-ground biomass is constrained by water deficits (Stegen et al., 2011). It is, however, not clear how rainfall influences tree dynamics other than constraining the upper limit, or what role rainfall may play in regulating rates of woody encroachment.

Most analyses of encroachment focus on specific areas and may be biased in favor of sites where encroachment has been observed. The most comprehensive analyses of encroachment in African savannas to date include Brandt et al. (2017) which used continent-wide passive microwave remote sensing, and Stevens et al. (2017) which compiled a meta-analysis of past woody cover change studies. Both these studies point to widespread encroachment in African drylands, with the latter study finding a mean increase of 0.25 % woody cover per year. Our study uses very high resolution (VHR) satellite imagery, sampled at 596 sites in 38 areas across drought-seasonal Africa, to (1) provide unbiased estimates of current trends in woody cover change in the savannas, and (2) explore how rates of change relate to environmental (climate, soil, herbivory, and fire) variables and estimates of potential woody cover based on local rainfall amounts.

3.2 Data and Methodology

3.2.1 Acquiring and sampling satellite imagery

We used the same dataset, image preprocessing steps, and classification framework as in a recent study on patterns in African woody vegetation structure (Axelsson

& Hanan, 2017) and refer the reader to this paper for a more thorough description of the methodology. Our sampling frame was sub-Saharan African savannas with a minimum of anthropogenic disturbances. This study used a subset of sites from the previous study where we had overlapping older (2002-2006) and newer (2011-2016) imagery. In all cases, we only acquired imagery from seasons when trees were in full leaf in the particular area. Most of the newer imagery were WorldView 2 while the older images were from the Quickbird 2 satellite. Due to limited image coverage, it is currently not possible to do a continental change analysis with VHR data from a single satellite. In total, we acquired overlapping imagery in 38 areas with a mean time difference of 9.9 years between image pairs. Within the overlapping imagery, we sampled 240 x 240 m sites guided by a 0.04° longitude/latitude grid which served as a base for site locations. The location of sites was, however, often adjusted to avoid locations with clear anthropogenic imprints such as settlements, roads, and agriculture, geomorphological features such as gullies and rock outcrops, or because of clouds and cloud shadows in the imagery. Where we needed to adjust site location, we selected the closest suitable location to the original point to reduce the potential for observer-bias in selecting the new site. Later, during the classification phase, some sites were eliminated due to difficulties in identifying woody plants because of a lack of green leaves or similar spectral signatures of trees and grasses. We ended up with 596 sites, and due to varying image quality, anthropogenic disturbances, and area of image overlap, there was variation in the number of sites per area (Figure 3.1).

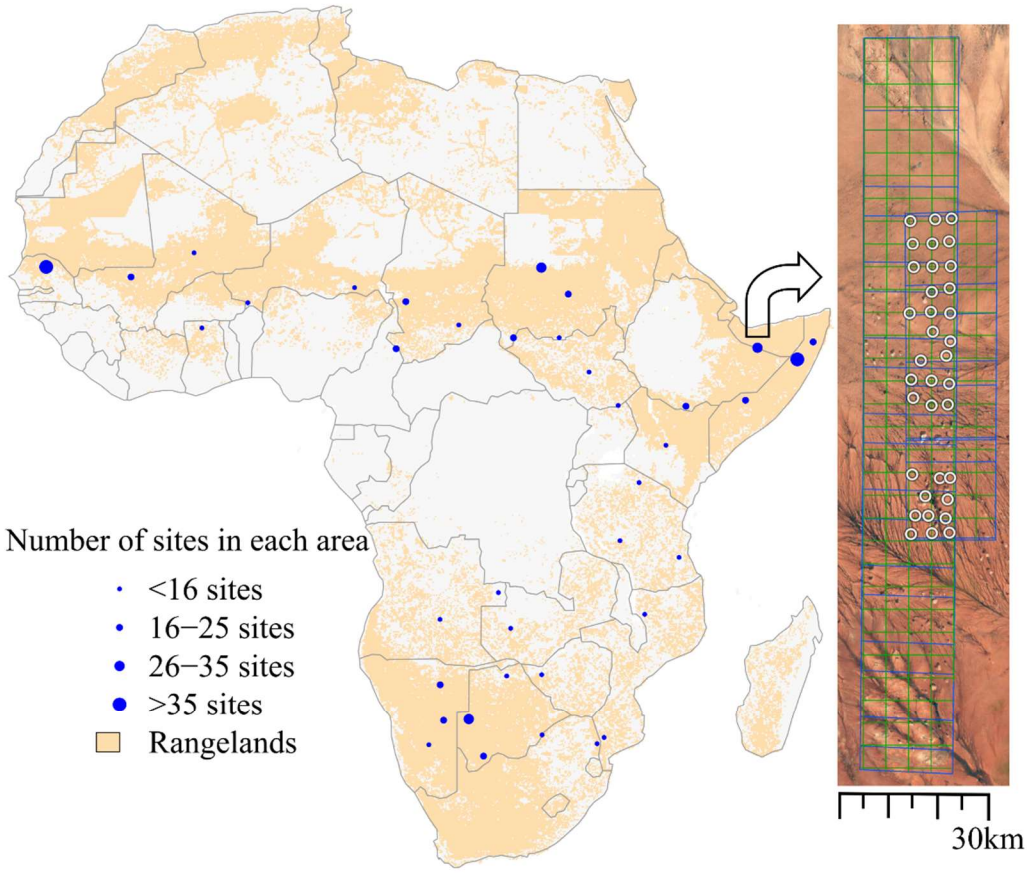

Figure 3.1 Location of the 38 study areas, containing 596 study sites, spread out over African rangelands (defined using the Anthropogenic biomes product (Ellis & Ramankutty, 2008)). The map to the right shows a study area on the border between Somalia and Ethiopia to illustrate the sampling strategy for study sites (white rings). The placement of sites was guided by a 0.04° longitude/latitude grid (green lines) in areas with overlapping older and newer satellite imagery (blue lines) with local adjustments to avoid anthropogenic influence, geomorphological features, and clouds.

3.2.2 Preprocessing and classification of satellite data

Preprocessing steps included Gram-Schmidt pan-sharpening of the blue, green, red, and near-infrared bands, and orthorectification using embedded RPC-information and an SRTM v2 DEM (Farr et al., 2007). The orthorectified imagery were resampled to 0.6 m ground resolution using the nearest neighbor method. Centered at the site coordinates, we then extracted a 400 x 400 pixel (240 x 240 m) area to represent each site. For classification of the woody pixels, we applied an unsupervised (ISODATA) classification approach dividing each image into 18 spectrally different classes. The results were smoothed using a kernel size of 3 pixels. Up to this point, processing was performed in ENVI 5.2 but the final classification step was done using a custom-built software. This step involved manually assigning the unsupervised classes into woody and non-woody cover types. The custom-built software helped us streamline the final classification step and perform it in an efficient and consistent manner. Examples of two sites with estimates of woody cover for the older and newer imagery are shown in Figure 3.2.

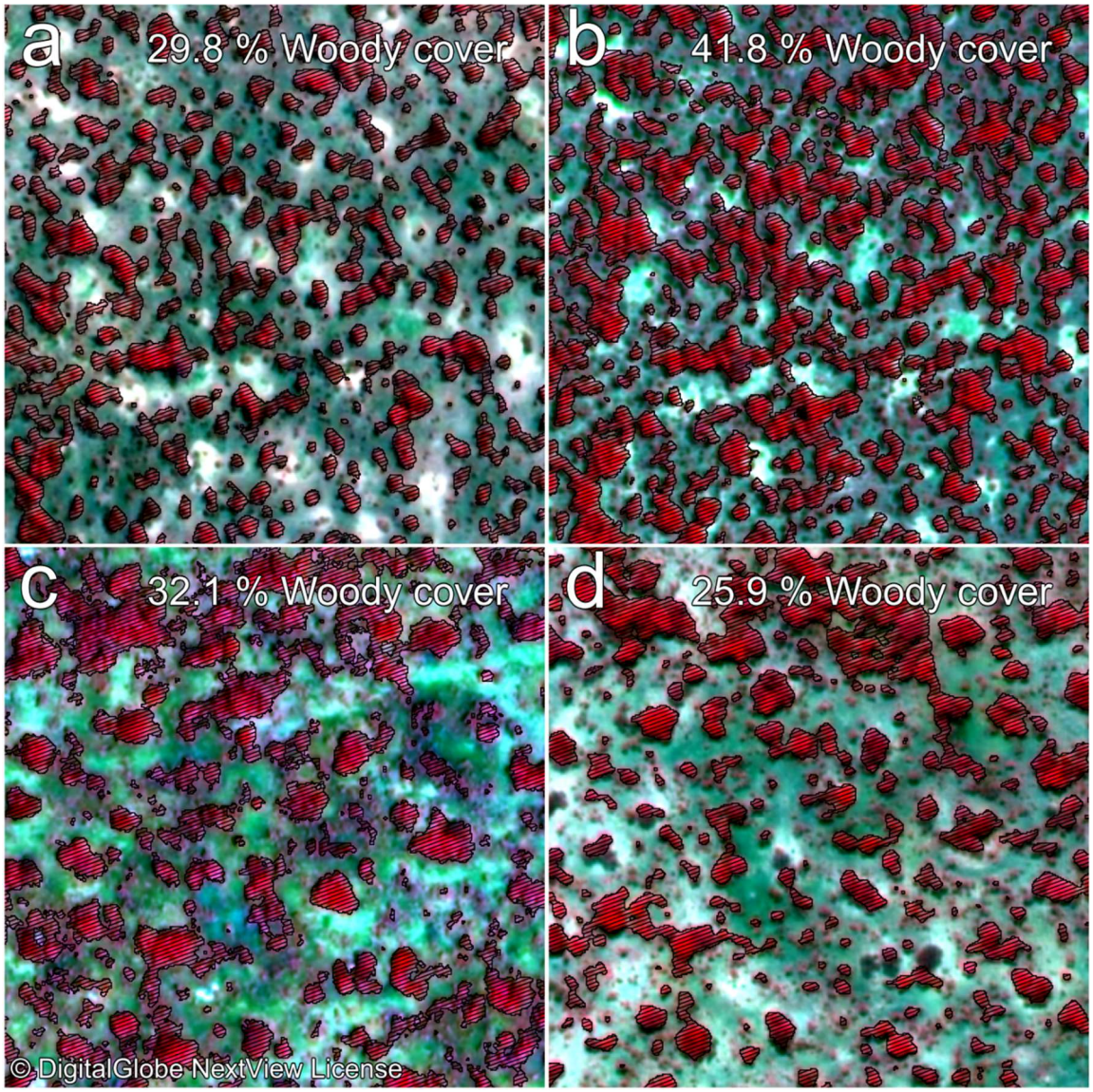

Figure 3.2 Woody cover estimated at two African savanna sites illustrating increasing (a, b) and decreasing (c, d) canopy cover through time (woody canopy indicated by hatched polygons). (a) False-color imagery for a site in western Niger (lat: 12.51311, long: 2.403536) taken in 2003, and (b) the same site with higher canopy cover in 2012. (c-d) Imagery depicting a reduction in woody cover between 2004 and 2013 for a site in South Sudan (lat: 9.510114, long: 24.63787).

3.2.3 Data used in the regression analysis

After image classification, we had estimates of woody cover from the older imagery (initial cover), the newer imagery (final cover), as well as acquisition dates for the imagery. Annual woody cover change was calculated as (final cover - initial cover) / time in years. We investigated relationships between woody cover change and several datasets that could have a causative impact on tree dynamics:

- *Mean annual precipitation (MAP)* was extracted from the Tropical Rainfall Measuring Mission (TRMM) 3B42 v7 product (0.25° x 0.25°) (Huffman et al., 2007). MAP was calculated individually for each site starting in January of the year of the first image acquisition and ending in December of the final acquisition.
- *MAP change* identifies change in rainfall relative to the years prior to the first image acquisition. It was calculated as the difference in MAP between the observation period (described above) and the period from January 1998 to December of the year prior to the observation period.
- *(Potential – Initial) cover* is the difference between rainfall-based potential woody cover and the initial cover, and measures how much woody cover can expand before it is limited by water deficits. Potential cover was calculated as 0.14*MAP-14.2 as described in Sankaran et al. (2005), but with the relationship capped at 100% cover. MAP was calculated from rainfall falling between the older and newer image acquisition dates.
- *Fire frequency* (fire events/year) was calculated from the MODIS MCD64A1 collection 5.1 burned area product (500 m resolution; Giglio et al., 2009), based on the number of fires occurring within the observation period. To avoid registering fires

identified in adjacent months as separate fires, we counted fire events in consecutive months as a single fire.

- *Cattle, sheep, & goat densities* were from the FAO Gridded Livestock of the World database, and adjusted to match FAOSTAT totals for the year 2005 (Wint & Robinson, 2007).
- *Population density* was from the Gridded Population of the World v4 product with UN-adjusted densities for the year 2010 (Doxsey-Whitfield et al., 2015).
- *Sand content* was from the top soil horizon (0-5cm) in the ISRIC/AfSIS 250 meter soil property maps of Africa (Hengl et al., 2015).

3.2.4 Regression analysis and considerations for spatial auto-correlation

We started by using ordinary least squares (OLS) regression (lm function in R) to identify significant correlative relationships with woody cover change. Due to the clustered spatial pattern of our sites, there was a clear risk of spatial auto-correlation that should be investigated and addressed. Spatial auto-correlation was evaluated by first constructing a neighborhood matrix where neighbor relations were set for sites closer than 90 km apart, then adding row standardized spatial weights, and finally calculating Moran's I (Moran, 1950) based on the spatial weights matrix and residuals from the OLS regression model. The distance 90 km was defined where spatial auto-correlation for the y-variable (woody cover change) reached its maximum. Calculations were made using the spdep package in R (Bivand et al., 2017). We found significant positive auto-correlation among residuals which leads to a higher risk of falsely identified relationships (Quesada et al., 2012). To account for spatial auto-correlation, we calculated relationships using simultaneous auto-regression (SAR; spautolm function in spdep R package). A spatial

structure (based on the spatial weights matrix described above) is then added to the linear regression model. This resulted in a model without spatially auto-correlated residuals and different significance levels for the predictors compared to the original regression model. It should, however, be noted that incorporating a spatial structure generally diminishes the significance of predictors with clear spatial gradients, such as climatic variables (Quesada et al., 2012). It could thus lead to a model that underestimates the significance of auto-correlated variables that are in fact causative. We therefore present results for both the original regression model and the SAR model and discuss their strengths and shortcomings.

3.3 Results

The mean annual change in woody cover for all 596 sites was 0.27 % per year, with 394 positive, 198 negative, and 4 with no change. The mean woody cover change was significantly greater than zero ($P<2.2e-16$). When we first averaged cover change for each area and then took the mean of the 38 areas we got 0.25 % per year, with 30 positive and 8 negative. The latter approach is likely more reliable since it removes much of the spatial auto-correlation among the individual sites. A density plot of annual woody cover change (Figure 3.3) shows that the distribution peaks close to zero. There was a higher concentration of woody cover losses in East Africa (Figure 3.4), likely due to the 2011 drought (Lyon & DeWitt, 2012) which impacted the whole region, and in particular southern Somalia, southern Ethiopia, and northern Kenya. Our estimates showed woody cover declines in the areas most heavily affected by the East African drought and a lack of large (>0.5 %/year) increases in the overall East African region.

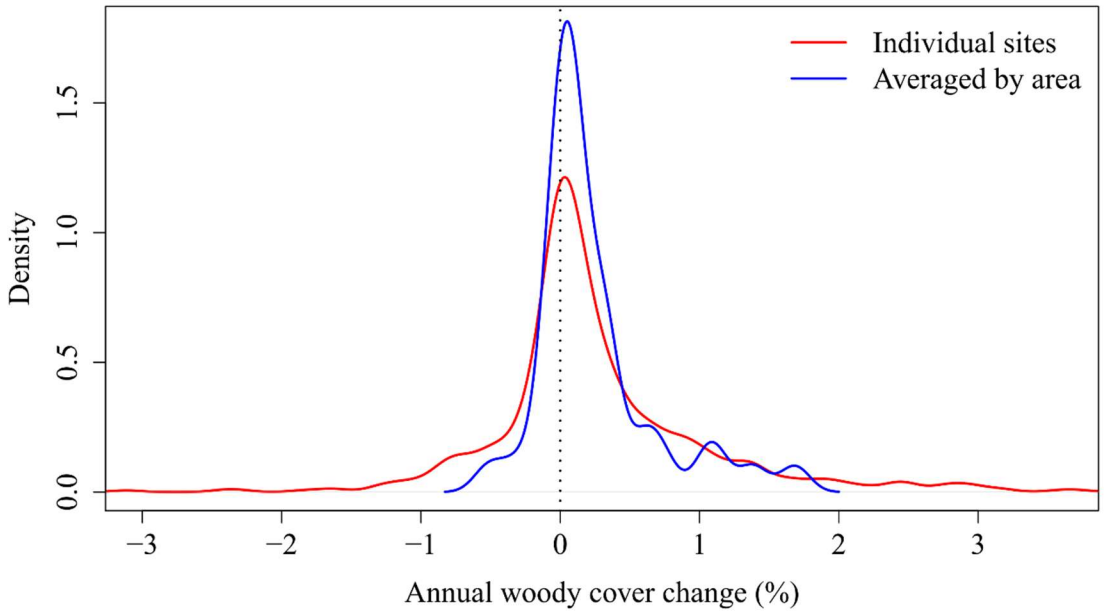

Figure 3.3 Density plot of annual change in woody cover with curves for the individual sites (596 samples) and for change averaged by area (38 samples). The distribution of the individual sites is more dispersed than the aggregated, but both peak near zero.

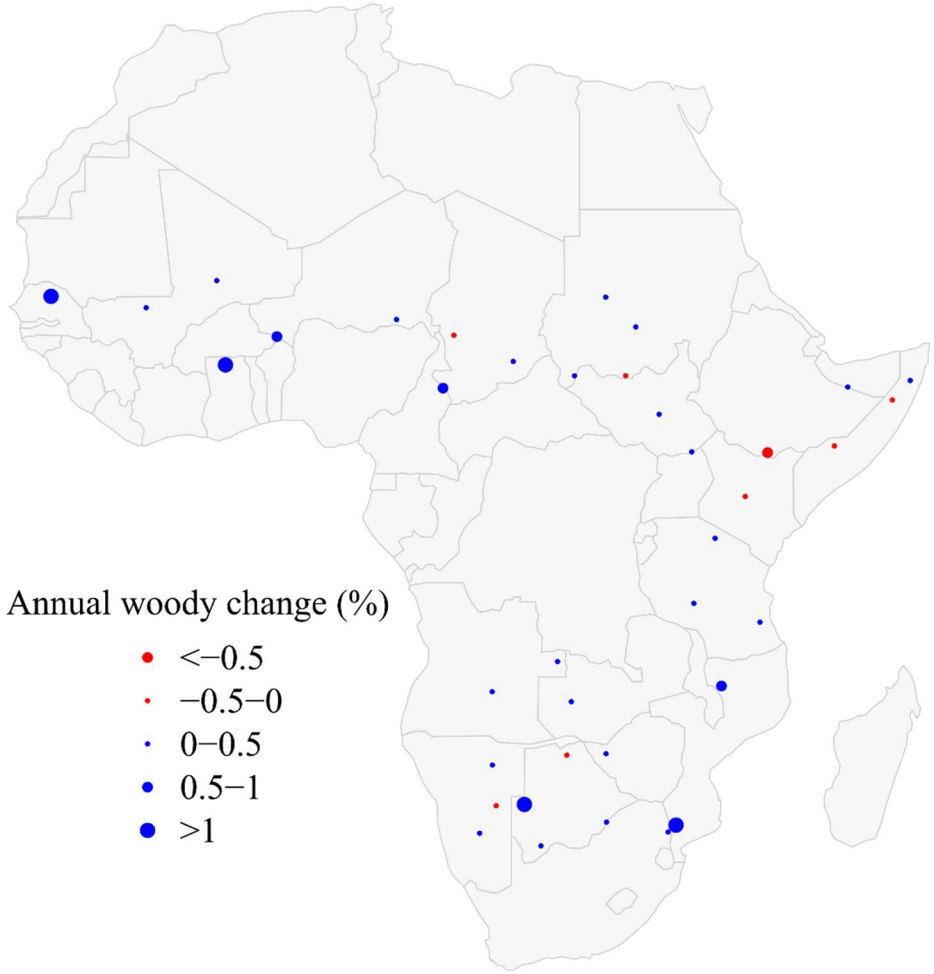

Figure 3.4 Mean annual change in woody cover in 38 study areas across African savannas. The average in each study area was calculated from a variable number of study sites, as shown in Figure 3.1.

3.3.1 Drivers of change in woody cover

Standard OLS regression between woody cover change and potential drivers resulted in an R-squared of 0.15 (Table 3.1), signaling that most of the variation in woody cover change remained unexplained. Initial woody cover and MAP were not significant individually, but the difference between potential cover and initial cover was highly significant ($P<0.001$). Since potential woody cover is defined based on mean annual

rainfall (per Sankaran et al., 2005), this implies that rates of increase in woody cover are positively correlated with available water resources. The other significant variables were change in MAP ($P<0.01$), which had a positive influence, and fire frequency ($P<0.01$) and cattle density ($P<0.05$), both of which had a negative effect on woody cover change. The positive sensitivity of woody cover to rainfall is consistent with the importance of MAP in determining potential cover. Similarly, the negative sensitivity to fire frequency is expected given the role of fire in suppressing sapling survival (Hanan et al., 2008). However, the negative effect of cattle density is inconsistent with expectations that cattle both reduce competition with herbaceous vegetation and reduce frequency of ground fires (Asner et al., 2004). The livestock densities were derived via disaggregation of census summary data for administrative areas (Wint & Robinson, 2007), perhaps limiting their utility in this analysis.

Table 3.1 Results of OLS regression between annual woody cover change and potential driver variables for the 596 African savanna sites.

	Estimate	Std. Error	t value	Pr (>|t|)	Significance
(Intercept)	-0.1648	0.2344	-0.703	0.482190	
MAP	-0.0003	0.0004	-0.805	0.421020	
Initial cover	0.0036	0.0043	0.844	0.398740	
(Potential - initial) cover	0.0158	0.0033	4.838	0.000002	***
MAP change	0.0014	0.0004	3.129	0.001840	**
Fire frequency	-0.5765	0.1777	-3.245	0.001240	**
Cattle	-0.0143	0.0062	-2.286	0.022640	*
Goat	0.0008	0.0032	0.253	0.800280	
Sheep	0.0016	0.0033	0.489	0.624710	
Population density	-0.0025	0.0039	-0.639	0.523380	
Sand content	0.0016	0.0030	0.525	0.600090	

Significance codes: '***' $P < 0.001$ '**' $P < 0.01$ '*' $P < 0.05$

Multiple R-squared: 0.146, Adjusted R-squared: 0.132, P-value 1.26e-15

The residuals of the OLS regression were spatially auto-correlated (Moran's I: 0.23, P<2.2e-16) which could compromise model reliability. We therefore complemented the OLS regression with results from a SAR model, which explicitly accounts for spatial auto-correlation by including a spatial structure among the predictors (Table 3.2). In this case, (potential-initial) woody cover and fire frequency remained significant, while change in MAP and cattle lose their significance. It is difficult to determine which of the two models is more correct since inclusion of a spatial structure in the regression model can decrease the role of spatially auto-correlated variables whether these are causative or not (Quesada et al., 2012).

Table 3.2 Results from simultaneous auto-regression (SAR) between annual woody cover change and potential driver variables for the 596 African savanna sites.

	Estimate	Std. Error	z value	Pr (>|z|)	Significance
(Intercept)	-0.0307	0.3302	-0.093	0.925840	
MAP	-0.0006	0.0006	-1.150	0.250367	
Initial cover	0.0071	0.0063	1.126	0.260154	
(Potential - initial) cover	0.0185	0.0055	3.360	0.000781	***
MAP change	0.0011	0.0007	1.565	0.117512	
Fire frequency	-0.5220	0.2009	-2.599	0.009362	**
Cattle	-0.0127	0.0082	-1.555	0.119891	
Goat	0.0016	0.0046	0.348	0.727861	
Sheep	0.0006	0.0035	0.160	0.872588	
Population density	-0.0013	0.0047	-0.285	0.775572	
Sand content	-0.0004	0.0042	-0.089	0.929088	

Significance codes: '***' P < 0.001 '**' P < 0.01

Nagelkerke pseudo-R-squared: 0.262, P-value: < 2.22e-16

We proceeded to further explore the relationship between woody cover change, rainfall, initial and potential cover (Figure 3.5). Here, a clear trend emerged with higher rates of encroachment where the initial cover is low and higher rates in high rainfall systems. As woody cover approaches its climatic maximum, the mean encroachment rate slows and eventually turns negative. Sites that have overshot the potential cover, i.e. negative (potential-initial) cover, are more likely to suffer mortality.

3.3.2 Estimating potential woody cover based on woody cover change trajectories

The relationship between woody cover change and initial cover (Figure 3.5a) opens up the possibility to use it to derive estimates for potential woody cover, similar to the relationship presented by Sankaran et al. (2005). In Figure 3.5a, woody cover change for the middle rainfall category (400-700 mm/year) decreases with increasing initial cover and turns negative at ~40 % cover. We infer that 40 % cover is a point of attraction for woody cover change that is equivalent to the potential woody cover for this rainfall interval. By identifying the point of attraction for MAP intervals of 100 mm/year up to 800 mm/year, we derived a linear relationship for potential woody cover (Figure 3.6). The remaining sites with MAP above 800 mm/year were placed in a single category. The derived linear relationship, Woody cover = 0.1415*MAP - 23.43, has a similar slope to that presented by Sankaran et al. (2005; Woody cover = 0.14*MAP – 14.2). The category with rainfall above 800 mm/year had a point of attraction above 100 % cover, indicating that the average growth of woody cover is dependent on water availability also in mesic savannas, and only

slows due to space restriction as it nears canopy closure. We noted that a number of sites fall outside of both our and Sankaran's line for potential woody cover. Most of these sites were from Somalia and Ethiopia, which could be related to the bimodal rainfall distribution (two rainy seasons) in that part of East Africa.

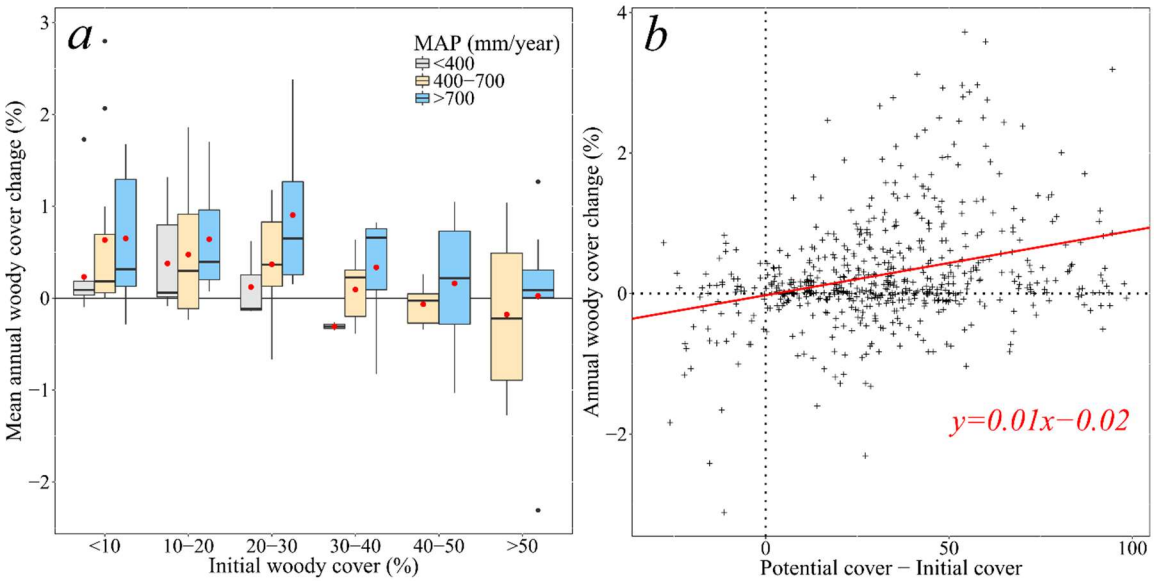

Figure 3.5 Relationship between woody cover change, initial woody cover, and rainfall. (a) Boxplot with woody cover change across intervals of initial woody cover and mean annual precipitation. Each sample represented the average woody cover change among sites in unique combinations of area, rainfall category, and initial cover category. The red points denote the mean change for each box. (b) Scatterplot with the individual sites along axes of woody cover change and (potential – initial) cover. The intercept of the regression line (red) was close to zero change (-0.02).

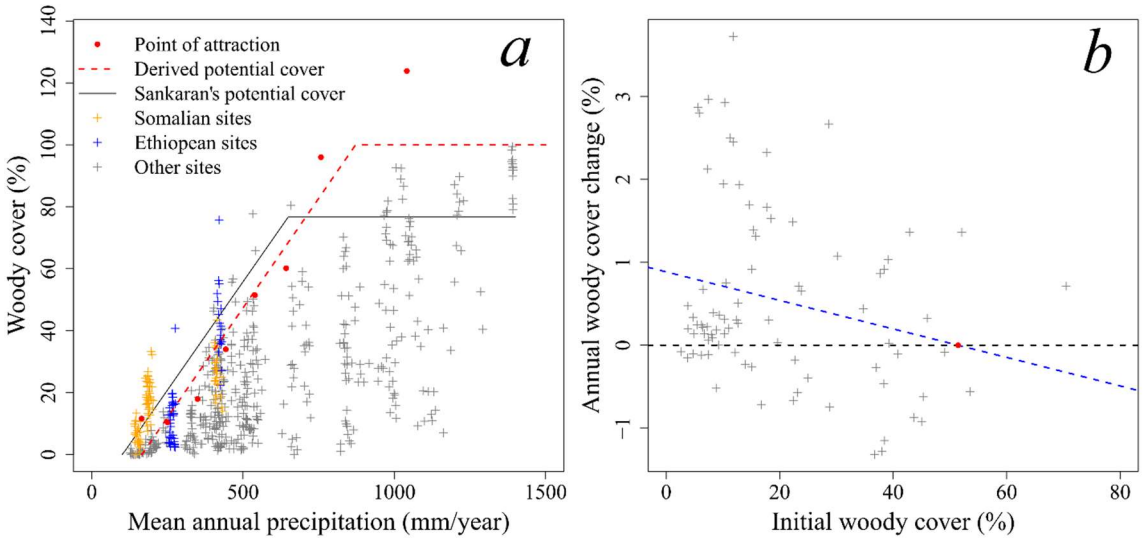

*Figure 3.6 Inference of resource-limited potential woody cover from woody cover growth rates estimated across gradients of initial cover and rainfall. (a) The derived potential woody cover (dashed red line; Woody cover = 0.1415*MAP - 23.43) calculated using linear regression of the points of attraction in each rainfall interval (red points). MAP for the points of attraction was calculated as the average MAP of the sites in each interval. We highlighted sites from Somalia and Ethiopia (yellow and blue dots) as these are overrepresented among sites with actual cover>potential cover. (b) Illustration of how the point of attraction was derived from the intersection between the regression line (blue) and the zero-change line (black). The graph is for the rainfall interval 500-600 mm/year where the intersection lands at a woody cover of 51 %.*

3.4 Discussion

3.4.1 Current trend of woody encroachment in African savannas

Over time, woody populations at individual sites undergo periods of growth and sometimes rapid dieback in response to disturbances and variation in environmental factors (Brandt, Tappan, et al., 2017). The wide spread of positive and negative changes in woody cover (Figure 3.5) is the result of this heterogeneity in growth stage and local conditions. However, this analysis points to a mean trend of ongoing woody encroachment for sites sampled across African savannas. Our estimated mean rate of change (0.25 %/year) was identical to the estimate in the meta-analysis by Stevens et al. (2017) even though the data used in that analysis covered other time periods and were more concentrated to the southern part of the continent. This reinforces the conviction of a consistent trend across African savannas. While our estimates were lower in some parts of East Africa, this was likely a result of the 2011 drought occurring within our relatively brief window of observation. In both the OLS and SAR regression analyses, water availability (potential cover – initial cover) and fire frequency were significant variables (Tables 3.1 & 3.2). Among the investigated variables, these are the ones that can be most clearly linked to current encroachment rates. As woody cover approaches its climatic maximum, water constraints slow growth and woody communities are more likely to suffer mortality through density-dependent regulation (Browning et al., 2008). Because of high competition from neighboring plants, individuals are more sensitive to droughts and interannual variation in rainfall. The role of fire in suppressing woody encroachment is well established. Frequent fires kill or top-kill smaller woody plants, thereby reducing the number of plants that reach a mature fire-tolerant size (Bond, 2008). The effectiveness by

which fires can suppress woody cover also depends on woody growth rates and thus water constraints. Higher growth rates lead to a higher likelihood for juvenile trees to reach a fire-tolerant size and escape the fire-trap (Wakeling et al., 2011). As our analysis avoided areas with high anthropogenic impacts, we found no relationship with population density (Tables 3.1 & 3.2). However, according to Brandt et al. (2017), there are substantial woody cover decreases in areas with high population growth due to deforestation and land clearing.

Change in precipitation and cattle density proved significant in the OLS regression, but these relationships could have been caused by spatial auto-correlation (Table 3.2). The low accuracy of livestock data at continental scales also makes it difficult to accurately estimate their influence in this type of analysis. While this analysis shows what factors control encroachment rates among individual sites, an explanation for the general trend of encroachment is still elusive. Woody encroachment is widespread across African savannas and neither strongly dependent on climatic zone nor soil texture (Tables 3.1 & 3.2). It is very possible that the hidden factor causing an overall increase in woody cover is the higher atmospheric CO_2 level, which has been proposed in several previous studies (Donohue et al., 2013; Higgins & Scheiter, 2012). If CO_2 acts as a global fertilizer, this could also increase potential woody cover (Stevens et al., 2016).

3.4.2 Derivation of potential woody cover based on change trajectories

The strong relationship between initial woody cover, MAP, and rates of woody cover change (Figure 3.5) shows that rainfall universally influences tree dynamics and growth, and not only by constraining the potential woody cover. Mean rates of woody

cover change are positively correlated to the difference between current and potential woody cover, suggesting that competition among trees is a key variable determining growth rates. A large gap between actual and potential cover leads to a surplus of water that boosts growth rates. While mesic savannas (MAP>~750 mm/year) are not considered water-limited in the sense that canopy closure is possible, their woody growth rates are nevertheless dependent on the difference between potential and initial woody cover. Conversely, a site with woody cover above its potential (possibly due to recent above-average rainfall) is more likely to experience water shortage and tree mortality. As this trend was consistent across intervals of MAP and initial woody cover, we were able to use it to derive a linear relationship for potential woody cover (Figure 3.6). While Sankaran et al. (2005) used a 99th quantile piecewise linear regression to derive potential cover, this method uses the woody cover change trajectories. The relationship we found had a similar slope to that in Sankaran et al. (2005) but was shifted to the right, possibly due to the influence of fire and browsing which can suppress woody cover growth rates. This approach also recognizes that episodic recruitment and rainfall variability can cause woody populations to temporarily over-shoot the potential cover based on long-term MAP, as opposed to the more rigid statistical method (the 99th quantile) used by Sankaran et al. (2005). Many sites in the dataset fell outside of both our and Sankaran's line, the majority of which came from areas of Somalia and Ethiopia (Figure 3.6a). The divergent pattern for these sites could be related to the bimodal rainfall distribution in the Horn of Africa. Plants are not only affected by the total rainfall amount but also its intra-annual distribution (Axelsson & Hanan, 2017; Good & Caylor, 2011), which can determine levels of infiltration and runoff as well as windows of opportunity for seedling growth.

As opposed to the potential cover estimated in Sankaran et al. (2005), we extended the relationship up to 100 % woody cover. The cap at ~80 % cover in Sankaran et al. (2005) emerged as a result of their methodology and the exclusive focus on savanna sites. The growth rate among sites with rainfall above 800 mm/year pointed to a point of attraction above 100 % (Figure 3.6a). Growth in woody cover is likely only slowed by space restriction as it nears canopy closure. Beyond canopy closure, water availability continues to impact forest communities by constraining above-ground woody biomass (Stegen et al., 2011).

3.5 Conclusions

We found that woody encroachment is ongoing and widespread across African savannas with a mean rate of 0.25 % per year. Although our results do not explain the overall trend, they show that change in woody cover is significantly related to a proxy for water availability (potential cover – initial cover) and fire frequency. The trend of higher encroachment rates with higher water availability (defined by the difference between actual and potential cover) was consistent across a range of mean annual precipitation from arid to mesic systems. Competition for water thus universally constrains tree growth, also in higher-rainfall (MAP>800 mm/year) savannas. Our approach to derive estimates of potential woody cover based on rates of canopy growth, and initial cover, demonstrates that temporal dynamics in woody populations can be used to infer resource limitations. Competition for water constrains tree population growth rates as canopy cover approaches potential cover and leads to higher mortality among populations that have over-shot their potential cover based on long-term average rainfall. The results of this study highlight the

central role of water availability and competition among trees in determining woody cover growth rates and potential canopy cover.

3.6 References

Ainsworth, E. A., & Long, S. P. (2005). What have we learned from 15 years of free-air CO2 enrichment (FACE)? A meta-analytic review of the responses of photosynthesis, canopy properties and plant production to rising CO2. *New Phytologist, 165*(2), 351-372.

Archer, S. R., Andersen, E. M., Predick, K. I., Schwinning, S., Steidl, R. J., & Woods, S. R. (2017). Woody plant encroachment: causes and consequences. In D. D. Briske (Ed.), *Rangeland Systems* (pp. 25-84): Springer.

Asner, G. P., Elmore, A. J., Olander, L. P., Martin, R. E., & Harris, A. T. (2004). Grazing systems, ecosystem responses, and global change. *Annu. Rev. Environ. Resour., 29*, 261-299.

Axelsson, C. R., & Hanan, N. P. (2017). Patterns in woody vegetation structure across African savannas. *Biogeosciences, 14*(13), 3239-3252. doi:10.5194/bg-14-3239-2017

Birhane, E., Treydte, A. C., Eshete, A., Solomon, N., & Hailemariam, M. (2017). Can rangelands gain from bush encroachment? Carbon stocks of communal grazing lands invaded by Prosopis juliflora. *Journal of Arid Environments, 141*, 60-67.

Bivand, R., Anselin, L., Berke, O., Bernat, A., Carvalho, M., Chun, Y., . . . Lewin-Koh, N. (2017). spdep: Spatial dependence: weighting schemes, statistics and models. In: R package version 06-11, URL https://CRAN.R-project.org/package=spdep.

Bond, W. J. (2008). What limits trees in C4 grasslands and savannas? *Annual Review of Ecology, Evolution, and Systematics, 39*, 641-659.

Bond, W. J., & Midgley, G. F. (2012). Carbon dioxide and the uneasy interactions of trees and savannah grasses. *Philosophical Transactions of the Royal Society B: Biological Sciences, 367*(1588), 601-612.

Brandt, M., Rasmussen, K., Peñuelas, J., Tian, F., Schurgers, G., Verger, A., . . . Fensholt, R. (2017). Human population growth offsets climate-driven increase in woody vegetation in sub-Saharan Africa. *Nature Ecology & Evolution, 1*, 0081.

Brandt, M., Tappan, G., Diouf, A. A., Beye, G., Mbow, C., & Fensholt, R. (2017). Woody vegetation die off and regeneration in response to rainfall variability in the West African Sahel. *Remote Sensing, 9*(1), 39.

Browning, D. M., Archer, S. R., Asner, G. P., McClaran, M. P., & Wessman, C. A. (2008). Woody plants in grasslands: post-encroachment stand dynamics. *Ecological Applications, 18*(4), 928-944.

Buitenwerf, R., Bond, W., Stevens, N., & Trollope, W. (2012). Increased tree densities in South African savannas:> 50 years of data suggests CO2 as a driver. *Global Change Biology*.

D'Odorico, P., Okin, G. S., & Bestelmeyer, B. T. (2012). A synthetic review of feedbacks and drivers of shrub encroachment in arid grasslands. *Ecohydrology, 5*(5), 520-530.

Dalle, G., Maass, B. L., & Isselstein, J. (2006). Encroachment of woody plants and its impact on pastoral livestock production in the Borana lowlands, southern Oromia, Ethiopia. *African Journal of Ecology, 44*(2), 237-246.

Daskin, J. H., Stalmans, M., & Pringle, R. M. (2016). Ecological legacies of civil war: 35-year increase in savanna tree cover following wholesale large-mammal declines. *Journal of Ecology, 104*(1), 79-89.

Donohue, R. J., Roderick, M. L., McVicar, T. R., & Farquhar, G. D. (2013). Impact of CO2 fertilization on maximum foliage cover across the globe's warm, arid environments. *Geophysical Research Letters, 40*(12), 3031-3035.

Doxsey-Whitfield, E., MacManus, K., Adamo, S. B., Pistolesi, L., Squires, J., Borkovska, O., & Baptista, S. R. (2015). Taking advantage of the improved availability of census data: a first look at the gridded population of the world, version 4. *Papers in Applied Geography, 1*(3), 226-234.

Ellis, E. C., & Ramankutty, N. (2008). Putting people in the map: anthropogenic biomes of the world. *Frontiers in Ecology and the Environment, 6*(8), 439-447.

Farr, T. G., Rosen, P. A., Caro, E., Crippen, R., Duren, R., Hensley, S., . . . Roth, L. (2007). The shuttle radar topography mission. *Reviews of Geophysics, 45*(2), 1-33. doi:10.1029/2005RG000183

Giglio, L., Loboda, T., Roy, D. P., Quayle, B., & Justice, C. O. (2009). An active-fire based burned area mapping algorithm for the MODIS sensor. *Remote Sensing of Environment, 113*(2), 408-420.

Good, S. P., & Caylor, K. K. (2011). Climatological determinants of woody cover in Africa. *Proceedings of the National Academy of Sciences, 108*(12), 4902-4907.

Hanan, N. P., Sea, W. B., Dangelmayr, G., & Govender, N. (2008). Do fires in savannas consume woody biomass? A comment on approaches to modeling savanna dynamics. *The American Naturalist, 171*(6), 851-856.

Hengl, T., Heuvelink, G. B., Kempen, B., Leenaars, J. G., Walsh, M. G., Shepherd, K. D., . . . Tamene, L. (2015). Mapping soil properties of Africa at 250 m resolution: Random forests significantly improve current predictions. *PloS one, 10*(6), e0125814.

Higgins, S. I., & Scheiter, S. (2012). Atmospheric CO2 forces abrupt vegetation shifts locally, but not globally. *Nature, 488*(7410), 209-212.

Honda, E. A., & Durigan, G. (2016). Woody encroachment and its consequences on hydrological processes in the savannah. *Phil. Trans. R. Soc. B, 371*(1703), 20150313.

Huffman, G. J., Bolvin, D. T., Nelkin, E. J., Wolff, D. B., Adler, R. F., Gu, G., . . . Stocker, E. F. (2007). The TRMM multisatellite precipitation analysis (TMPA): Quasi-global, multiyear, combined-sensor precipitation estimates at fine scales. *Journal of Hydrometeorology, 8*(1), 38-55.

Kgope, B. S., Bond, W. J., & Midgley, G. F. (2010). Growth responses of African savanna trees implicate atmospheric [CO2] as a driver of past and current changes in savanna tree cover. *Austral Ecology, 35*(4), 451-463.

Kulmatiski, A., & Beard, K. H. (2013). Woody plant encroachment facilitated by increased precipitation intensity. *Nature Climate Change, 3*, 833-837. doi:10.1038/nclimate1904

Lyon, B., & DeWitt, D. G. (2012). A recent and abrupt decline in the East African long rains. *Geophysical Research Letters, 39*(2).

Moran, P. A. (1950). Notes on continuous stochastic phenomena. *Biometrika, 37*(1/2), 17-23.

Morgan, J. A., Milchunas, D. G., LeCain, D. R., West, M., & Mosier, A. R. (2007). Carbon dioxide enrichment alters plant community structure and accelerates shrub growth in the shortgrass steppe. *Proceedings of the National Academy of Sciences, 104*(37), 14724-14729.

Quesada, C., Phillips, O., Schwarz, M., Czimczik, C., Baker, T., Patino, S., . . . Almeida, S. (2012). Basin-wide variations in Amazon forest structure and function are mediated by both soils and climate. *Biogeosciences, 9*(6).

Roques, K., O'connor, T., & Watkinson, A. (2001). Dynamics of shrub encroachment in an African savanna: relative influences of fire, herbivory, rainfall and density dependence. *Journal of Applied Ecology, 38*(2), 268-280.

Sankaran, M., Augustine, D. J., & Ratnam, J. (2013). Native ungulates of diverse body sizes collectively regulate long-term woody plant demography and structure of a semi-arid savanna. *Journal of Ecology, 101*(6), 1389-1399.

Sankaran, M., Hanan, N. P., Scholes, R. J., Ratnam, J., Augustine, D. J., Cade, B. S., . . . Ludwig, F. (2005). Determinants of woody cover in African savannas. *Nature, 438*(7069), 846-849.

Stegen, J. C., Swenson, N. G., Enquist, B. J., White, E. P., Phillips, O. L., Jørgensen, P. M., . . . Núñez Vargas, P. (2011). Variation in above-ground forest biomass across broad climatic gradients. *Global Ecology and Biogeography, 20*(5), 744-754.

Stevens, N., Erasmus, B., Archibald, S., & Bond, W. (2016). Woody encroachment over 70 years in South African savannahs: overgrazing, global change or extinction aftershock? *Phil. Trans. R. Soc. B, 371*(1703), 20150437.

Stevens, N., Lehmann, C. E., Murphy, B. P., & Durigan, G. (2017). Savanna woody encroachment is widespread across three continents. *Global Change Biology, 23*(1), 235-244.

Van Auken, O. (2009). Causes and consequences of woody plant encroachment into western North American grasslands. *Journal of Environmental Management, 90*(10), 2931-2942.

Wakeling, J. L., Staver, A. C., & Bond, W. J. (2011). Simply the best: the transition of savanna saplings to trees. *Oikos, 120*(10), 1448-1451.

Wint, W., & Robinson, T. P. (2007). *Gridded livestock of the world 2007*: Food and Agriculture Organization of the United Nations Rome.

4 MODELING SAVANNA WOODY STRUCTURE AND PATTERNING

Abstract

The vegetation structure in African savannas is shaped by different ecosystem processes, including fire, overland flow of surface water, and competition and facilitation between neighboring plants. The effect of many processes changes along precipitation and soil texture gradients, causing non-linear effects in plant responses. Here, we present a modeling study aimed at reproducing and explaining trends in vegetation structure in relation to environmental factors. The savanna model can reproduce several trends in vegetation structure, earlier estimated using very high resolution satellite remote sensing. In agreement with earlier observations, we find that increases in woody cover in relation to rainfall is more a result of increasing crown sizes than tree densities across the full precipitation gradient (150-1400 mm/year). We also reproduced trends in increasing woody plant aggregation in relation to aridity, high precipitation variability, and finer soil texture. Variation in interannual precipitation had a large impact on all analyzed woody properties. Woody plant aggregation rose sharply during dieback events, indicating that facilitative plant interactions are strongly tied to decreases in precipitation.

4.1 Introduction

Models are commonly used tools for experimentation and building credibility around a specific theoretical perspective. The coupling of modeled and observed data can be especially powerful as it can offer explanations for observed trends in the form of mechanisms and feedbacks. This study focuses on African savannas, which are characterized by tree-grass interactions, frequent fires, and high variability in rainfall. They

are complex ecosystems and models can be useful for disentangling and explaining the key factors that influence vegetation structure in these landscapes.

Several earlier savanna models focus on explaining mechanisms for tree-grass coexistence, often with focus on either fire or the water cycle. The models by Higgins et al. (2000) and Staver & Levin (2012) describe interactions between trees and grasses in fire-dominated savannas. Here, abundant grass growth fuels frequent fires, which suppress woody plant dominance. Other models, for example the work by Laio, Porporato, Fernandez-Illescas et al. (2001), focus on capturing the water cycle in great detail to explain tree-grass dynamics in drier systems where fires are less common. Here, soil type plays a key role controlling infiltration, retention, and soil water potential. These types of models are sometimes spatially explicit, but more often model tree and grass populations as numbers representative of a particular landscape size. A third group of models focus on describing plant dynamics during the formation of periodic vegetation patterns (PVPs) in arid systems (Rietkerk et al., 2002; von Hardenberg et al., 2010). The key here is to capture both competition for soil water and overland flows from bare to vegetated patches. While these models are spatially explicit, they generally model vegetation as one entity and do not separate woody plants from grasses.

The above-mentioned models are largely successful at explaining observed vegetation structures and patterns in the ecosystems they set out to simulate. To construct a new model that works in both arid systems and mesic fire-prone systems, and for simulating plant interactions and the spatial pattern of the vegetation, it is necessary to incorporate elements from all these models. Such a new model can simulate variation in vegetation structure across the full range of mean annual precipitation (MAP), from the

arid to the wet, and also capture ecosystem responses to long-term changes in precipitation. The differences in the temporal scale of important ecosystem processes cause some problems. The vegetation structure of savannas is shaped over several decades, if not centuries, and the model needs to run a long time before reaching a state that is representative of the set environmental conditions. Models capturing the effects of fire and maturation of savanna trees therefore often simulate the development over hundreds of years (Higgins et al., 2000). On the other hand, models capturing soil water dynamics in drylands usually require much shorter time steps, sometimes simulating the drying and wetting of the soil over individual rainfall events (Porporato et al., 2001).

This study aimed to model the vegetation structure at 876 African savanna sites, previously described by Axelsson & Hanan (2017), with the purpose of capturing and explaining the main ecosystem processes that shape the vegetation. That study used very high resolution satellite imagery and a crown delineation method to estimate woody cover, tree density, mean crown sizes, and the level of spatial aggregation among woody plants at each site. Some of the key findings of the earlier study include: (1) increases in woody cover along the rainfall gradient was more a result of increasing crown sizes than variation in the number of trees; (2) the level of aggregation among woody plants increased with high rainfall variability, while also being influenced by MAP, soil texture, and slope; and (3) woody cover and mean tree crown size had a unimodal relationship with sand content where mid-textured soils featured higher cover and larger trees.

Modeling variation in plant density, crown sizes, and spatial tree patterns requires simulating the growth of individual trees using a spatially explicit model. We modeled responses in the vegetation to the same environmental factors as in the remote

sensing study: rainfall, soil texture, slope, and fire. Factors we lack good data for, such as grazing and browsing pressure, were assumed constant for all sites.

4.2 Model description

The developed savanna model simulates establishment, growth and mortality of herbaceous vegetation and individual trees over monthly time steps in a 200x200 m landscape. It was implemented in R and C code and allows variation in monthly rainfall rates, soil type, slope, fire, and grazing. Water content and above-ground herbaceous biomass are modeled per 1 m² cells, whereas woody plants are represented by crown circles that can establish and grow anywhere on the underlying grid. To avoid any edge effects, the model uses periodic boundary conditions, and all neighborhood effects that would affect cells or trees outside of the grid are transferred to the opposite side of the boundary. A list of all model variables and coefficients is found in Appendix B.

4.2.1 Vegetation attributes

The model offers support for different woody functional types, but only one type (a typical savanna tree) was used to generate the results presented in this paper. We have separated herbaceous vegetation into living and dead grasses. Dead grasses do not consume water, but are important as fuel for fires and provide positive effects in the form of shading and enhancing infiltration (Resco de Dios et al., 2014). Trees and herbaceous vegetation are characterized by the attributes shown in Table 4.1.

Table 4.1 Attributes of woody plants and herbaceous vegetation as used in the model.

Woody plant attributes	**Description**	**Value**
$\mathrm{nSeedlings}_W$	Number of seedlings dispersed each month	25

$Crown\ radius_{seedling}$	Crown radius for seedlings	0.03 m
$Z_{seedling}$	Root depth of seedlings	200 mm
$Max\ radius_W$	Maximum crown radius	6 m
Z_{max}	Maximum root depth	2200 mm
LAI_W	Leaf area index of the canopy	2
$Water\ use_W$	Water use per woody root cover	8 mm
GR_W	Maximum monthly radial growth rate of the crown	0.012 m
Inf_W	Controls the positive effect on infiltration rates per woody root cover	0.4
$LSTOL_W$	Light stress tolerance; controls growth restrictions and mortality from insufficient light conditions	0.3
$WSTOL_W$	Water stress tolerance; controls growth restrictions and mortality from water stress	0.15
$FTOL_W$	Fire tolerance; controls the chance to survive high fire intensities.	1.0
$Crown\ radius_W$	Radius of crown (m); individual for each plant	
$Root\ radius_W$	Radius of root system calculated as $1.5 \cdot Crown\ radius_W$ (m)	
Z_W	Depth of root system calculated as $Z_{seedling} + (Z_{max} - Z_{seedling})\sqrt{(Crown\ radius_W - Crown\ radius_{seedling})/Max\ rad}$	

Herbaceous attributes	**Description**	**Value**
Z_H	Herbaceous root depth	400 mm
SLA_H	Specific leaf area	8 m² per kg
$Water\ use_H$	Monthly water use by living grasses	5 mm per kg/m²
GR_H	Maximum monthly growth rate of living grasses	0.02 kg/m²
MR_H	Maximum monthly mortality rate of grasses	0.1 kg/m²
Inf_H	Controls the positive effect on infiltration rates from both living and dead grasses	0.1/kg/m²
DR_H	Decomposition rate of dead grasses	5% per month
$LSTOL_H$	Tolerance to low light conditions	0.12
$WSTOL_H$	Tolerance to water stress	0.06

4.2.2 Relative soil moisture and soil attributes

The relative soil moisture, s (range 0 to 1), is calculated based on the soil water content, Wat (mm), the soil depth, Z_r (set to 2200 mm), and soil porosity, n (eq. 1). This

soil moisture term is used in several previous models and follows the approach by Laio, Porporato, Ridolfi et al. (2001). Following their calculation of the water balance, we base the relationships between s and water potentials on empirical relationships with soil texture from Clapp and Hornberger (1978) using the power curve of soil moisture (eq. 2).

$$s = \frac{Wat}{nZ_r} \quad \text{eq. 1}$$

$$\Psi_s = \bar{\Psi}_s s^{-b} \quad \text{eq. 2}$$

Here, $\bar{\Psi}_s$ and b are texture-specific coefficients and Ψ_s is the water (matric) potential. Solving s yields the relative soil moisture for different water potentials. By varying the soil texture class, we control the soil class specific attributes in Table 4.2.

Table 4.2. Soil attributes specific to each texture class. Values for each class are based on empirical relationships derived by Clapp and Hornberger (1978). Values for matric potentials are from Laio, Porporato, Ridolfi et al. (2001), except for field capacity, which is commonly set to 0.033 MPa. We used the same s^* and s_w for both woody and herbaceous vegetation.

Soil attributes	**Description**	**Matric potential**
n	Porosity; the available space for water in the soil	
Ks	Saturated hydraulic conductivity; controls infiltration rates	
s_{fc}	Field capacity; controls soil water drainage	-0.033 Mpa
s^*	Point where plants start to close stomata	-0.03 MPa
s_w	Plant wilting point	-3 MPa
s_h	Hygroscopic point	-10 MPa

4.2.3 Infiltration properties

The infiltration capacity of a cell is influenced by soil texture, nearby woody plants, and both living and dead herbaceous vegetation. Vegetation enhances infiltration

by increasing macroporosity around roots and increasing organic matter in the soil. The influence of woody plants is represented by the mean woody root cover inside a 4.5 m radius around the center of each cell.

$$Inf_{ij} = Inf_W \cdot Woodyrootcover_{mean\ 4.5m} + Inf_H \cdot H_{ij} + Inf_S \cdot Ks \quad \text{eq. 3}$$

H is the herbaceous biomass (kg/m²), whereas Inf_W and Inf_H scale the influence from woody and herbaceous vegetation. The coefficient Inf_S (set to 10) scales the influence from the soils saturated hydraulic conductivity and is the same for all soil types.

4.2.4 Rainfall and diffusion of surface water

Precipitation falls, creates overland flows, and infiltrates at time scales far shorter than the monthly time steps used by the model. If all the monthly precipitation was applied at once, the water holding capacity of the soil would be overwhelmed. To incorporate these processes, we adjusted the amount of precipitation (P) falling and creating surface water (Q) to reflect a typical week of the month:

$$Q = P_{monthly} \cdot 12/52 \quad \text{eq. 4}$$

Coefficients for water consumption have therefore been adjusted accordingly to reflect weekly consumption. The surface water will move across the landscape and create higher water content in cells with higher infiltration capacity. Low infiltration capacities (due to fine-textured soils and little vegetation) will cause the surface water to move further and aggregate in cells with higher infiltration capacity. The process is composed of two steps that iterate. In the first (eq. 5), water infiltrates, and in the second (eq. 6), water diffuses between neighboring cells at a rate determined by D_Q (set to 0.8). Here, i, j denote the cell coordinates. If not all water has infiltrated after 60 iterations, the process is terminated and

the remaining water is assumed to leave the system as runoff. The maximum number was set following calibration with the observed data (Axelsson & Hanan, 2017), which exhibited a drop in woody cover on fine-textured soils, and we thus assume that runoff generation is a significant process in causing the observed drop. Less vegetation, clayey soils, and high rainfall in a month thereby contribute to both spatial redistribution of water and runoff generation.

$$Q_{i,j} = Q_{i,j} - Inf_{i,j} \qquad (Inf_{i,j} = Q_{i,j} \text{ if } Q_{i,j} < Inf_{i,j}) \quad \text{Infiltration} \qquad \text{eq. 5}$$

$$Q_{i,j} = Q_{i,j} - D_Q Q_{i,j} + \frac{D_Q}{4}\left(\sum_{\delta=+/-1}\left[Q_{i,j+\delta} + Q_{i+\delta,j}\right]\right) \quad \text{Diffusion (flat terrain)} \qquad \text{eq. 6}$$

On flat terrain, surface water diffuses equally in all direction. The effect of slope is to diffuse more water downhill than in other directions. This effect is applied linearly up to 1% slope, where all surface water is directed in a single direction.

4.2.5 Light availability

Light availability affects evaporation and plant light stress. We use Beer's law to calculate a light availability index that ranges from 0 to 1:

$$LightA_{ground} = e^{-k_{ext}(H \cdot SLA_H + Woodycover_{mean\ 4.5m} \cdot LAI_W)} \qquad \text{eq. 7}$$

The value for the light extinction coefficient k_{ext} (set to 0.5) was taken from estimates in grasslands and savannas by Zhang et al. (2014). The influence of woody plants is represented by the mean woody cover in a 4.5 m radius around cell centers multiplied by the leaf area index, LAI_W . Overlapping crowns are summarized so that $Woodycover_{mean\ 4.5m}$ can exceed 1 in dense patches. Using the same type of index, we

also calculate the light availability individually for each tree crown, $LightA_w$, based on other overlapping tree crowns. $Woodycover$ is then calculated as the woody cover of larger trees within the area of the plant's crown circle. As tree heights are not modeled, we assume larger crowns are taller and will shade overlapping smaller trees.

4.2.6 Evaporation of top-soil water

Evaporation is based on the relative soil moisture in the top soil layer (s_{top}) down to the soil depth Z_{evap} (set to 100 mm). It is calculated after newly fallen rain, Wat_{new}, has infiltrated and drained to field capacity (eq. 8). The maximum evaporation, E_{max}, is based on light availability and an evaporation coefficient, k_{evap} (set to 0.06; eq. 9). Shading decreases evaporation (Metzger et al., 2014; Raz-Yaseef et al., 2010), and here we let shading from both woody and herbaceous vegetation affect evaporation rates. The evaporation (mm) is constant above the wilting point and then linearly decreases to the hygroscopic point (eq. 10); an approach borrowed from (Laio, Porporato, Ridolfi, et al., 2001).

$$s_{top} = s + \frac{Wat_{new}}{nZ_{evap}} \quad \text{(cannot exceed } s_{fc}\text{)} \qquad \text{eq. 8}$$

$$E_{max} = n \cdot Z_{evap} \cdot LightA_{ground} \cdot k_{evap} \qquad \text{eq. 9}$$

$$Evap = \begin{cases} 0 & if \quad s_{top} \leq s_h \\ \frac{s_{top} - s_h}{s_w - s_h} \cdot E_{max} & if \quad s_h < s_{top} \leq s_w \\ E_{max} & if \quad s_w < s_{top} \end{cases} \qquad \text{eq. 10}$$

4.2.7 Water consumption and plant stress

Herbaceous vegetation consumes water in relation to the biomass of living grasses, H_{living}, in a cell (eq. 11), whereas woody plants consume water in relation to their

root coverage (eq. 12). The woody root cover of a cell is calculated as the sum of the coverage of the individuals with roots in the cell and can thus exceed 1.

$$Wat_H = Water\ use_H \cdot H_{living} \quad \text{eq. 11}$$

$$Wat_W = Water\ use_W \cdot Woody\ rootcover \quad \text{eq. 12}$$

Plant water stress is calculated after drainage to field capacity (eq. 13), evaporation of top-soil water, and water consumption by herbaceous vegetation (eq. 14). It is assumed that consumption by herbaceous vegetation mainly takes place in the upper part of the soil profile, thereby suppressing the growth of woody plants by reducing water flow to deeper soil depths (Holdo & Brocato, 2015; Riginos, 2009). Woody plants have more variable root depths, and we apply competition from woody plants on a more long-term basis by reducing the soil moisture at the end of each month. Plant water stress is calculated following Porporato et al. (2001), where the stress level, WS_H, ranges from 0 to 1 (eq. 15).

$$s_{herb} = s + \frac{Wat_{new}}{nZ_H} \text{ (cannot exceed } s_{fc}) \quad \text{eq. 13}$$

$$s_{herb} = s_{herb} - \left(\frac{Evap + Wat_H}{nZ_H}\right) \quad \text{eq. 14}$$

$$WS_H = \begin{cases} 1 & if \quad s_{herb} \leq s_w \\ \left[\frac{s^* - s_{herb}}{s^* - s_w}\right]^3 & if \quad s_w < s_{herb} \leq s^* \\ 0 & if \quad s^* < s_{herb} \end{cases} \quad \text{eq. 15}$$

Water stress for woody plants is calculated using the same equations as for herbaceous vegetation. The rooting depth is then replaced by the individual rooting depth for each plant, Z_W, and we base the stress level on the water balance in the cell where the stem is located. This approach results in herbaceous vegetation and younger trees, with more shallow root systems, becoming more dependent on recent rainfall, Wat_{new}, than do adult trees.

In addition to water stress, both herbaceous and woody plants can suffer stress induced by insufficient light conditions (Valladares & Niinemets, 2008). Holmgren et al. (2012) found hump-back shaped plant responses to drought under different irradiance levels indicating that intermediate light conditions are often optimal. This is reflected in the model, where low light availability increases light stress and high light availability increases evaporation leading to higher water stress. Light stress, LS, is calculated from light availability (eq. 16), creating an exponential response curve which is then capped at 1. Light stress for herbaceous vegetation is based on light conditions at the ground level, $LightA_{ground}$, whereas light availability for trees, $LightA_w$, is based on overlapping tree crowns as described in section 4.2.5. The overall plant stress level, PS, is a function of both light stress and water stress (eq. 17), resulting in a stress index ranging from 0 to 1.

$$LS = 2/e^{10\cdot(LightA-0.05)} \quad \text{(cannot exceed 1)} \qquad \text{eq. 16}$$

$$PS = LS + WS - (LS \cdot WS) \qquad \text{eq. 17}$$

4.2.8 Plant establishment, growth, and mortality

Establishment of new woody plants is applied every month by dispersing $\mathrm{nSeedlings}_W$ number of seedlings at random positions across the landscape. Their initial size and root depth are determined by $Crown\ radius_{seedling}$ and $Z_{seedling}$. Whether plants grow or suffer mortality depends on their stress levels as well as their tolerance of light and water stress. If the tolerances to both water and light stress are higher than the respective stress levels, plants will grow in relation to their growth rates and the overall stress level (eq. 18 & 20). Grasses will die if either of the stress thresholds is exceeded, and

the die-off is in proportion to the stress level, PS_H (eq. 19 & 20). Dead grasses will continue to be a part of the herbaceous biomass and decompose at the rate DR_H (eq. 21). In the case of woody plants, the maximum crown size, $Max\ radius_W$, restricts their sizes (eq. 22). For herbaceous vegetation, self-shading limits excessive growth (Zimmermann et al., 2010). The herbaceous biomass is part of equation 7 for calculating $LightA_{ground}$, which controls light stress for grasses, and this constrains the maximum amount of grasses. Mortality risks for trees, $pMort_W$, are based on the difference between water stress, light stress, and their respective stress thresholds (eq. 23 & 24). If a mortality risk is larger than a random number ranging from 0 to 1, the tree will suffer mortality.

$$Growth_H = GR_H \cdot (1 - PS_H) \quad if \quad LS_H < LSTOL_H \ and \ WS_H < WSTOL_H \qquad \text{eq. 18}$$

$$Mort_H = MR_H \cdot PS_H \quad if \quad LS_H > LSTOL_H \ or \ WS_H > WSTOL_H \qquad \text{eq. 19}$$

$(cannot\ exceed\ H_{living})$

$$H_{living} = H_{living} + Growth_H - Mort_H \qquad \text{eq. 20}$$

$$H_{dead} = H_{dead} + Mort_H - (H_{dead} \cdot DR_H) \qquad \text{eq. 21}$$

$$Growth_W = GR_W \cdot (1 - PS_W) \cdot \left(1 - \left(\frac{Crown\ radius_W}{Max\ radius_W}\right)^2\right) \quad if \ LS_W < LSTOL_W \ and \ WS_W < WSTOL_W \qquad \text{eq. 22}$$

$$pMort\ LS_W = LS_W - LSTOL_W \qquad \text{eq. 23}$$

$$pMort\ WS_W = WS_W - WSTOL_W \qquad \text{eq. 24}$$

4.2.9 Fire and grazing disturbances

In the case of a fire, all herbaceous plants (living and dead) burn and generate a fire intensity (FI) in proportion to their biomass. Byram's fireline intensity equation (eq. 25) states that the intensity (MW/m) is in proportion to the energy content of grasses (set

to 20 kJ/g), the rate of spread (set to 1 m/s), and the amount of fuel (Byram, 1959). Here, the fuel content is set to the mean herbaceous biomass within a 2.5 m radius from the center of each cell. The tolerance of trees to withstand a fire is a function of the tolerance of the species, $FTOL_W$, and their sizes. The risk of mortality is calculated according to equation 26, which forms a sigmoidal response curve, as illustrated in Figure 4.1.

$$FI = H_{mean\ 2.5m} \cdot \text{EnergyContent} \cdot \text{RateOfSpread} \qquad \text{eq. 25}$$

$$pMort\ Fire = 0.5 - 0.5 \cdot \frac{1.2 \cdot FTOL_W \cdot Crown\ radius_W - 0.6 \cdot FI + 3}{\sqrt{10 + (1.2 \cdot FTOL_W \cdot Crown\ radius_W - 0.6 \cdot FI + 3)^2}} \qquad \text{eq. 26}$$

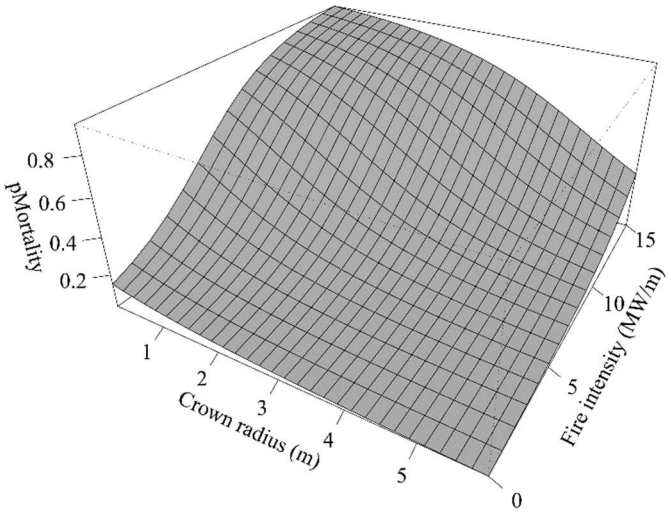

Figure 4.1 Woody plant mortality risk in relation to plant size and fire intensity. The sigmoidal response curve creates a fire-trap effect where the mortality risk varies greatly with plant size (Bond, 2008).

Grazing is modeled as a monthly removal of grasses in each cell (% of herbaceous biomass). More grasses usually mean more grazers, and by calculating it as a percentage of available grasses, we can apply the same grazing regime across the rainfall gradient. Herbivores are assumed to graze preferentially on living grasses. If living grasses are not sufficient to satisfy the grazing rate, dead grasses are consumed.

4.2.10 Lateral diffusion of remaining soil moisture

By the end of each month, water losses through plant consumption and evaporation are subtracted from the relative soil moisture, and water exceeding the field capacity will drain (eq. 27). All the water in the soil column is thereby vertically spread out homogenously. There is also a lateral homogenization process, whereby water moves to equalize local differences in water potentials. This is modeled by diffusing the relative soil moisture 20 times using equation 6 with the diffusion coefficient, D_Q, set to 0.1.

$$s = s + \frac{Wat_{new} - Evap - Wat_H - Wat_W}{nZ_r} \qquad \text{(cannot exceed } s_{fc}\text{)} \qquad \text{eq. 27}$$

4.2.11 Realism of the model

The model was designed to offer an explanation for the trends and patterns found in Axelsson & Hanan (2017), and we experimented with different mechanisms in order to reproduce the same relationships with environmental factors. It was important to run the model with monthly time steps to capture seasonal fluctuations in rainfall, but also to incorporate processes that occur on hourly and daily timescales such as overland flows and soil drainage. This mismatch in time-scales meant that it was necessary to adjust some variable values, for example water consumption by trees and grasses, to make the different processes work together. Certain concepts, such as the tolerance of larger trees to withstand

fire and the ability of plants to increase infiltration rates, are well described in the literature, but without definitive numbers to use. Our aim was thus not to model every detail realistically, but to capture and describe the main processes that control woody vegetation structure and pattern formation in savannas. We also recognize that some potentially important factors, such as browsing, temperature, and variation in tree characteristics, are left out in this analysis.

4.3 Data and Methodology

To compare modeled landscapes with real observations, we used estimates of woody vegetation properties at 876 African savanna sites described in Axelsson & Hanan (2017). That study used very high resolution satellite imagery and a tree crown delineation method to estimate woody cover, tree density, mean crown size, and the level of spatial aggregation among trees. The image dates varied between late 2011 and early 2016. We used the following data, extracted for each site, as input to the model:

1. Monthly fire event data from the MODIS MCD64A1 collection 5.1 burned area product (500 m resolution) for the years 2001–2015 (Giglio et al., 2009). In the regression analysis described below, we used fire frequency derived from this time series.
2. Monthly precipitation from the Tropical Rainfall Measuring Mission (TRMM) 3B42 v7 product (0.25º resolution) (Huffman et al., 2007). Data were extracted using the bilinear interpolation method, and we used the years 2001-2015 to feed the model with synchronized precipitation and fire event time series. These data

were also used to calculate MAP and precipitation variability (the coefficient of variation (cv) of the time series) for use in the regression analysis described below.

3. Soil texture data came from the ISRIC/AfSIS soil property maps of Africa (250 m resolution; top 5 cm of the soil profile) (Hengl et al., 2015). As the model input variable is soil texture class, we used the map's estimates of clay, silt, and sand content together with the mean estimates of these categories for each soil class in (Cosby et al., 1984) and picked the soil texture class as the one with the closest match for each site.
4. Slope (%) was derived from the SRTM v2 elevation data (3 arcsec resolution) (Farr et al., 2007) using a kernel size of 10 after having smoothed the elevation data with a low-pass filter of width 7. As the model input range for slope is limited to 0-1 %, we truncated all higher values to 1.

To estimate the vegetation structure at each site, we ran the model for 60 years and repeated the 15-year time series of precipitation and fire event data during the running time. The initial landscapes were bare of vegetation, but had soil moisture at field capacity, which gave the vegetation an initial growth boost and facilitated early establishment of trees. The grazing pressure was set to 3 % for all sites. At the end of each site simulation, we saved woody cover, woody plant density (plants per hectare), mean crown diameter (m), woody plant aggregation (Besag's L transformation of Ripley's K at 20 m (Besag, 1977; Ripley, 1977)), and herbaceous biomass (kg/m²) from the modeled landscapes. Positive values of Besag's L-statistic indicate an aggregated plant pattern, whereas negative values indicate regularly spaced plants. As the variables vary seasonally, we used the mean values from the final 12 months. For crown diameter, plant density, and

aggregation, we filtered out all woody plants <1 m crown radius, to reduce the impact from smaller trees and better conform to the results from the remotely sensed estimates that could not detect small trees (Axelsson & Hanan, 2017).

To compare the responses to environmental factors (MAP, precipitation cv, sand content, slope, and fire frequency) for both the modeled and observed landscapes we used boosted regression trees (BRT's, in the dismo R package). The settings in the BRT models were family=Gaussian, tree complexity=3, learning rate=0.01, and bag fraction=0.5.

4.4 Results

The responses in woody vegetation properties to environmental factors (Figure 4.2) indicate that variation in woody cover and mean crown sizes are strongly dependent on MAP, both in the observed and modeled data. The modeled tree densities have a higher variability and follow MAP in the dry end, but later reach an asymptote. Precipitation variability, sand content, and slope have only minor relative influences over woody cover and crown sizes across the modeled landscapes, whereas density is negatively influenced by higher rainfall variability. The effect of fire frequency is negative on woody cover and tree density and has a unimodal response curve for mean crown size (see Figure 4.3 for explanation). We do not have observed results for herbaceous biomass, but show the modeled results because of its interactions with woody plants. It is non-linearly related to MAP, with an increasing trend in the dry end before being suppressed by woody vegetation (Figure 4.2). The least amount of grasses is found in landscapes with a closed woody canopy, where light limitations are detrimental to grass growth. Aggregation of woody

plants (L-statistic at 20 m) is higher in dry systems with high rainfall variability and on fine-textured soils in accordance with the observed data (Figures 4.4 & 4.5). The BRT model showed higher aggregation on flatter ground in the observed data, which was not reproduced by the model.

The model reproduced the general trend for the effect of sand content on woody cover and plant aggregation, but the relative influence of soil type was generally low for the modeled sites (Figure 4.2). This might be because the relationship changes with the rainfall gradient (Figure 4.5) and may also be related to how the relative influences in the BRT models are calculated. The relative influences are partly based on how many times a variable is selected for splitting in the BRT model (Elith et al., 2008). For the modeled sites, the sand content was grouped into soil type bins, and this reduced complexity in the data may negatively affect the relative influences. To test this, we replaced the original sand content values with the binned values also for the observed dataset, and this resulted in dramatically lower relative influences.

Correlations between modeled woody vegetation properties and the estimates from satellite data (Figure 4.6) indicate fair agreement for woody cover and mean crown sizes and no agreement for tree density and aggregation. Woody cover and crown sizes have higher correlation with environmental factors through their strong, relatively linear, relationship with MAP (Axelsson & Hanan, 2017), which facilitates the match between observed and modeled landscapes. Tree density and aggregation, on the other hand, are characterized by non-linear responses and weaker correlation with environmental factors (Axelsson & Hanan, 2017).

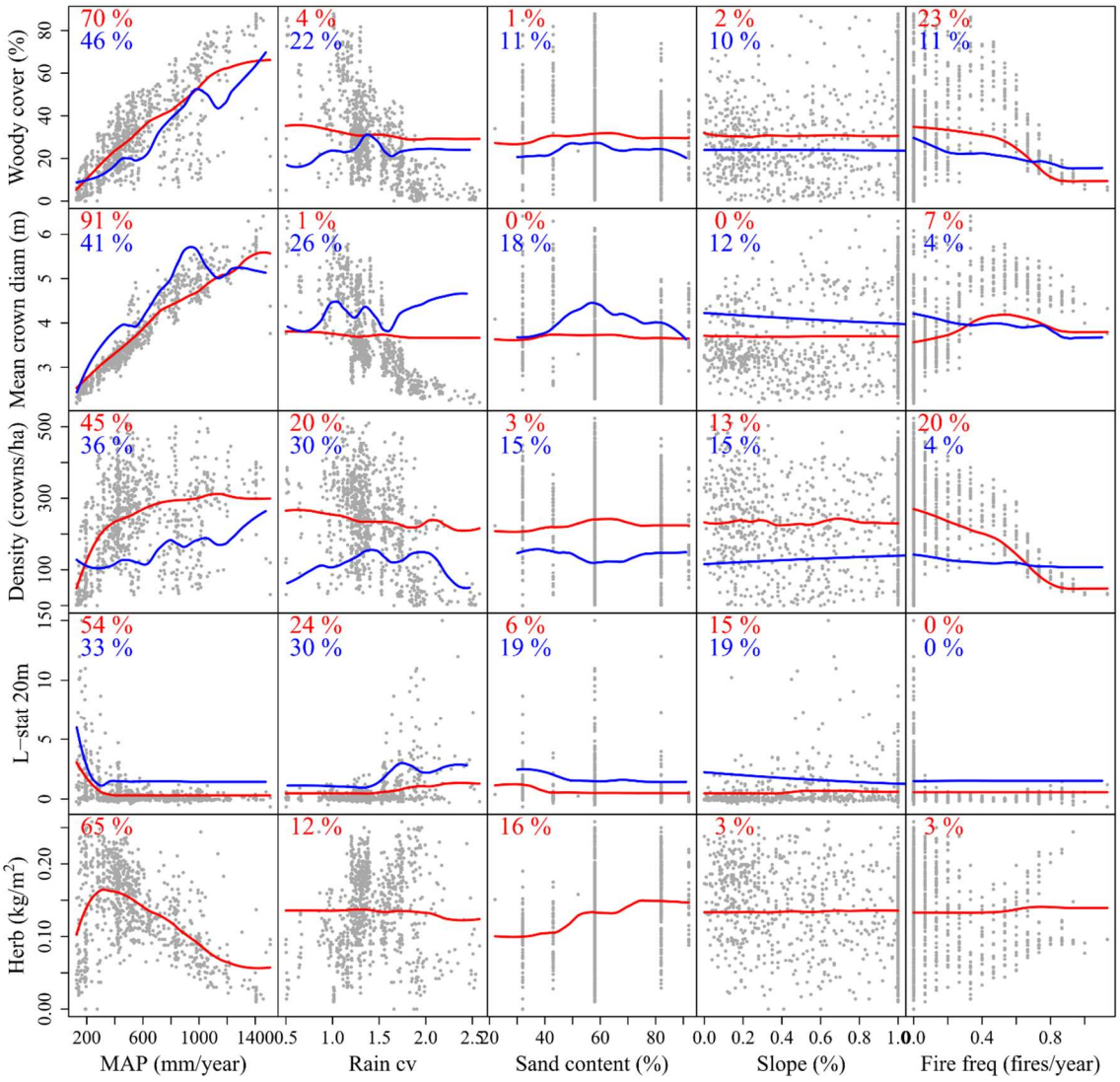

Figure 4.2 BRT responses ("partial dependencies") for modeled sites (red lines) and estimates from satellite data (blue lines). The lines represent responses to environmental factors when accounting for the average effect of the other four factors. The respective relative influences for each environmental factor (%) are shown in the top-left corner of each graph using the same color coding. Gray dots represent the modeled values for the 876 African savanna sites. Note that for the slope variable, the observed values range up to 14 %, whereas slope values in the model were capped at 1. We therefore only display the first part (0-1 %) of the observed BRT responses for slope.

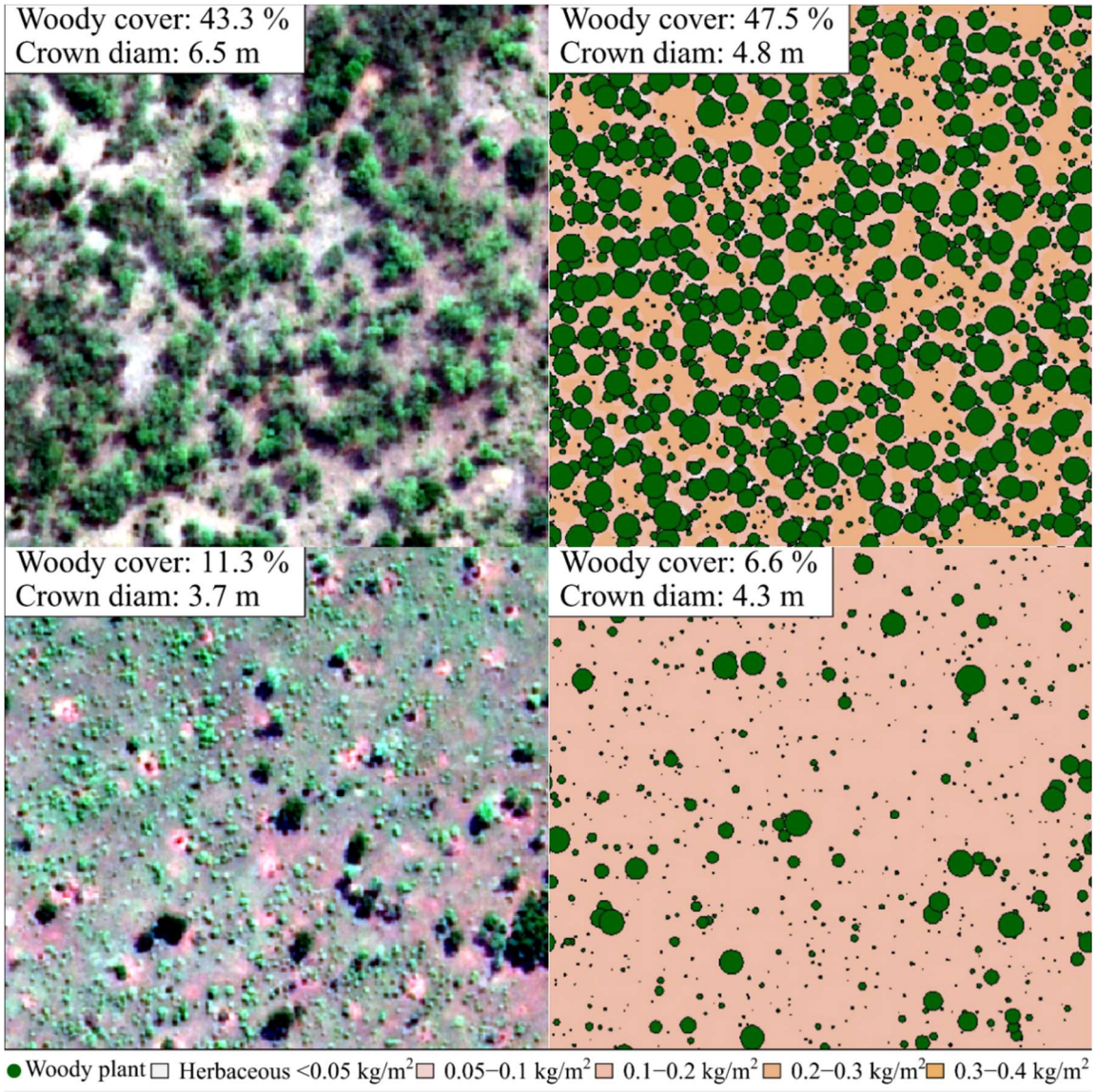

Figure 4.3 Examples of observed and modeled mesic savannas in South Sudan with different fire frequencies. The top site (Lat. 6.680127, Long. 30.96909, MAP 834 mm/year) and the bottom site (Lat. 6.517448, Long. 30.92804, MAP 855 mm/year) had fire frequencies at 0.5 and 1.1 fires per year, respectively. At medium fire frequency, the fires kill many of the smaller trees which also improves water availability for the fire-tolerant larger trees. This leads to an increase in mean crown size at medium fire frequencies among the modeled landscapes. At the higher fire frequency, few trees escape the fire-trap

and the tree population is dominated by the smaller, suppressed plants, leading to a reduction in mean crown size.

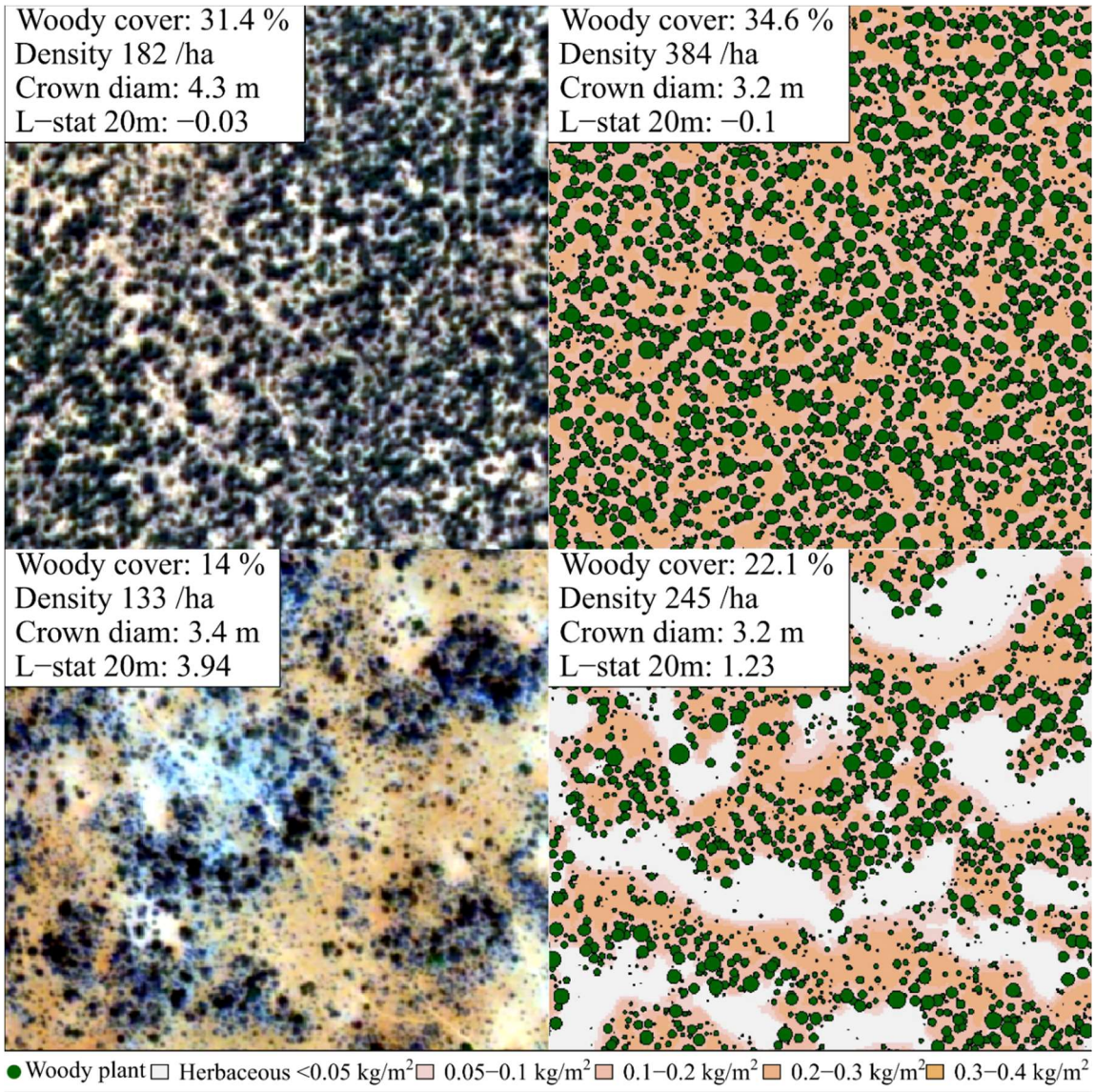

Figure 4.4 Examples of observed and modeled landscapes with lower and higher levels of tree aggregation. The top pair is from a site in Botswana (Lat. -22.0941, Long. 20.80593, MAP 422 mm/year, Rain cv 1.36, Loamy sand, Slope 0.17 %, Fire freq. 0.07). Here, the landscape has a low value for aggregation, as there are no large tree-less patches and many trees grow in rows with bare or grassy patches on the sides. The bottom pair is from

Somalia (Lat. 4.048934, Long. 44.07875, Rain cv 1.56, Clay loam, Slope 0.55%, fire freq. 0). The more variable precipitation, combined with a fine-textured soil, contribute to a landscape with aggregated woody plants. The gentle slope means that much of the surface water is directed downhill, leading to a banded pattern with bare ground between vegetated patches.

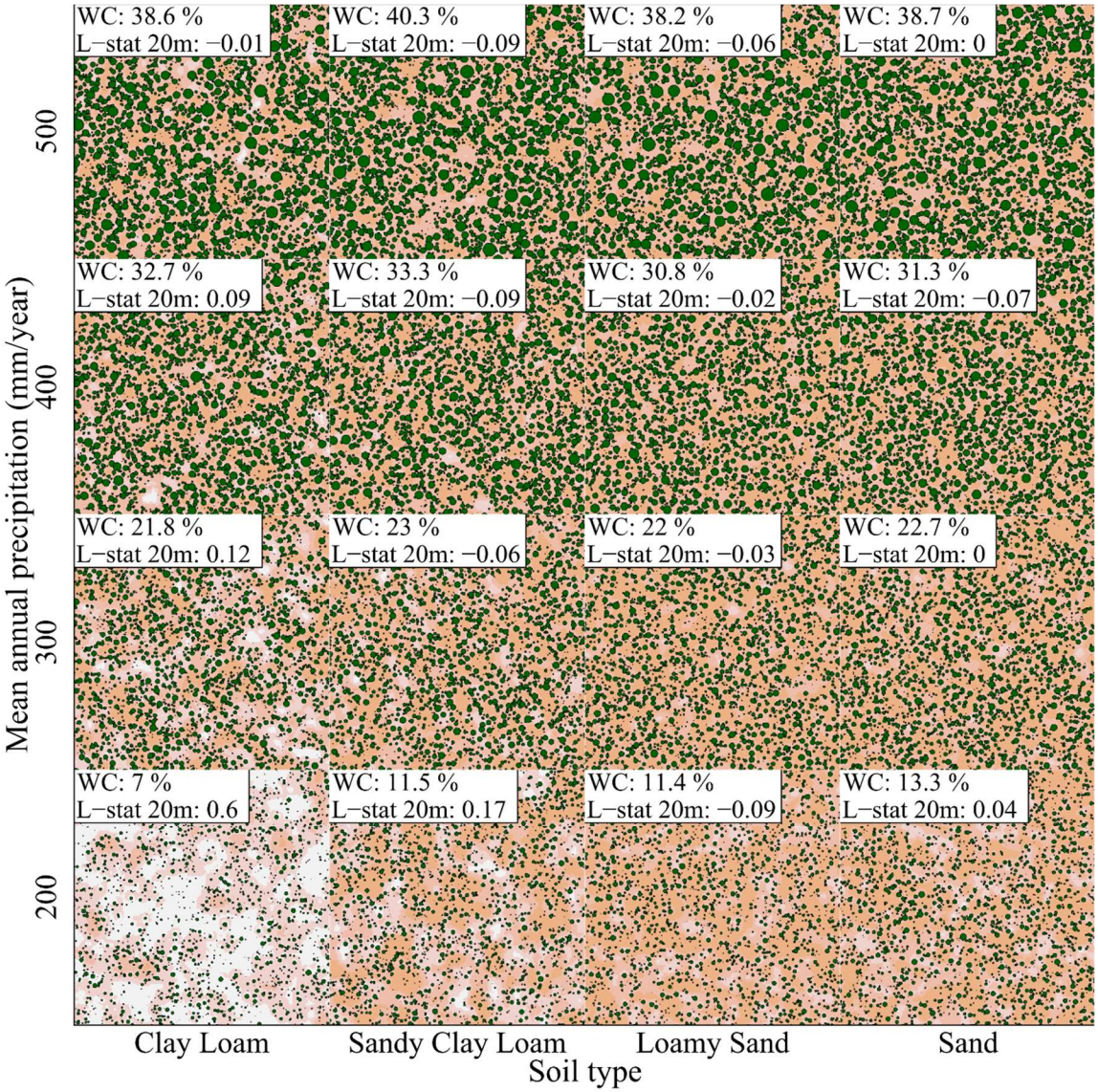

Figure 4.5 Modeled landscapes illustrating the effects of soil type and MAP in influencing woody cover and the level of tree aggregation in a landscape. The landscapes were

modeled with 0 % slope, no fires, and by repeating a year with normally distributed monthly rainfall (rain cv 1.3) for 60 years. Woody cover is higher on the sandy soil at the dry end and highest on the medium-textured sandy clay loams at higher rainfall, which corresponds with the inverse texture hypothesis. The lowest woody cover and highest level of woody plant aggregation are on the clay loam at low rainfall. The landscapes follow the same legend as in figures 4.3 & 4.4.

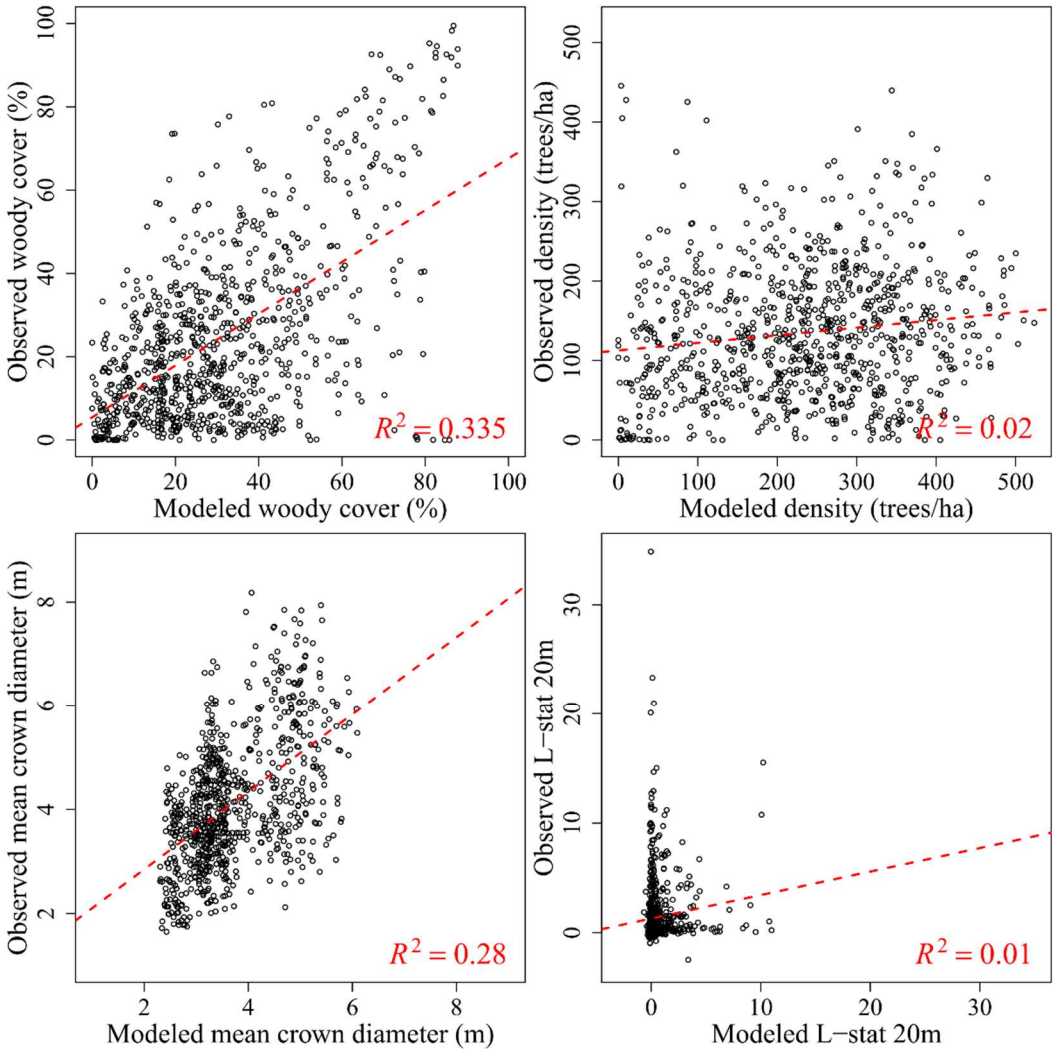

Figure 4.6 Regressions between estimates from satellite imagery (observed) and modeled woody vegetation properties for the 876 African savanna sites.

By running the model for a single site and recording statistics for every month, we can study how the woody properties fluctuate over time (Figure 4.7). The woody properties exhibited strong responses to interannual variation in rainfall, with distinct growth and decline phases. The strong temporal fluctuations further explain the relatively weak correlations between modeled and observed landscapes (Figure 4.6), as the simulations are likely to sometimes be out of phase from when the satellite image was recorded. By re-running the model with the soil type changed to clay, it was clear that the clayey soil negatively affected woody cover and mean crown size for this site. This effect was not clear in the BRT regression analysis (Figure 4.2), perhaps because the relationship changes along the rainfall gradient. The trend may also be clearest for clay soil, and only one of the 876 sites had this soil type. Woody plant aggregation showed distinct peaks during the decline phase and these were accentuated on the clayey soil. This indicates that facilitation between trees strongly influences survival during droughts. An example of a site with a periodic vegetation pattern in Senegal (Figure 4.8) shows how the landscape evolves during the decline and growth phases. The vegetation died off into an organized pattern and was most reminiscent of the observed periodic pattern at the peak of the die-off.

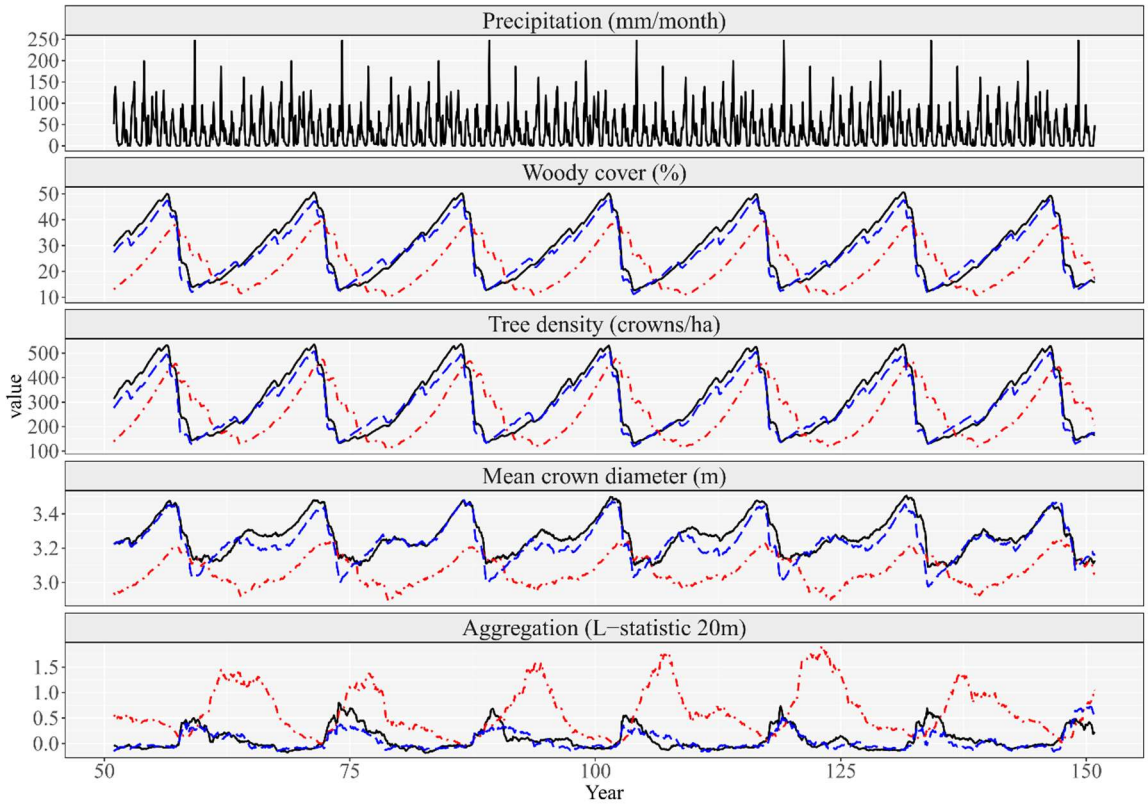

Figure 4.7 Variation in modeled woody attributes for a site in Botswana (black solid line; MAP 420 mm/year, Rain cv 1.2, Sandy clay loam, Fire freq. 0). To investigate the effect of soil type, we modeled the same site with the soil type changed to clay (red dotted line) and sand (blue dashed line). All woody attributes show a great sensitivity to interannual variation in rainfall, with phases of growth and decline that coincide with the precipitation time series (2001-2015) that was repeated every 15 years. The level of aggregation peaks during the die-off and is accentuated on the clayey soil. There is little difference between the sand and the sandy clay loam, but the vegetation on the clayey soil has lower woody cover, driven both by fewer trees and smaller crown sizes, and a delayed response curve, possibly caused by the higher water-holding capacity of clays.

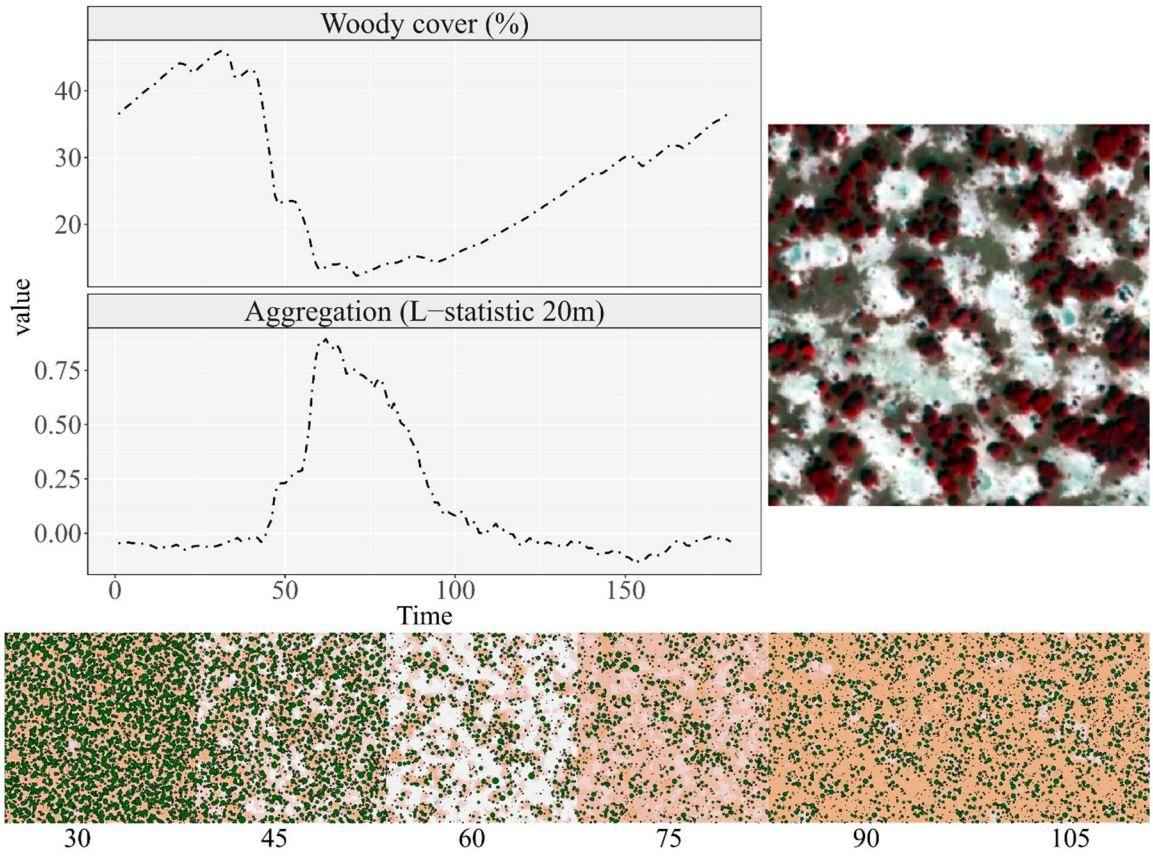

Figure 4.8 Timeline with changes in the modeled landscape during a decline phase for a site in Senegal (Lat. -14.47543, Long. 15.64887, MAP 421 mm/year, Rain cv 1.7, Sandy clay loam, Slope 0.08 %, Fire freq. 0). This site exhibited a periodic vegetation pattern with clear differences between the vegetated patches and the surrounding bare ground. During the modeling of the site, the vegetation fluctuated greatly and was most reminiscent of the observed vegetation structure at the low-point at time 60. The vegetation thus dies off into an aggregated pattern and then grows out of it in the following growth phase. The landscapes follow the same legend as in figures 4.3 & 4.4. Although the time scale is in months, it is representative of more long-term processes.

4.5 Discussion

4.5.1 Modeling woody cover, plant density, and crown sizes

One of the key findings in Axelsson & Hanan (2017) was that increases in woody cover are more a result of increasing crown sizes than increasing tree densities. Our modeling results reproduce this pattern, with strong positive relationships between woody cover, crown sizes, and MAP (Figure 4.2). Landscapes with low rainfall (~300 mm/year) often feature many smaller woody plants, with relatively low resource needs, that use water from a small area around each plant. With increasing rainfall, trees can grow larger, and the larger trees with more developed root systems will often outcompete nearby smaller plants. In wet systems with large trees and high woody cover, survival of smaller plants often depends on light availability, which limits their numbers. Overall, tree densities are therefore less controlled by MAP than are mean crown sizes.

The approach to model tree crowns as circles works well for savannas but may limit woody cover as it approaches canopy closure. At the high end of woody cover (>70 %), the model underestimated woody cover in relation to the observed estimates (Figure 4.6). This is likely due to the inflexible nature of the circular crowns, which caused a high degree of crown overlap. Natural tree crowns are more flexible in terms of branching out into open gaps where sunlight is available and are therefore better at forming a closed canopy.

The observed woody cover and crown sizes were influenced by rainfall variability, but with fluctuating response curves (Figure 4.2) that may be caused by data overfitting in the BRT model. In the modeled responses, rainfall variability had little

influence over woody cover and crown sizes, but a weak negative effect on tree density. This trend results from the more pronounced dry seasons, associated with high rainfall variability, which can increase tree mortality. Sand content had a unimodal influence on woody cover and crown sizes in the observed data, and similar, but much weaker, responses for the modeled landscapes. The modeled landscapes had lower woody cover and crown sizes on fine-textured soils (Figure 4.7), but the relationship is clearest for clay soil, which was rare among the analyzed savanna sites. The relationship also changes with MAP (Figure 4.5) in agreement with the inverse texture hypothesis (Noy-Meir, 1973). At the wet end, woody cover is lower on the sandy soil due to increased deep percolation, and at the dry end, woody cover is lower on the clay soil due to increased runoff generation. It is, however, not clear if runoff is a dominant flux in arid systems, and this effect may be achieved using different modeling mechanisms. Noy-Meir (1973) mentioned runoff as a possible driver, but proposed that increased evaporation on clayey soils was the dominant mechanism suppressing woody cover. Later, Fensham et al. (2015) suggested that the higher wilting point in clayey soils impedes water extraction. In our simulations, the relative soil moisture rises from the addition of infiltrated water until the system reaches a balance point where water losses are similar to water additions. This point is higher on clayey soils and the system compensates for the high wilting point by keeping higher soil moisture levels. The higher wilting point, alone, was thus not sufficient for explaining a drop in woody cover on clayey soils. A study by English et al. (2005) in grasslands and savannas in the southwestern USA found that soil water content levels were consistently higher on clayey soils, and relatively more water was retained in the top soil layer on clays. It is possible that soil water retention in the top soil layer can result in higher evaporative

losses and also negatively affect more deep-rooted woody plants. To model this mechanism, it would be necessary to separate the soil into layers which we never did in this modeling study. This would also favor grasses on fine-textured soils, whereas in our simulations grass growth was favored by coarse-textured soils (Figure 4.2), where the higher infiltration capacity resulted in less overland flows to woody patches.

We modeled the effect of fire on tree mortality following observations that larger trees, with thicker bark, are far less sensitive to high fire intensities than younger plants (Bond, 2008). As opposed to the savanna model by Higgins et al. (2000), we did not model top-killing of trees. Many savanna tree species can survive a fire with the top burnt but the root-system intact, and then re-sprout without having to invest in root development (Bond, 2008). Our modeled effects of fire do, however, fit relatively well with the observed data. The simulations indicate that among the woody properties, tree density and woody cover were most affected by fire and there was a unimodal effect on mean crown size in relation to fire frequency (Figures 4.2 & 4.3).

4.5.2 Modeling woody plant aggregation

One important reason for modeling individual trees using a spatially explicit model design was to simulate neighbor interactions and the spatial pattern of woody plants. Our modeling results agree with the observations from satellite data that landscapes with more aggregated woody plants are associated with low MAP, high rainfall variability, and fine-textured soils (Figure 4.2). The model simulations indicate two processes that lead to higher levels of aggregation: (1) overland flows and (2) vegetation dieback phases. Overland flows redistribute water to vegetated patches. This is increased on fine-textured soils, which increase the contrast in infiltration capacity between vegetated and non-

vegetated patches (Niemeyer et al., 2014). It is also related to rainfall patterns, where more intense rainfall events will cause more overland flows. Vegetation dieback phases cause distinct peaks in woody plant aggregation (Figure 4.7). This indicates that local facilitative tree-tree interactions play a major role for woody survival during droughts. In the simulations, local facilitation occurs from shading, which lowers evaporation rates and increased infiltration capacity near trees, where the former is the more important factor during droughts. During severe water shortages, evaporation becomes a greater factor relative to competition from neighboring trees, resulting in the mortality of more isolated trees. Systems with high rainfall variability are more likely to experience periods of severe water shortage and vegetation contraction. As higher aridity, in general, results in more aggregated plants; this is also enhanced by the harsher conditions on clayey soils, here modeled through increased runoff generation. The model results are thus in correspondence with the stress-gradient hypothesis, which states that facilitative interactions increase with higher environmental stress (He et al., 2013). During the re-growing phase following the dieback, woody aggregation drops as new trees establish and grow in the open. Competition and facilitation between trees thus appear strongly linked to the different phases of vegetation growth and dieback.

The effect of slope did affect the alignment of the vegetation in the simulated landscapes (Figure 4.4) but had relatively small influence over the woody properties (Figure 4.2). In contrast, the observed woody aggregation did have a negative relationship with slope, which may be the result of rill formation on steeper slopes (Saco & Moreno-de las Heras, 2013). As opposed to the modeled overland flows, rills lead the water away and do not contribute to local redistribution of water resources.

4.5.3 Vegetation growth and dieback phases

The modeled landscapes feature great fluctuations in woody structure over time (Figure 4.7) as a result of interannual variation in rainfall. These phases are a natural component of drylands with highly variable precipitation and are supported by observations in the field (Brandt et al., 2017; Wiegand et al., 2006). It is, however, clear that the growth response among trees is exaggerated, and the modeled trees respond too fast to increasing precipitation. A study on woody encroachment using the same data set (Axelsson & Hanan, 2018) showed that most of the sites had relatively small changes in woody cover over a 10-year period. In the model, the sensitivity to increased rainfall is controlled by the maximum monthly growth rate and the soil depth, which acts as a reservoir that dampens the effect of smaller rainfall fluctuations. The reasons for the high sensitivity in the modeled growth rates were (a) shortening the running time of the model and (b) making sure that the vegetation at some of the arid sites survived. With a slower growth rate, the windows of opportunity for sapling growth during the modeled 15 years of rainfall were sometimes not sufficient for reaching a more drought-tolerant size with deeper roots. In the field, woody plants in drylands grow slowly and may rarely receive the longer periods of above-average precipitation necessary for sapling survival. The observed woody cover in some of these sites may be the result of wet periods many decades ago.

4.5.4 Vegetation dieback as possible origin of periodic vegetation patterns

As the simulations indicated that the most aggregated vegetation patterns emerged from dieback (Figure 4.8), this may offer a clue to how periodic vegetation patterns first form. Observations from the Sahel indicate that some of the most distinct periodic patterns emerged from dieback in the last century. According to Barbier et al.

(2006), a 3000 km² area of homogenous savanna in south-western Niger underwent a dramatic shift to a highly aggregated periodic vegetation structure during a period with droughts and decreased precipitation between 1956 and 1996. Similar developments were also observed in Sudan during the droughts of the 1970s and 1980s (Deblauwe et al., 2011). It is thus possible that these patterns first form during prolonged droughts in environments where edaphic conditions facilitated water redistribution via overland flows. Over time, soil erosion in bare patches may serve to reinforce the periodic pattern, and a significant wet period would be necessary to turn it back into a homogenous savanna.

4.6 Conclusions and Model applications

We set out to construct a savanna vegetation model that incorporates several aspects of the natural environment (mean annual rainfall, rainfall variability, soil type, slope, fire), to examine if we can reproduce observed trends from a remote sensing analysis and offer explanations to observed variation in vegetation structure. We showed how MAP influences tree density and crown sizes, where woody density increases with MAP at the dry end, but crown sizes are the main driver of increasing woody cover across the full range of rainfall. Our modeled landscapes followed the trend predicted by the inverse texture hypothesis, with suppression of woody cover on clayey soils in drylands, but we cannot be sure if this was modeled using the correct process, as the same trend can be modeled using different processes and the scientific community is divided on the driving mechanism. Further, our simulations indicated that the level of aggregation among woody plants is strongly tied to facilitative effects during dieback events, which also can offer an explanation for how periodic vegetation patterns first emerge.

The model proved useful for simulating spatial interactions among plants and for modeling landscape development over time. For further studies, it would be useful to gather (or generate) longer time series of monthly precipitation for better calibration of the sensitivity of tree growth to interannual fluctuations in rainfall. The model may also prove useful for modeling interactions between different woody functional types. In this study, we used a single type of tree to avoid having different tree characteristics influence the results.

4.7 Appendix B: List of model variables and coefficients

Variable	Description
$Crown\ radius_W$	Radius of crown (m); individual for each plant
E_{max}	Maximum evaporation in a cell based on light availability (mm).
$Evap$	Evaporation of soil water in a cell (mm).
FI	Fire intensity in a cell (MW/m)
$Growth_H$	Monthly growth of herbaceous vegetation in a cell (kg/m²).
$Growth_W$	Monthly radial growth of a tree crown (m).
H	Herbaceous aboveground biomass (kg/m²).
H_{dead}	Aboveground biomass of dead herbaceous vegetation in a cell (kg/m²).
H_{living}	Aboveground biomass of living herbaceous vegetation in a cell (kg/m²).
$H_{mean\ 2.5m}$	Herbaceous vegetation around a cell calculated as the mean herbaceous biomass in a circle with radius 2.5 m from the cell center.
Inf_{ij}	Infiltration rate for a cell; depends on soil type and the local herbaceous biomass and woody root cover.
$LightA_{ground}$	Light availability at the ground level for a cell (ranges from 0 to 1); depends on shading from both herbaceous and woody plants.
$LightA_w$	Light availability for a tree crown; based on shading from larger overlapping crowns (ranges from 0 to 1).
LS	Light stress for vegetation (ranges from 0 to 1).

$Mort_H$	Herbaceous mortality in a cell (kg/m²).
$P_{monthly}$	Precipitation falling during a month (mm).
$pMort\ Fire$	Mortality risk from fire for a woody plant (ranges from 0 to 1).
$pMort\ LS_W$	Mortality risk from light stress for a woody plant (ranges from 0 to 1).
$pMort\ WS_W$	Mortality risk from water stress for a woody plant (ranges from 0 to 1).
PS	Plant stress as a function of water and light stress (ranges from 0 to 1).
Q	Surface water (mm).
$Root\ radius_W$	Radius of root system of a woody plant calculated as $1.5 \cdot Crown\ radius_W$ (m)
s	Relative soil moisture in a cell (ranges from 0 to 1).
s_{herb}	Relative soil moisture in the upper soil level down to the soil depth Z_H (ranges from 0 to 1).
s_{top}	Relative soil moisture in the top soil down to the soil depth Z_{evap} (ranges from 0 to 1).
Wat	Water content in the soil (mm)
Wat_H	Water consumed by herbaceous vegetation in a cell (mm).
Wat_W	Water consumed by woody plants in a cell (mm).
Wat_{new}	Newly infiltrated water in a cell (mm). Calculated after drainage to field capacity.
$Woodycover_{mean\ 4.5m}$	Woody cover for a cell calculated as the mean woody cover in a circle with radius 4.5 m from the cell center.
$Woody\ rootcover$	Woody root cover in a cell.
$Woodyrootcover_{mean\ 4.5m}$	Cover of woody plant roots for a cell calculated as the mean root cover in a circle with radius 4.5 m from the cell center.
WS	Water stress for vegetation (ranges from 0 to 1).
Z_W	Depth of root system calculated as $Z_{seedling} + (Z_{max} - Z_{seedling})\sqrt{(Crown\ radius_W - Crown\ radius_{seedling})/Max\ radius_W}$

Coefficient	Description	Value
$Crown\ radius_{seedling}$	Crown radius for seedlings	0.03 m
D_Q	Diffusion rate for overland flows between neighboring cells.	0.8
DR_H	Decomposition rate of dead grasses	5% per month
EnergyContent	Energy content of herbaceous vegetation	20 kJ/g
$FTOL_W$	Fire tolerance; controls the chance to survive high fire intensities.	1.0

GR_H	Maximum monthly growth rate of living grasses	0.02 kg/m²
GR_W	Maximum monthly radial growth rate of the crown	0.012 m
Inf_H	Controls the positive effect on infiltration rates from both living and dead grasses	0.1/kg/m²
Inf_S	Scales the influence from the soils saturated hydraulic conductivity.	10
Inf_W	Controls the positive effect on infiltration rates per woody root cover	0.4
k_{evap}	Evaporation coefficient	0.06
k_{ext}	Light extinction coefficient	0.5
Ks	Saturated hydraulic conductivity; controls infiltration rates.	Varies with soil type
LAI_W	Leaf area index of the woody canopy	2
$LSTOL_H$	Tolerance of woody plants to low light conditions	0.12
$LSTOL_W$	Light stress tolerance of woody plants; controls growth restrictions and mortality from insufficient light conditions	0.3
MR_H	Maximum monthly mortality rate of grasses	0.1 kg/m²
$Max\ radius_W$	Maximum crown radius	6 m
n	Porosity; the available space for water in the soil.	Varies with soil type
$\mathrm{nSeedlings}_W$	Number of seedlings dispersed each month	25
RateOfSpread	Fire spread rate.	1 m/s
s^*	Point where plants start to close stomata.	Varies with soil type
s_h	Hygroscopic point.	Varies with soil type
s_{fc}	Field capacity; controls soil water drainage.	Varies with soil type
s_w	Plant wilting point.	Varies with soil type
SLA_H	Specific leaf area	8 m² per kg
$WSTOL_H$	Tolerance to water stress of herbaceous vegetation	0.06
$WSTOL_W$	Water stress tolerance of woody plants; controls growth restrictions and mortality from water stress	0.15
$Water\ use_H$	Monthly water use by living grasses	5 mm per kg/m²
$Water\ use_W$	Water use per woody root cover	8 mm
Z_{evap}	Soil depth from which water evaporates.	100 mm
Z_H	Herbaceous root depth	400 mm
Z_{max}	Maximum root depth for woody plants	2200 mm
Z_r	Soil depth	2200 mm
$Z_{seedling}$	Root depth of woody plant seedlings	200 mm

4.8 References

Axelsson, C. R., & Hanan, N. P. (2017). Patterns in woody vegetation structure across African savannas. *Biogeosciences, 14*(13), 3239-3252. doi:10.5194/bg-14-3239-2017

Axelsson, C. R., & Hanan, N. P. (2018). Rates of woody encroachment in African savannas reflect water constraints and fire disturbance. *Journal of Biogeography, 0*(0). doi:doi:10.1111/jbi.13221

Barbier, N., Couteron, P., Lejoly, J., Deblauwe, V., & Lejeune, O. (2006). Self-organized vegetation patterning as a fingerprint of climate and human impact on semi-arid ecosystems. *Journal of Ecology, 94*(3), 537-547.

Besag, J. (1977). Comments on Ripley's paper. *Journal of the Royal Statistical Society B, 39*(2), 193-195.

Bond, W. J. (2008). What limits trees in C4 grasslands and savannas? *Annual Review of Ecology, Evolution, and Systematics, 39*, 641-659.

Brandt, M., Tappan, G., Diouf, A. A., Beye, G., Mbow, C., & Fensholt, R. (2017). Woody vegetation die off and regeneration in response to rainfall variability in the West African Sahel. *Remote Sensing, 9*(1), 39.

Byram, G. M. (1959). Combustion of forest fuels. *Forest fire: Control and use, 1*, 61-89.

Clapp, R. B., & Hornberger, G. M. (1978). Empirical equations for some soil hydraulic properties. *Water Resources Research, 14*(4), 601-604.

Cosby, B., Hornberger, G., Clapp, R., & Ginn, T. (1984). A statistical exploration of the relationships of soil moisture characteristics to the physical properties of soils. *Water Resources Research, 20*(6), 682-690.

Deblauwe, V., Couteron, P., Lejeune, O., Bogaert, J., & Barbier, N. (2011). Environmental modulation of self-organized periodic vegetation patterns in Sudan. *Ecography, 34*(6), 990-1001.

Elith, J., Leathwick, J. R., & Hastie, T. (2008). A working guide to boosted regression trees. *Journal of Animal Ecology, 77*(4), 802-813.

English, N. B., Weltzin, J. F., Fravolini, A., Thomas, L., & Williams, D. G. (2005). The influence of soil texture and vegetation on soil moisture under rainout shelters in a semi-desert grassland. *Journal of Arid Environments, 63*(1), 324-343. doi:http://dx.doi.org/10.1016/j.jaridenv.2005.03.013

Farr, T. G., Rosen, P. A., Caro, E., Crippen, R., Duren, R., Hensley, S., . . . Roth, L. (2007). The shuttle radar topography mission. *Reviews of Geophysics, 45*(2), 1-33. doi:10.1029/2005RG000183

Fensham, R. J., Butler, D. W., & Foley, J. (2015). How does clay constrain woody biomass in drylands? *Global Ecology and Biogeography, 24*(8), 950-958.

Giglio, L., Loboda, T., Roy, D. P., Quayle, B., & Justice, C. O. (2009). An active-fire based burned area mapping algorithm for the MODIS sensor. *Remote Sensing of Environment, 113*(2), 408-420.

He, Q., Bertness, M. D., & Altieri, A. H. (2013). Global shifts towards positive species interactions with increasing environmental stress. *Ecology letters*.

Hengl, T., Heuvelink, G. B., Kempen, B., Leenaars, J. G., Walsh, M. G., Shepherd, K. D., . . . Tamene, L. (2015). Mapping soil properties of Africa at 250 m resolution:

Random forests significantly improve current predictions. *PloS one, 10*(6), e0125814.

Higgins, S. I., Bond, W. J., & Trollope, W. S. (2000). Fire, resprouting and variability: a recipe for grass–tree coexistence in savanna. *Journal of Ecology, 88*(2), 213-229.

Holdo, R. M., & Brocato, E. R. (2015). Tree–grass competition varies across select savanna tree species: a potential role for rooting depth. *Plant Ecology, 216*(4), 577-588.

Holmgren, M., Gómez-Aparicio, L., Quero, J. L., & Valladares, F. (2012). Non-linear effects of drought under shade: reconciling physiological and ecological models in plant communities. *Oecologia, 169*(2), 293-305.

Huffman, G. J., Bolvin, D. T., Nelkin, E. J., Wolff, D. B., Adler, R. F., Gu, G., . . . Stocker, E. F. (2007). The TRMM multisatellite precipitation analysis (TMPA): Quasi-global, multiyear, combined-sensor precipitation estimates at fine scales. *Journal of Hydrometeorology, 8*(1), 38-55.

Laio, F., Porporato, A., Fernandez-Illescas, C., & Rodriguez-Iturbe, I. (2001). Plants in water-controlled ecosystems: Active role in hydrologic processes and response to water stress: IV. Discussion of real cases. *Advances in water resources, 24*(7), 745-762.

Laio, F., Porporato, A., Ridolfi, L., & Rodriguez-Iturbe, I. (2001). Plants in water-controlled ecosystems: Active role in hydrologic processes and response to water stress: II. Probabilistic soil moisture dynamics. *Advances in water resources, 24*(7), 707-723. doi:http://dx.doi.org/10.1016/S0309-1708(01)00005-7

Metzger, J. C., Landschreiber, L., Gröngröft, A., & Eschenbach, A. (2014). Soil evaporation under different types of land use in southern African savanna ecosystems. *Journal of Plant Nutrition and Soil Science*.

Niemeyer, R., Fremier, A., Heinse, R., Chávez, W., & DeClerck, F. (2014). Woody vegetation increases saturated hydraulic conductivity in dry tropical Nicaragua. *Vadose Zone Journal, 13*(1).

Noy-Meir, I. (1973). Desert ecosystems: environment and producers. *Annual review of Ecology and Systematics, 4*, 25-51.

Porporato, A., Laio, F., Ridolfi, L., & Rodriguez-Iturbe, I. (2001). Plants in water-controlled ecosystems: Active role in hydrologic processes and response to water stress: III. Vegetation water stress. *Advances in water resources, 24*(7), 725-744.

Raz-Yaseef, N., Rotenberg, E., & Yakir, D. (2010). Effects of spatial variations in soil evaporation caused by tree shading on water flux partitioning in a semi-arid pine forest. *Agricultural and Forest Meteorology, 150*(3), 454-462.

Resco de Dios, V. R., Weltzin, J. F., Sun, W., Huxman, T. E., & Williams, D. G. (2014). Transitions from grassland to savanna under drought through passive facilitation by grasses. *Journal of Vegetation Science*.

Rietkerk, M., Boerlijst, M. C., van Langevelde, F., HilleRisLambers, R., van de Koppel, J., Kumar, L., . . . de Roos, A. M. (2002). Self-organization of vegetation in arid ecosystems. *The American Naturalist, 160*(4), 524-530.

Riginos, C. (2009). Grass competition suppresses savanna tree growth across multiple demographic stages. *Ecology, 90*(2), 335-340.

Ripley, B. D. (1977). Modelling spatial patterns. *Journal of the Royal Statistical Society. Series B (Methodological), 39*(2), 172-212.

Saco, P. M., & Moreno-de las Heras, M. (2013). Ecogeomorphic coevolution of semiarid hillslopes: Emergence of banded and striped vegetation patterns through interaction of biotic and abiotic processes. *Water Resources Research, 49*(1), 115-126.

Staver, A. C., & Levin, S. A. (2012). Integrating theoretical climate and fire effects on savanna and forest systems. *The American Naturalist, 180*(2), 211-224.

Valladares, F., & Niinemets, Ü. (2008). Shade tolerance, a key plant feature of complex nature and consequences. *Annual Review of Ecology, Evolution, and Systematics, 39*(1), 237.

von Hardenberg, J., Kletter, A. Y., Yizhaq, H., Nathan, J., & Meron, E. (2010). Periodic versus scale-free patterns in dryland vegetation. *Proceedings of the Royal Society B: Biological Sciences, 277*(1688), 1771-1776.

Wiegand, K., Saltz, D., & Ward, D. (2006). A patch-dynamics approach to savanna dynamics and woody plant encroachment–insights from an arid savanna. *Perspectives in Plant Ecology, Evolution and Systematics, 7*(4), 229-242.

Zhang, L., Hu, Z., Fan, J., Zhou, D., & Tang, F. (2014). A meta-analysis of the canopy light extinction coefficient in terrestrial ecosystems. *Frontiers of earth science, 8*(4), 599-609.

Zimmermann, J., Higgins, S. I., Grimm, V., Hoffmann, J., & Linstädter, A. (2010). Grass mortality in semi-arid savanna: the role of fire, competition and self-shading. *Perspectives in Plant Ecology, Evolution and Systematics, 12*(1), 1-8.

5 SYNTHESIS AND CONCLUSIONS

5.1 Summary and key findings

Savannas exhibit significant variability in vegetation structure, including the density and cover of woody plants, sizes of trees, and their spatial patterns, resulting from variation in climate, soils, and topography, and various disturbances including fire, herbivory, and periodic droughts that may have enduring impacts on woody populations. This dissertation aimed to examine how woody vegetation structure and directional changes in African savanna woody cover vary with changing environmental conditions. The analyses were based on access to very high spatial resolution (VHR; <1 m) satellite imagery from sites sampled across African savannas, and the development of a suite of analysis software, including for analysis of woody populations in VHR data, and a process-based model of tree-grass interactions and woody population dynamics in savanna ecosystems. The primary results of this research are summarized below.

Chapter 2: Patterns in woody vegetation structure across African savannas

- Variation in woody cover in relation to mean annual precipitation (MAP) is more a function of increasing tree sizes than a function of variation in tree density.
- Woody cover was higher on mid-textured soils than either more clayey or sandy soils, and this was driven by larger crown sizes.
- Woody plants exhibit higher levels of aggregation in systems with more variable rainfall, lower overall rainfall, and fine-textured soils. These factors were also associated with the occurrence of periodic vegetation patterns (PVPs).

Chapter 3: Rates of woody encroachment in African savannas reflect water constraints and fire disturbance

- Across the study areas, there was a mean increase in woody cover of 0.25 % per year.
- Variation in woody cover change was significantly related to woody cover deficits (potential woody cover – initial woody cover) and fire frequency.
- Given the relationship between woody cover change and the potential woody cover, it was possible to derive estimates of potential woody cover from change dynamics in woody cover.

Chapter 4: Modeling savanna woody structure and patterning

- Woody cover and mean crown sizes increased with MAP across the full rainfall range. Woody density increased with MAP at the dry end, but the relationship reached an asymptote at ~400 mm/year.
- The modeled landscapes followed the patterns along rainfall and soil texture gradients that lead to the formulation of the inverse texture hypothesis (Noy-Meir, 1973), with higher woody cover on sandy soils at the dry end and higher woody cover on medium-textured soils in mesic systems. The model was calibrated to suppress woody growth on clayey soils in drylands in correspondence with earlier observations, but it is not clear whether the correct mechanism was used, as the same effect can be achieved from both higher runoff generation and increased evaporation of top-soil water.

- The modeled landscapes had higher woody plant aggregation in systems with low and variable rainfall and on fine-textured soils. This was in correspondence with the findings in chapter 2.
- Dieback events resulted in peaks in aggregation, indicating that tree-tree facilitative effects were most influential during droughts and controlled plant survival. This also offers an explanation for how strongly aggregated periodic vegetation patterns may emerge during prolonged droughts.

5.2 Variability in woody vegetation structure in tropical savannas: a synthesis

This research set out to examine how environmental factors influence woody vegetation structure and change in woody cover in African savannas. Many of the factors that influence woody cover have been analyzed in previous studies (e.g. Sankaran et al., 2008), whereas less research has focused on its constituents, tree density and crown size, and the spatial pattern of trees. With access to VHR imagery for sites spread out over the African continent, I was able to estimate these woody vegetation properties and link them to environmental factors. Any such analysis is limited to the datasets available. Whereas it is clear that biological factors, such as density of browsers and grazers, have strong impacts on the landscapes, I did not consider those datasets sufficiently reliable for the study. Instead, I used mean annual precipitation (MAP), rainfall seasonality, sand content, slope, and fire frequency. The classification approach, based on unsupervised classification followed by manual assignment of classes using custom-built software, worked well for this study, which featured great variation in the reflectance properties of the vegetation between sites, as well as different satellite sensors and solar and viewing angles. It was

necessary to apply a flexible methodology that allowed for adaptions to conditions at each site.

One limitation with the analysis is that crown delineation is complicated, and in cases of overlapping crowns it is sometimes only possible to clearly distinguish the individual crowns at the ground level during field assessments. As with all remotely sensed products, the estimates based on the delineated crowns cannot be considered as accurate as field observations. The estimates are based on the assumption that errors associated with the delineation are similar between sites, and the found relationships should then result from correlation between the estimated and true woody properties. I cannot exclude the possibility that the tree crown delineation methodology caused a few artifacts among the responses in woody properties. Specifically, the drop in tree density for medium-textured soils (Figure 2.7) may have resulted from incorrect delineation at some sites in that particular range of sand content, especially since the ensuing modeling study did not reproduce that pattern. It should also be noted that the focus of the remote sensing analysis (chapter 2) was not on the absolute numbers, but on identifying trends in woody vegetation properties and linking them to environmental factors. Similarly, the model presented in chapter 4 is not a prediction model, but a tool to better understand and explain how different ecosystem processes interactively shape woody vegetation structure in a savanna landscape.

The findings in chapter 2 contribute to our understanding of savanna ecology and dynamics. As savannas greatly contribute to the global carbon cycle (Poulter et al., 2014), it is important to understand the woody composition in terms of crown sizes and tree densities. To help interpret and explain the results, I constructed the model presented

in chapter 4, which simulates how rainfall, soil type, slope, and fire impacts the vegetation in a savanna landscape. The model results show that most of the observed trends in woody vegetation properties, can be explained from modeled ecosystem processes, which adds support to both the validity of the found relationships and to the mechanisms proposed to cause them.

The model further provided a view of the evolution of the landscape over time (Figure 4.7). Whereas the growth response of the trees was exaggerated, the general pattern of growth and dieback phases in relation to interannual variation in rainfall is modeled realistically. This also underscores the importance of the temporal aspect when studying savannas. My own recognition of the temporal aspect, and the importance of interannual variation in rainfall, also grew as the project proceeded. In chapter 2, I used rainfall seasonality (coefficient of variation of mean monthly rainfall) as a potential driver in the regression analysis. In chapter 4, I instead used rainfall variability (coefficient of variation of the full time-series of monthly precipitation estimates). In hindsight, it would have been better to also use rainfall variability in the former analysis since it incorporates both seasonal and interannual variations. It also would have been better to pursue a longer time series of monthly precipitation in the modeling study. In chapters 2 & 3, I used TRMM data (Huffman et al., 2007) because of the higher spatial resolution, whereas a long time series was deemed less important. This decision carried over to chapter 4 where I used the same data. Given the importance of interannual variation in rainfall in the modeled landscapes, it would have been appropriate to use Climatic Research Unit (CRU) data (Harris et al., 2014), which provides a longer time series at lower spatial resolution. For

further studies using the model, it is recommended that the sensitivity in tree growth to fluctuations in precipitation is calibrated using this or other long-term datasets.

The simulations indicated that the level of aggregation among trees is strongly linked to the dieback and growth phases. Isolated trees were more vulnerable to succumb during dieback, but once the rains returned, competition became the dominant neighborhood effect and new plants established in the open. This apparent shift from facilitation to competition is in agreement with the stress-gradient hypothesis and supports earlier observations of such temporal shifts in semi-arid systems (Sthultz et al., 2007). The temporal aspect may also play an important role in how PVPs form and evolve. If plants do not grow into aggregated patterns, it is necessary to include the temporal aspect. Periodic vegetation patterns may then form during prolonged droughts and evolve with expansions and contractions following wet and dry periods, where it is the contractions that create the strong periodicity. Erosion of soil resources in the bare patches and possibly soil crust formation may then play a key role in maintaining a periodic pattern long after the droughts end.

5.3 Patterns of woody cover change: a synthesis

The study on woody encroachment (chapter 3) found a trend of increasing woody cover (0.25 % per year) that could not be tied to any of the environmental factors in the study. Higher atmospheric CO_2 concentrations is a possible driver of this trend, in correspondence with modeling studies that have simulated the effect of increasing CO_2 (Brandt et al., 2017; Higgins & Scheiter, 2012). The results are important as they support the trend in woody encroachment found in other studies (Brandt et al., 2017; Stevens et al., 2017) using different data and methods. The novel contribution of the current study,

however, is to highlight the role of water availability in controlling rates of change in woody cover. I found that the difference between potential and initial woody cover was strongly related to estimates of change during the 10-year observation period. This relationship held in both water-limited and mesic savannas and exists with or without the trend of woody encroachment. Woody cover varies naturally over time, with phases of growth and decline resulting from the growth stage of the vegetation, disturbances, and, foremost, interannual variation in rainfall, as shown in chapter 4. The relationship between woody cover change and the woody cover deficit (potential – initial cover) highlights the importance of potential woody cover when studying encroachment and offers clues about where to expect the fastest rates of encroachment. It is also important to note that in mesic savannas, woody growth rates affect the ability of trees to outgrow and escape frequent fires and can therefore have nonlinear effects on woody cover by facilitating landscape transition to a forest state.

If the general trend in encroachment results from increasing atmospheric CO_2, it is important that future research clarifies how it affects woody communities and interacts with other environmental factors and disturbances. Some studies suggest that CO_2 acts by increasing water-use efficiency and should have a clear impact in water-limited drylands (Higgins & Scheiter, 2012). Other studies suggest that CO_2 will have the greatest effect in mesic savannas by helping juvenile trees escape the fire trap (Bond & Midgley, 2000). In chapter 3, I found similar trends of encroachment across the MAP gradient. I also found that the relationship between woody cover change and woody cover deficit (potential – initial cover) existed both in dryland and mesic savannas. This pattern may indicate that a CO_2-fueled boost to water use efficiencies has similar impacts across the rainfall gradient.

It is, however, not clear whether CO_2 boosts woody growth rates, raises the potential woody cover, or both. The relationship in chapter 3 suggests that raising the potential cover will simultaneously boost growth rates. Increasing water use efficiencies may result in higher potential woody cover in water-limited systems (Stevens et al., 2016), and this would, naturally, have large implications for dryland ecosystems and their ability to act as a terrestrial carbon sink.

5.4 Looking to the future

Trends in the development of remote sensing instruments indicate that the scientific community will be having greater access to data of increasingly higher spatial resolution. VHR data have fewer "mixed" pixels and require different processing and analysis techniques than coarser-scaled products. In systems with sparse (<~ 25%) woody cover, coarser resolution data cannot be used to reliably estimate woody cover (Gaughan et al., 2013; Gessner et al., 2013), and more fine-scaled products are needed. This research shows that VHR imagery can prove very useful for studying dryland vegetation and offers a methodology for how to process and analyze the data. The use of VHR data for large scale assessments also opens novel areas of research. Large scale estimates of tree cover from coarse resolution remote sensing data have been available for some time (Hansen et al., 2003) and have fueled a plethora of literature on factors that control woody (e.g. Accatino & De Michele, 2016; Good & Caylor, 2011). Access to VHR imagery can similarly open new fields of research on more detailed structural vegetation properties which will further contribute to our understanding of these ecosystems.

This research is also an example of how remote sensing analysis can be aided by model simulations for interpretation and understanding of observed results. The goal is to understand the physical and biological processes that shape ecosystems and one approach is to compare remote sensing observations to results from model simulations. Disagreements between modeled and observed results can signal that interpretations are incorrect or that additional factors influence the results. The presented model still needs further refinement, for instance in terms of realistically modeling plant responses to changes in rainfall over longer time frames. Additional factors and processes, such as temperature, could be incorporated in future versions of the model, especially if it was to be used to simulate ecosystems with high temperature seasonality. Temperature affects evapotranspiration and cold temperatures may induce mortality. It would thus be necessary to include temperature if constructing a model that works in both tropical Africa, tropical systems on other continents, and in more temperate climates. However, the current model offers a solid platform for simulating tree-tree and tree-grass interactions in a savanna landscape.

5.5 References

Accatino, F., & De Michele, C. (2016). Interpreting woody cover data in tropical and subtropical areas: Comparison between the equilibrium and the non-equilibrium assumption. *Ecological Complexity, 25*, 60-67.

Bond, W. J., & Midgley, G. F. (2000). A proposed CO2-controlled mechanism of woody plant invasion in grasslands and savannas. *Global Change Biology, 6*(8), 865-869.

Brandt, M., Rasmussen, K., Peñuelas, J., Tian, F., Schurgers, G., Verger, A., . . . Fensholt, R. (2017). Human population growth offsets climate-driven increase in woody vegetation in sub-Saharan Africa. *Nature Ecology & Evolution, 1*, 0081.

Gaughan, A. E., Holdo, R. M., & Anderson, T. M. (2013). Using short-term MODIS time-series to quantify tree cover in a highly heterogeneous African savanna. *International Journal of Remote Sensing, 34*(19), 6865-6882.

Gessner, U., Machwitz, M., Conrad, C., & Dech, S. (2013). Estimating the fractional cover of growth forms and bare surface in savannas. A multi-resolution approach based on regression tree ensembles. *Remote Sensing of Environment, 129*, 90-102.

Good, S. P., & Caylor, K. K. (2011). Climatological determinants of woody cover in Africa. *Proceedings of the National Academy of Sciences, 108*(12), 4902-4907.

Hansen, M., DeFries, R., Townshend, J., Carroll, M., Dimiceli, C., & Sohlberg, R. (2003). Global percent tree cover at a spatial resolution of 500 meters: First results of the MODIS vegetation continuous fields algorithm. *Earth Interactions, 7*(10), 1-15.

Harris, I., Jones, P., Osborn, T., & Lister, D. (2014). Updated high-resolution grids of monthly climatic observations–the CRU TS3. 10 Dataset. *International journal of climatology, 34*(3), 623-642.

Higgins, S. I., & Scheiter, S. (2012). Atmospheric CO2 forces abrupt vegetation shifts locally, but not globally. *Nature, 488*(7410), 209-212.

Huffman, G. J., Bolvin, D. T., Nelkin, E. J., Wolff, D. B., Adler, R. F., Gu, G., . . . Stocker, E. F. (2007). The TRMM multisatellite precipitation analysis (TMPA): Quasi-global, multiyear, combined-sensor precipitation estimates at fine scales. *Journal of Hydrometeorology, 8*(1), 38-55.

Noy-Meir, I. (1973). Desert ecosystems: environment and producers. *Annual review of Ecology and Systematics, 4*, 25-51.

Poulter, B., Frank, D., Ciais, P., Myneni, R. B., Andela, N., Bi, J., . . . Liu, Y. Y. (2014). Contribution of semi-arid ecosystems to interannual variability of the global carbon cycle. *Nature, 509*(7502), 600-603.

Sankaran, M., Ratnam, J., & Hanan, N. (2008). Woody cover in African savannas: the role of resources, fire and herbivory. *Global Ecology and Biogeography, 17*(2), 236-245.

Stevens, N., Erasmus, B., Archibald, S., & Bond, W. (2016). Woody encroachment over 70 years in South African savannahs: overgrazing, global change or extinction aftershock? *Phil. Trans. R. Soc. B, 371*(1703), 20150437.

Stevens, N., Lehmann, C. E., Murphy, B. P., & Durigan, G. (2017). Savanna woody encroachment is widespread across three continents. *Global Change Biology, 23*(1), 235-244.

Sthultz, C. M., Gehring, C. A., & Whitham, T. G. (2007). Shifts from competition to facilitation between a foundation tree and a pioneer shrub across spatial and temporal scales in a semiarid woodland. *New Phytologist, 173*(1), 135-145.